Swiss Potential for Geothermal Energy and CO2 Storage
Synthesis Report

Author(s):

Driesner, Thomas; Gischig, Valentin; Hertrich, Marian (iD); Loew, Simon (iD); Maurer, Hansruedi; Mazzotti, Marco; Saar, Martin O. (iD); Wiemer, Stefan (iD); Zappone, Alba Simona (iD); Moscariello, Andrea; Guglielmetti, Luca; Valley, Benoît; Holliger, Klaus; Laloui, Lyesse; Lecampion, Brice; Krause, Rolf; Amann, Florian; Meier, Peter; Spada, Matteo; Lateltin, Olivier

SCCER S SoE

SWISS COMPETENCE CENTER for ENERGY RESEARCH
SUPPLY of ELECTRICITY

Swiss Potential for Geothermal Energy and CO$_2$ Storage

Synthesis Report

Impressum

Publisher
ETH Zurich

Editors
Domenico Giardini, Gianfranco Guidati (ETHZ)

Authors
Thomas Driesner, Valentin Gischig, Marian Hertrich, Simon Löw, Hansruedi Maurer, Marco Mazzotti, Martin O. Saar, Stefan Wiemer, Alba Zappone (ETHZ), Andrea Moscariello, Luca Guglielmetti (Uni Geneva), Benoit Valley (Uni Neuchatel), Klaus Holliger (Uni Lausanne), Lyesse Laloui, Brice Lecampion (EPFL), Rolf Krause (USI), Florian Amann (RWTH Aachen), Peter Meier (Geoenergie Suisse), Matteo Spada (PSI), Olivier Lateltin (Swisstopo)

Contact
Domenico Giardini (domenico.giardini@erdw.ethz.ch)

Editorial and Layout
Barbara Naegeli, Silvia Passardi (ETH Zurich)

Title Image
Installation of the monitoring sensors at the Bedretto Laboratory for Geosciences and Geoenergies. © Swiss Seismological Service at ETH Zurich, 2020 (Image: Luxwerk.ch).

Executive Summary

In the aftermath of the Fukushima disaster the Swiss Federal Office of Energy proposed the Energy Strategy 2050 which is largely based on the report by Prognos (2012). The main objective was the strong growth of renewable electricity generation to compensate the nuclear power plants that shall retire within 20–30 years. Specific goals were set for hydropower and the new renewables: photovoltaics, wind and geothermal power plants. The latter were planned to deliver 4.4 TWh/a by 2050.

During the lifetime of the SCCER-SoE, the political debate in Switzerland and elsewhere evolved from a mere replacement of nuclear power towards the more holistic objective to reduce the overall greenhouse gas emissions to net-zero, meaning that any residual emission of fossil CO$_2$ shall be compensated, either in Switzerland or abroad.

This change of focus shed the light on the overall *energy* system of which the *electricity* system is only a sub-system. And indeed, the majority of fossil CO$_2$ emissions in Switzerland stem from the provision of heat (space heat, domestic hot water, industrial process heat) and mobility services (gasoline and diesel vehicles). Both the recent update of the Energy Perspectives 2050+ by Prognos (2020) and the results of the JASM Project (Marcucci et al., 2021) highlight the importance of CO$_2$-free heat supply for the aforementioned sectors.

The objective of SCCER-SoE, namely to generate electricity from geothermal heat, requires the creation and safe operation of deep geothermal reservoirs, capable of delivering heat at temperatures of 150–200 °C. At a geothermal gradient of 30 °C/km, this requires a depth of 4–6 km, well inside the crystalline baserock. Here, the natural permeability needed for the circulation of any heat transfer fluid is virtually absent, requiring a whole array of novel stimulation and monitoring techniques.

Such techniques were at the heart of the geothermal research in SCCER-SoE, ranging from lab-scale experiments, to field experiments at 10-meter scale in the Grimsel Test Center, to finally reach the 100-meter scale at the Bedretto lab. Tests at Grimsel showed that permeability could be increased by orders of magnitude, while controlling the inevitable rock movements that may be perceived as induced seismicity at the surface. Research continues at the Bedretto lab where first stimulation campaigns were successfully executed at the end of 2020.

Once we will manage to deliver geothermal heat from the crystalline baserock to the surface, the options for using this heat are manifold: district heating networks or some industrial processes in the food sector may require heat at temperatures between 80–100 °C. Higher temperatures in excess of 100 °C may be used by other industries or by the emerging field of CO$_2$ capture processes. Heat at a temperature of 150 °C and above may eventually be used for electricity generation.

Complementary to the development of stimulation techniques for deep reservoirs in crystalline rocks, we added the element of heat storage in sedimentary rocks at the beginning of Phase II of the SCCER-SoE. Researchers contributed actively to successful drilling campaigns in the Geneva area and later also in Bern. When successful, this approach allows to store excess thermal energy from waste to energy plants in summer to eventually supply heat via district heating networks in winter.

Another element of any future net-zero greenhouse gas emission strategy is the permanent storage of CO$_2$. This can be captured from waste to energy or cement plants, but also from wood combined heat and power plants. The necessary volumes to be stored are in the order of 10–20 Mt$_{CO_2}$/a, where only a geological storage seems realistic. Research within SCCER-SoE led to a significant reduction of the estimated the domestic storage potential. We therefore recommend a two-pronged approach, first to maximize the efforts to understand the Swiss subsurface, both by a reanalysis of existing data and by the acquisition of new data, and second to promote and join a European initiative for a CO$_2$ transport and storage infrastructure.

Acronyms and Abbreviations

ATLS	Advanced Traffic Light System
BULGG	Bedretto Underground Laboratory for Geosciences and Geoenergies
CCS	CO$_2$ Capture and Storage
CPG	CO$_2$-Plume Geothermal
DGE	Deep Geothermal Energy
EGS	Enhanced Geothermal System
GIS	Geographical Information System
JASM	Joint Activity Scenarios & Modelling
HP	Heat Pump
GHG	Greenhouse Gases
GSHP	Ground Source Heat Pump
GTS	Grimsel Test Site
PV	Photovoltaics
SCCER	Swiss Competence Center for Energy Research
SCCER-SoE	SCCER Supply of Electricity
SED	Swiss Seismological Service
SGS	Swiss Geological Survey
SMB	Swiss Molasse Basin
sMCDA	spatial Multi-Criteria Decision Analysis
STEM	Swiss TIMES Energy System Model
kWh	kilowatt-hour
GWh	gigawatt-hour, 1 GWh = 10^6 kWh
TWh	terawatt-hour, 1 TWh = 10^9 kWh
PJ	peta-joule, 1 PJ = 0.277 TWh, 1 TWh = 3.6 PJ

Table of Contents

1   Geothermal Energy - an Untapped Resource

Geothermal energy is heat stored in the rock masses below our feet. It can be used to heat our houses, to run industrial processes or to generate electricity. Recent studies clearly indicate the value of geothermal heat for achieving the net-zero emission target of the Swiss Federation. Over the past seven years, the SCCER-Supply of Electricity addressed the challenges that are associated with the extraction of heat from the subsurface.

1.1   What is Geothermal Energy?

Geothermal energy refers to the thermal energy in the subsurface that can be extracted to supply heat to buildings and industry, or to generate electricity. It stems from the early stages of earth formation and is still fed by radioactive decay processes. The temperature of the earth core is approx. 6000 °C. Towards the surface, the temperature decreases and on the last kilometers the geothermal gradient in Switzerland is roughly 30 °C per kilometer.

Today, geothermal energy in Switzerland is exploited mainly via heat pumps at shallow depth of less than 400 m to supply space heating and domestic hot water (Figure 1). The ground temperature in this region is 10–20 °C, close to the average ambient surface temperature. Many technical options exist, Laloui and Loria (2019) give an overview with special focus on energy geostructures.

New opportunities appear for greater depths and temperatures. From 2000 m onward, temperatures are in the range of 80 °C which can be used for district heating networks or for low-temperature industrial processes. Once 100 °C are reached at more than 3000 m depth, power generation cycles can be employed that are commercially available today. For source temperatures between 100 and 200 °C the efficiency will be in the order of 10–15 %. The residual heat is rejected in a condenser against the environment and is generally *not at a useful temperature level anymore*. Alternatively, medium temperature industrial processes may be supplied, the advantage being that almost all heat can be directly used.

In order to extract thermal energy from the underground, two heat transport processes are possible: conduction which is generally slow but sufficient for ground heat probe applications and advection which is a much more efficient way of extracting and transporting heat. Advection implies the circulation of a fluid - generally water - through the rocks. Such a process requires a sufficient permeability and an adequate permeability structure for efficient heat extraction. Permeability of rock masses spans many orders of magnitude and takes various forms. In sedimentary rocks as sand- or limestone it can be part of the initial rock fabric (primary permeability) or increased by dissolution (karstification) or fracturing (secondary permeability). In magmatic rocks such as granite the primary permeability is very small and rock mass permeability is largely controlled by the presence of fractures.

In case of sedimentary rocks, heat can be extracted by pointing a borehole into an aquifer, a layered structure with high natural permeability, and by pumping hot water to the surface. This approach is often termed hydrothermal (see Figure 1). In Switzerland, such aquifers are mainly found in the Mesozoikum (the blue layers in Figure 2), which refers to a series of 70–250 mio years old sedimentary rocks, that are close to the surface in Northern Switzerland, and that are found in increasing depth towards the Alps and the east.

In the case of crystalline basement rock, fracture zones with sufficient permeability for exploitation in an hydrothermal manner are potentially present, but difficult to find. Here, the permeability has to be artificially engineered (petrothermal approach, see Figure 1). This is called enhanced geothermal systems (EGS). During a stimulation phase, fractures in the rocks are either generated or enlarged by injecting water under high pressure. The deformation
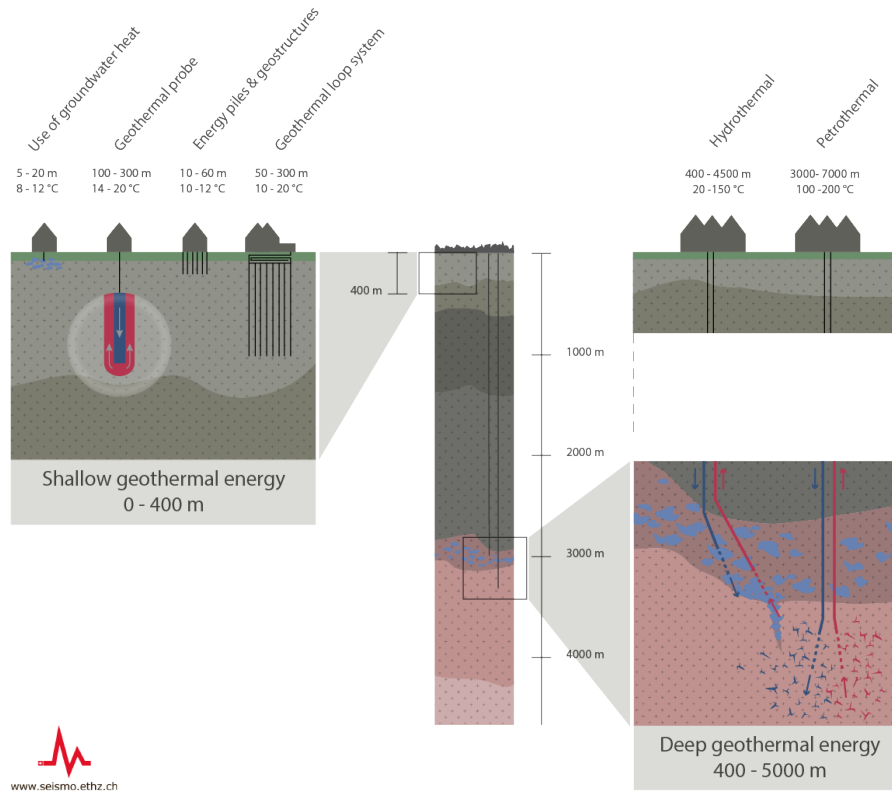
Figure 1: *Types of geothermal energy resources and installation (Swiss Seismological Service at ETH Zurich).*

and failure of the rock mass can lead to rapid rock displacements that can be perceived at the surface as induced earthquakes.

1.2 Swiss Energy Strategy

The Swiss Federal Energy Act was accepted in its revised version by the Swiss electorate on 21 May 2017. It aims at increasing the share of renewable energy in the supply mix, while abandoning in the long runs the use of nuclear power. Geothermal electricity production was explicitly mentioned in the Swiss Energy Strategy 2050: 4.4 TWh of electrical energy per year shall be produced in 2050 (Prognos, 2012).

The Swiss energy strategy has recently been completely revised, with the additional objective to reduce the Swiss greenhouse gas emissions to net-zero in 2050 (Prognos, 2020). During the process, it was well understood that geothermal energy can play a crucial role to supply baseload energy, not only in electricity generation but especially for direct heat use for districts, agriculture and industrial processes. Similar conclusions were reached within the Joint Activity Scenarios & Mod-

elling (JASM) where researchers of all eight SC-CER collaborated to generate net-zero scenarios (Marcucci et al., 2021).

Furthermore, it was understood that the net-zero emission target can only be reached when CO_2 is actively collected from large scale emitters and locked away from the atmosphere. The only realistic option to do this at the necessary scale of 10 Mt_{CO_2}/a and more is in the subsurface.

1.3 Heat Production Today

The final energy demand for space heating, domestic hot water and industrial process heat was 101.5 TWh in 2019 (Figure 3). The largest share of 60 TWh was supplied by fossil oil and gas. Geothermal heat contributed 3 TWh, where the majority came from shallow borehole heat exchangers and ground water, coupled to brine-water and water-water heat pumps, respectively (Link, 2021).

Only a small fraction of 0.22 TWh was used directly without elevating the temperature via a heat pump, mainly in thermal baths. The direct use of geothermal heat for space heat from deep aquifers is found only in Riehen and it supplied a
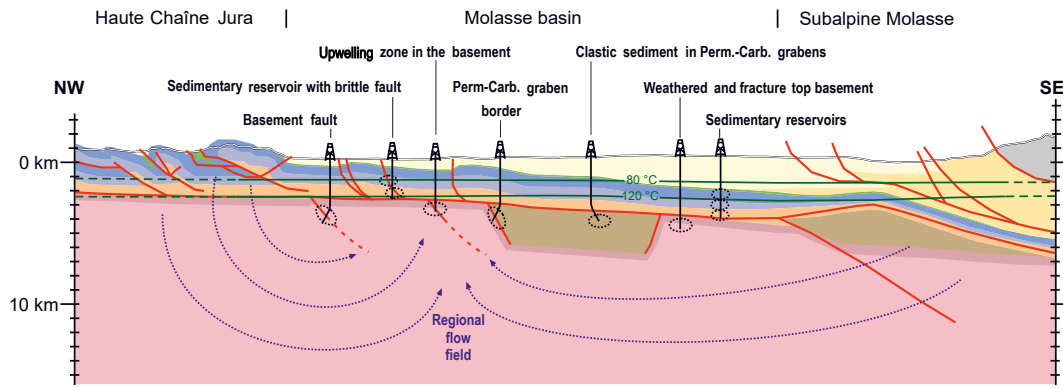
Figure 2: *Simplified geological cross-section through the Swiss plateau with potential targets for geothermal projects (Valley and Miller, 2020).*
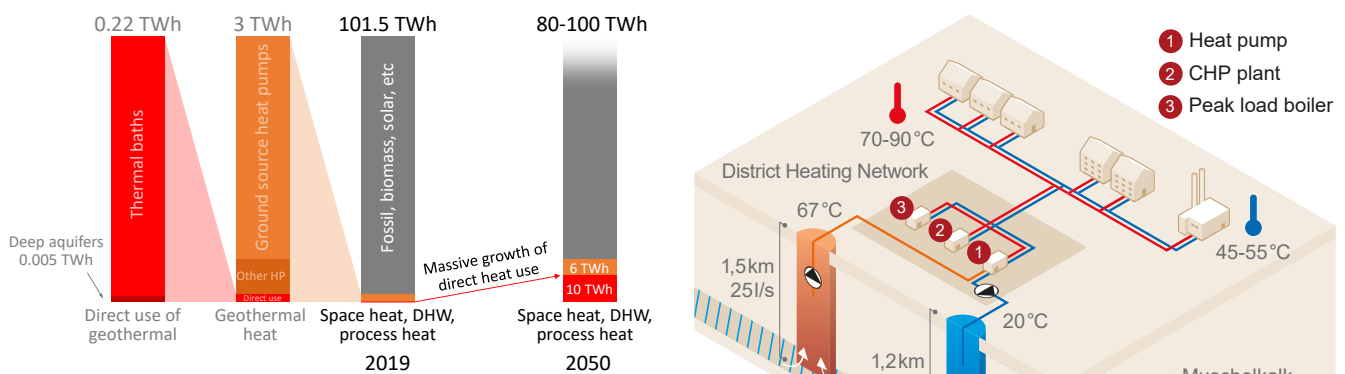
Figure 3: *The role of geothermal energy for the supply of domestic and industrial heat.*

Figure 4: *Cartoon representation of the Riehen geothermal project (source: Erdwärme Riehen).*

tiny 0.005 TWh in 2019 (Figure 4).

The centerpiece is a geothermal plant that has been in operation since 1994 and pumps warm water at around 66 °C from a depth of over 1500 meters. This is fed into the approximately 37 km long local district heating network. The municipality of Basel is now planning a second deep well. The new geothermal plant "geo2riehen" is scheduled to go into operation in 2025.

Both the Energieperspektiven 2050+ and the JASM scenarios foresee a strong growth of geothermal heat use in 2050. The fraction used by heat pumps via borehole heat exchangers will grow further but is limited especially in densely populated cities. A massive growth to 10 TWh/a is foreseen for the direct use of deep geothermal heat, for the purposes of space heating, domestic hot water and low temperature (< 150 °C) industrial processes.

1.4 New Projects

A range of new projects aiming primarily at heat production are now entering the phases of explo-

ration and resource characterization in Switzerland. Some examples are listed here.

GEothermie 2020 (Geneva): This geothermal development program driven by Services Industriels de Geneve (SIG) and the Canton of Geneva, aims at implementing geothermal energy in the Canton of Geneva with a stepwise approach starting from shallow installation to gradually move toward deeper targets to cover 20 % of the cantonal heat demand by 2035. SCCER-SoE researchers actively contributed to the prospection phase (Moscariello et al., 2020). An essential element of this strategy is also the creation of a high temperature underground thermal energy storage, that will be capable of storing heat from a waste-to-energy plant in summer, and deliver it to a district heating network in winter (see also www.heatstore.eu).

Two wells have been drilled into deep reservoirs
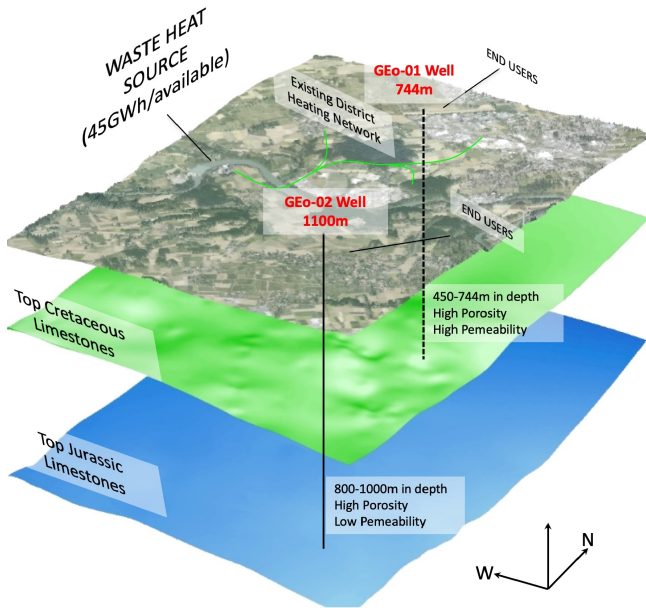
Figure 5: *Illustration of the Geneva project aiming to develop an underground thermal energy storage connected to a waste-to-energy plant.*

in the Mesozoic carbonate sequence. The Geo-01 well is 744 m deep and produces at present 50 l/s of hot water at 33 °C which corresponds to 20–30 GWh/a of thermal power suitable to supply 2000-3000 households. A second well (GEo-02) reached approx. 1400 m in depth. This well encountered a carbonate reservoir at high hydrostatic pressure but lower permeability than expected and some differences in the predicted stratigraphy. The well will be re-entered, sampled and tested for a long period of time in order to assess well deliverability and reservoir connectivity. The mixed results obtained by the drilling campaign to date attest for the importance of continuing the efforts in exploring the subsurface in order to reach a satisfactory level of understanding to ensure high chance of drilling success.

The effectiveness of exploration approaches, concepts and models developed for the Geneva Basin will provide a solid framework to assist the continued effort to explore for direct heat production and subsurface storage potential in sedimentary basins at shallow to medium depths and demonstrate again the great potential and value of geothermal energy amongst the renewable energy portfolio available in Switzerland.

City of Davos: The municipality of Davos relies on indigenous and renewable energies as well as energy efficiency. An important part of the political energy strategy is the increased use of geothermal energy. To this end, Davos already launched a pilot project some ten years ago to eventually produce 4 GWh/year of heat (GEOTEST, 2019).

Energeô La Côte: Four sites are currently under investigation in the Canton Vaud, in the regions of Nyon, Gland / Vinzel (first drilling site), Aubonne and Etoy. The target reservoir is the Dogger limestone located at about 2500 m in depth which will be drilled by a doublet to produce hot water at about 80 °C (https://www.energeo.ch/)

AGEPP (Lavey-les-Bains): this project located in Canton Vaud aims at producing hot water at 110 °C with an expected flow rate of 40 l/s using a "singlet" solution, by drilling one well reaching 2300 m in depth which will serve as production well. The goal is to install an Organic Rankine Cycle (ORC) power plant to supply 15.5 GWh/a of heat and 4.5 GWh/a of electricity to about 900 households (https://www.agepp.ch/)

1.5   Challenges

Geothermal energy is right below our feet. Assuming a minimum useful temperature of 40 °C the layer between 1 and 6 km depth under the Swiss Mittelland contains 3'000'000 TWh of thermal energy, over four orders of magnitude more than the annual heat demand. The challenge is to either find the right spots where natural permeability is high and hot water can be extracted with minimum effort (hydrothermal), or to create artificial permeability by hydraulic stimulation of tight rocks (petrothermal).

The present synthesis report summarizes the work done by researchers of SCCER-SoE over the past seven years and addresses the aforementioned challenges. Section 2 tackles the problems of subsurface exploration and drilling, i.e. how to find good locations and how to get there efficiently. Section 3 addresses the central topic of the deep geothermal reservoir, including its creation, characterization and simulation. The bulk of the work done in SCCER-SoE was devoted to this matter, especially the challenge to create sufficient permeability in tight crystalline rocks. Section 4 is devoted to the related topic of subsurface CO₂ storage, a subject that was found to be of paramount importance for reaching the Swiss net-zero GHG emission targets. Finally, Section 5 tackles issue of risks and sustainability.

2 Exploration and Drilling

It is well known that geothermal energy is available in abundance below our feet. Depending on the desired temperature level, a depth of several kilometers has to be reached. The issue is to find the right spots and to get there. Therefore the topics of exploration and drilling are crucial for a successful deployment of geothermal heat and electricity production. How to create and operate a deep geothermal reservoir is the subject of the subsequent Section 3.

2.1 Subsurface Characterization

The development of deep geothermal projects is a multidisciplinary activity with several goals, namely (i) to identify the most favorable subsurface targets by integrating datasets from different sources, (ii) to quantify the associated uncertainties and risks that have to be mitigated by proper exploration programs, and (iii) to deliver results to project developers, policy makers and public authorities, in a accessible and ready-to-use manner to enable an optimal allocation of financial resources.

The so-called Play-based exploration approach, coupled to an accurate Play Fairway Analysis contributes to achieve these goals. An exploration program is based on the collection and interpretation of different datasets (geology, geochemistry, geophysics) to improve the knowledge of subsurface conditions such as temperature, permeability, reservoir volume and petrophysical properties. However, uncertainties always remain and these propagate into levels of risk that can hinder the development of a project. Therefore, the most appropriate methods have to be identified, designed and executed to fill the knowledge gaps and reduce uncertainties. A summary of the main geothermal exploration methods coupled to the subsurface parameter to be quantified is presented in Table 1.

When looking at the Swiss subsurface, geothermal projects can be developed in a wide variety of geological setting, including sedimentary basins and crystalline rocks, characterized by a large heterogeneity of lithologies and petrophysical conditions. Hence, a combination of activities has to be developed in order to allow industrial developers and decision makers to feel confident in geothermal projects.

Acquisition of high-resolution exploration and monitoring methods. Several geophysical methods such as gravity, deep electrical resistivity tomography (DERT), passive seismic and 2D and 3D active seismic including Vertical Seismic Profiling (VSP) using Distributed Acoustic Sensing (DAS), can be employed and combined for both exploration and time-lapse monitoring during production to reduce the subsurface uncertainty in terms of target identification, characterization, geologic risks (i.e. hydrocarbon accumulations) and reservoir performance.

Reservoir characterization. The quantification of the petrophysical parameters (i.e. porosity, permeability, thermal properties) and hydraulic properties distribution is a crucial step to assess

Table 1: *Correlation between exploration methods and subsurface parameters.*

	Geologic mapping	Fluid geochemistry	Gravity	Magnetic	Magnetotelluric	Electrical resistivity tomography	Active seismic	Passive seismic	Minero/petro observations	Thermal gradient holes	Exploration well
Porosity	orange		green				orange				green
Permeability	orange				orange	orange					green
Saturation					green	green		red			green
Fluid quality and type		green			orange						green
Fluid circulation paths		green			orange	orange					green
Clay content	orange				green	green			green		green
Magnetic mineral content	orange			green					green		green
Metallic mineral content	orange								green		green
Mechanical properties	red		red				green		orange		green
Tectonic structures	green		light orange			red	red				green
Temperature at depth		green			red					orange	green

the geothermal potential of a reservoir and predict its long-term behavior and sustainability. This can be achieved by field geologic observations, laboratory analysis, fracture characterization based on borehole images, production and tracer testing employing environmentally friendly tracers.

Thermal-Hydraulic-Mechanical-Chemical (THMC) models have the goal to produce predictive simulations of underground fluid flow, heat transport, geomechanics, and chemical reactions to estimate the efficiency, feasibility, and safety of a project. TH simulations focus on (i) assessing thermo-hydrological challenges to heat storage in the complex subsurface and (ii) on quantifying overall thermal efficiency using plausible-yet-simplified realizations of the underground heterogeneity as well as pre-existing hydrological conditions.

Machine learning applied to exploration and reservoir characterization. Machine Learning (ML) and Artificial Intelligence (AI) are methods that are broadly used in hydrocarbon industry, however, in geothermal applications their integration into project development workflows is still immature. These methods have the huge potential to allow geoscientist and decision makers to develop sets of geothermal plays, therefore allowing the evaluation of different development scenarios for which uncertainty and associated risks can be quantified. Increasing interest is being directed towards big data, thanks to the increasing amount of data that is collected during exploration phases. This data can be integrated using ML and AI to produce 3D static and dynamic model to improve the data interpretation process. Additionally, ML and AI can help coupling subsurface elements with surface components (i.e. energy demand scenarios, infrastructures planning) to provide a complete vision of the most efficient production configurations.

2.2 GeoMol – Geological Model of the Swiss Molasse Basin

The geological model of the Swiss Molasse Basin (GeoMol), first published in 2015, provides a simplified representation of the subsurface of the Swiss Midlands located between the Jura Mountains to the north and the Alps to the south. The model features the major fault systems and 12 basin-wide geological horizons based mainly on geophysical data, wells and surface geology. Initially, the model was part of the "INTERREG IV B" Alpine Space program, which produced a coherent geological 3D model of the North Alpine Foreland Basin and Po Basin. Pilot regions within the model provided more detail and addressed the potentials of geothermal energy, CO$_2$ storage and additionally earthquake hazard in the Po Basin. The Swiss Geological Survey (SGS), using the seismic interpretations of Sommaruga et al. (2012), modeled the Swiss portion of the North Alpine Foreland Basin.

As nearly half of the Swiss area were pilot regions with a higher detail, the SGS collaborated with five partners to complete an improved model. This was first published by the SGS in 2017 (Landesgeologie, 2017) and has been updated on an annual basis since then. Updates to the model are made at both a regional as well as a local scale. Regional updates usually cover a large area – for example a canton that has been remodeled using additional or previously unavailable data. Local updates typically cover a much smaller area (for example a fault zone) and include model corrections. The updates are described in the release notes, which accompany the models published in the GeoMol viewer (viewer.geomol.ch). Additionally to the structure of the Swiss Molasse Basin a temperature model of the subsurface is now included in GeoMol.

The anticipated use of the model lies primarily in the early phases of geothermal and CO$_2$ storage exploration as well as the visualization of the subsurface. While the SGS cannot provide detailed information, we are aware of the model being used or having been used in the planning stages of six different geothermal projects. The uppermost layer of the model – Top Bedrock – came to use in three projects related to transportation. Academia has also shown interest in the model and has applied it in three studies regarding subsurface exploration.

In producing the GeoMol model and its updates, a number of specialists had unique access to subsurface data of the Swiss Molasse Basin. These studies in turn provide an improved scientific understanding of the basin (Clerc, in prep. Gruber, 2017; Mock, 2017).

2.3 Fairways Analysis for Deep Geothermal Energy

Subsurface models like GeoMol provide opportunities for identifying geothermal plays and assessing the suitability for geothermal development. Valley and Miller (2020) proposed such an analysis in a
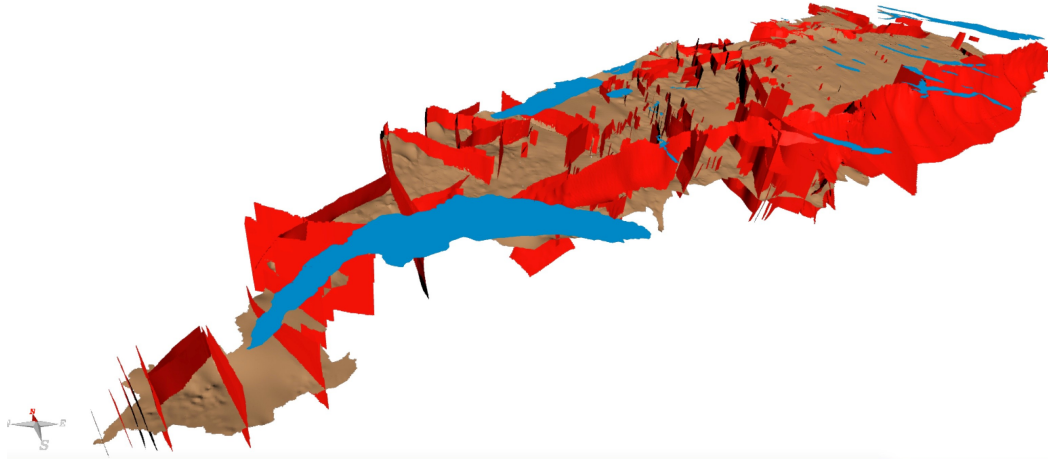
Figure 6: *Representation of the "Top Dogger" surface (brown) and fault zones (red) from the GeoMol19 model. View is from the SSW to NNE with a 3x vertical exaggeration. The model terminates along the southern edge of the Jura Mountains to the north, the Alps to the south, Lake Constance to the NE and Lake Geneva & France to the SW. The triangle zone of the Alpine front forms the large surfaces in the SE (see viewer.geomol.ch).*

quantitative play-fairway approach for Switzerland. The objective was to value the available data within a systematic, evolutive quantitative framework.

We first reviewed the available data sets and proposed conceptual classifications of geological and structural settings favorable for deep-seated fluid circulation in Switzerland. We took the available data to determine best-estimate stress models, which are then used to compute slip and dilation tendency on the main faults identified in the database. We also combined all available information to provide quantitative mapping of the fairway score (favorability maps) for geothermal exploration.

The results obtained show that with the available data, sharp contrasts in favorability can be highlighted on the Swiss plateau and these contrasts can guide exploration (see Figure 7). However, these results should be considered preliminary because of our simplifying assumptions, the paucity of data, and the scale of Switzerland which may not be appropriate for local scale exploration planning. Particularly, an attempt should be done to calibrate and validate the approach using appropriate data assimilation techniques. The difficulty is that direct evidence from geothermal projects or deep drilling on the Swiss plateau are sparse. The methodology and approach for generating favorability maps, however, can be applied in future studies with the availability of additional data, more sophisticated modeling and analysis, and findings from future exploration projects.

2.4 Model-based Heat Flow Analysis for the Canton of Aargau

With reported specific heat-flow values of up to 140 mW/m², the subsurface in the Canton of Aargau is an area of interest for deep geothermal energy exploration. The nature of this heat-flow anomaly was recently analyzed by using a combination of geophysical magnetotelluric exploration, geological modeling, and geophysical simulation, all focusing on the Permocarboniferous Trough (Niederau et al., 2020; Shah et al., 2020a; Shah et al., 2020b). This east-west striking graben system (Figure 8), is assumed to be connected to the origin of the heat-flow anomaly (Rybach et al., 1987; Griesser and Rybach, 1989).

To achieve a complete characterization of the heat-flow values as well as their spatial uncertainty, the project followed a workflow comprising: (i) self-consistent integrated implementation and analysis of various geoscientific data types such as temperature and stratigraphic logs from boreholes, geological cross sections and tectonic maps, (ii) development of a fit-for-purpose geological model of the Permocarboniferous Trough with focus on parameters controlling heat transport, and (iii) numerical simulations of the dominant heat-transport processes in the area.

Due to its nature as a pilot study, the developed workflow was designed to be adaptable, so that new data can be integrated seamlessly in order to update the model. This model-based core of the
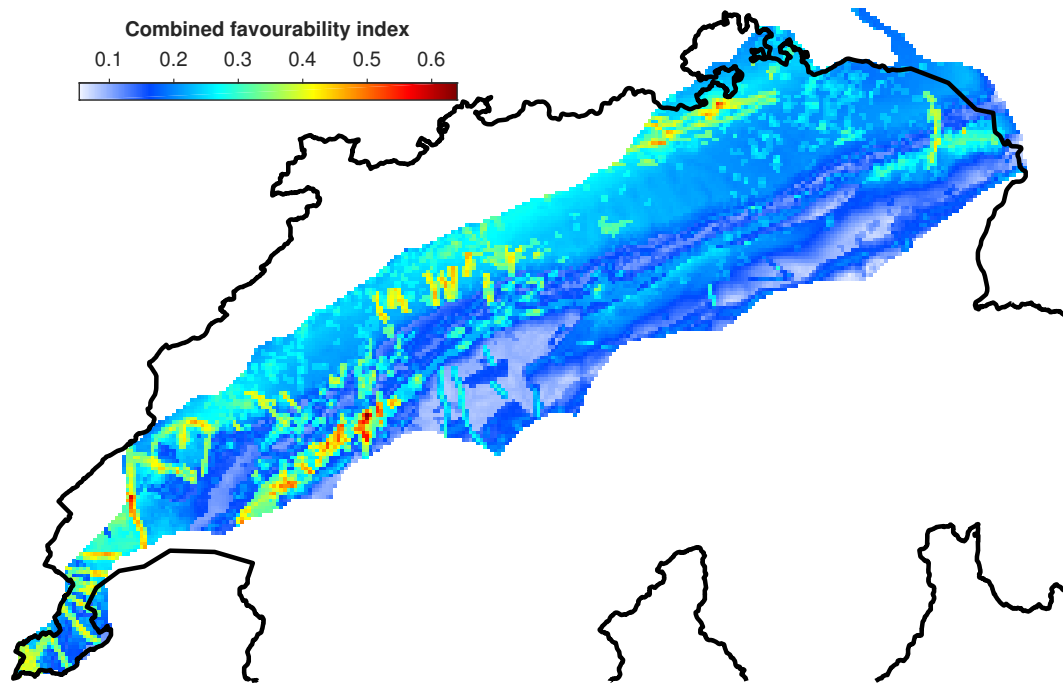
Figure 7: *Combined favorability index map for the target at 120 °C (Valley and Miller, 2020).*
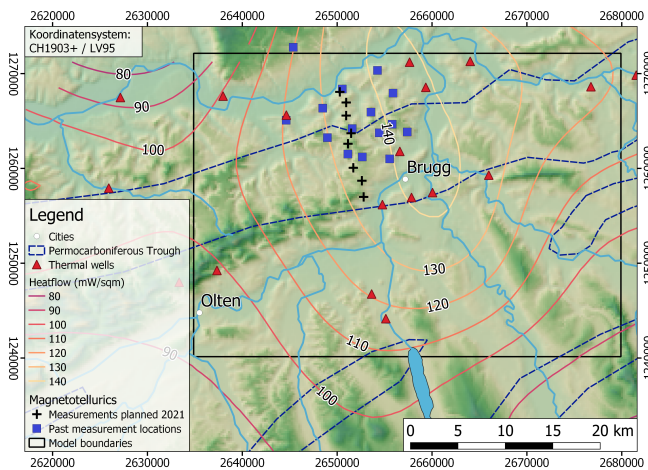
Figure 8: *Study area showing the outline of the geological, and heat-transport models.*

project was complemented by magnetotelluric field-studies, aiming to further constrain the geometry and depth of the graben system.

A vital part of this project was to investigate the effect of uncertain geological structures on the simulated subsurface temperatures and hence heat flow. In addition to borehole lithology, other input data for the geological model were: (i) interpretations of migrated seismic sections, (ii) interfaces from GeoMol (Team GeoMol, 2015), (iii) information from magnetotelluric measurements.

Perturbation of these uncertain input data within a reasonable uncertainty interval yields an ensem-

ble of geological models, which is conditioned in sequential steps in a Bayesian Inference Framework (Wellmann et al., 2018), readily implemented in the geological modeling software GemPy (Varga et al., 2019). Ensemble conditioning is done sequentially, using multiple likelihoods, e.g. geological knowledge, gravity measurements and temperature measurements from boreholes (see red triangles in Figure 8), discarding unrealistic geometries and models whose simulated gravity and temperatures do not fit observations. The resulting, conditioned ensemble will thus comprise realistic geological models fitting gravity and temperature measurements. The top in Figure 9 shows an example of a geological cross section of the PermoCarboniferous Trough through one of the models. For analysing uncertainty, concepts such as model topology (Thiele et al., 2016) or information entropy (Wellmann and Regenauer-Lieb, 2012) were used.

An example of latter is shown in the bottom Figure 9, which shows the cell entropy for a model ensemble comprising 50 different models where the depth of the Permocarboniferous Trough was varied. Entropy is zero where no uncertainty is present, i.e. where the same geological unit is present throughout the model ensemble. If, however, the geological unit at a certain location in the model differs between ensemble members, the information entropy is increased. As we vary the base of the Permocarboniferous Trough, the ensemble uncertainty at its
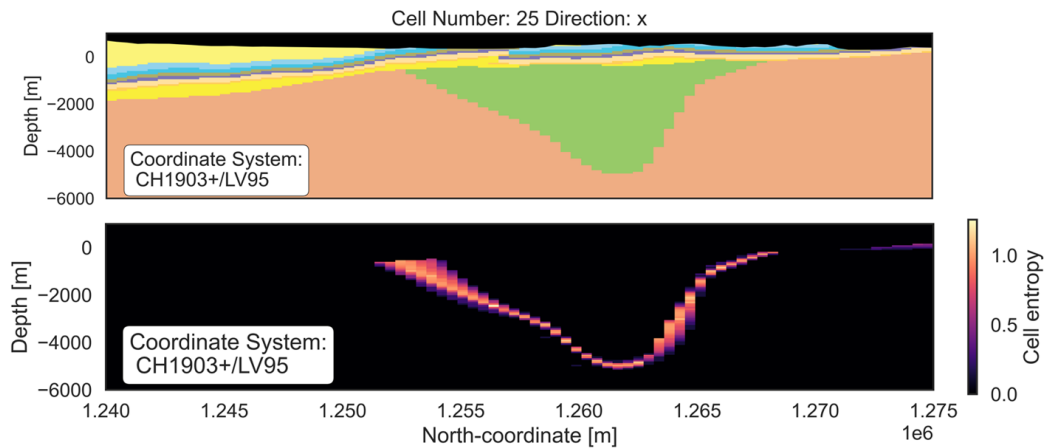
Figure 9: *Top: Cross section of a geological model of the Permocarboniferous Trough. Bottom: Information entropy of the model ensemble due to perturbation of normal fault location.*

contact to underlying crystalline basement is highest, as represented by the increased information entropy in the bottom Figure 9.

During a pilot survey in 2016, magnetotelluric (MT) data were measured at 14 sites in the area of the heat flow anomaly in Canton Aargau (see blue squares in Figure 8). The survey showed that the MT data are affected by severe electromagnetic noise that originates from power lines and the dense infrastructure in the region. The low signal-to-noise ratio required to develop advanced processing tools that allow in-depth statistical analyses in order to separate the natural signal from noise (resistics.io: in review Shah et al., 2020a).

Nevertheless, the collected MT data show that they contain valuable information about the subsurface structure such as depth to the crystalline basement, electromagnetic strike direction of permeable faults and sensitivity to the electrically conductive filling of the permo-carboniferous trough which is embedded in the more resistive crystalline basement (Shah et al., 2020b, in review).

The next MT survey will be conducted in Summer 2021 on additional locations (see black crosses in Figure 8) and is expected to benefit from improved measurement setups and newly developed data processing techniques.

2.5 Advanced Drilling Technologies

Drilling and completion activities account for more than 50 % of the overall project costs (Stefánsson, 1992; Tester et al., 2006) of any geothermal development project. Costs increase exponentially with well depth (Fitzgerland, 2013; Lukawski et al.,

2014), which is especially relevant when accessing deep (> 3 km) geothermal resources, typically found in hard crystalline rocks (such as granites).

This is mainly due to the fact that drilling using conventional state-of-the-art rotary drilling methods is a very inefficient process. Especially, drilling deep wells in hard rocks results in substantial technical difficulties, including extensive wearing of the drilling tools requiring frequent bit replacement and slow penetrations into the hard rock, thereby affecting the overall economics of geothermal projects (Fay, 1993; Diaz et al., 2018). Research and development is therefore needed, and innovative drilling methods – employing unconventional rock-breaking approaches – are being investigated (Teodoriu, 2011; Rudolf von Rohr et al., 2015; Jamali et al., 2017; Reinsch et al., 2018; Rossi et al., 2020a). Two novel drilling technologies have been studied: Combined Thermo-Mechanical Drilling (CTMD) and Plasma-Pulse Geo-Drilling (PPGD).

2.5.1 Combined Thermo-Mechanical Drilling (CTMD)

The basis of Combined Thermo-Mechanical Drilling (CTMD) technology, is thermal spallation drilling. This method is based on removing the rock not by means of mechanical action, rather by thermal loading (Rudolf von Rohr et al., 2015; Kant et al., 2018; Vogler et al., 2020a; Kant et al., 2017). It has been shown to be effective in hard rocks (Höser et al., 2018). Nevertheless, the required conditions to achieve rock spallation hinder its further use for deep wells, where different formations, including softer materials, are encountered.

As a further development of thermal spallation drilling and to ease the implementation of thermal-based drilling approaches under deep conditions, we investigated a novel hybrid technology called Combined Thermo-Mechanical Drilling (CTMD) (Rossi et al., 2020d; Rossi et al., 2020b; Rossi et al., 2020c). It integrates a thermal assistance, e.g., by flame jets, into a conventional rotary drill bit (see Figure 10). The CTMD technology is based on the fact that rock materials, when exposed to high temperatures and heating rates (by flame-jetting), experience extensive cracking (Rossi et al., 2018b). Thereby, this thermal cracks weaken the rock material and therefore facilitate the rock removal performed by conventional drilling cutters (Rossi et al., 2018a; Rossi et al., 2020e). This increases drilling performance, especially but not exclusively, in hard crystalline rocks.

Besides extensive laboratory investigations of the concept, we demonstrated the technology in a real-scale drilling rig (Rossi et al., 2020b; Rossi et al., 2020c). This field test provided evidence for enhanced drilling performance in granite rock, i.e. increased penetration rates and improved drill bit lifetime. This promising results have shown the readiness of the CTMD technology to improve the drilling performance under field conditions. Nonetheless, further research and technical developments are required to extend the application of this method under deep drilling conditions.
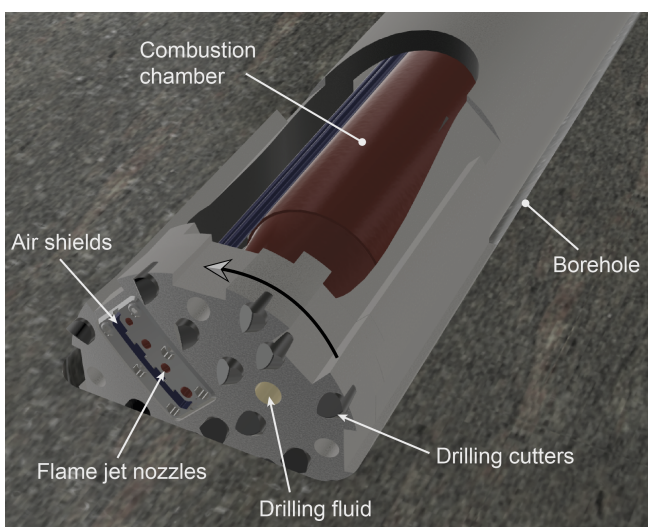
Figure 10: *Schematic view of the Combined Thermo-Mechanical Drilling (CTMD) technology applied to a 5.5-inch drill bit (Rossi et al., 2020a).*
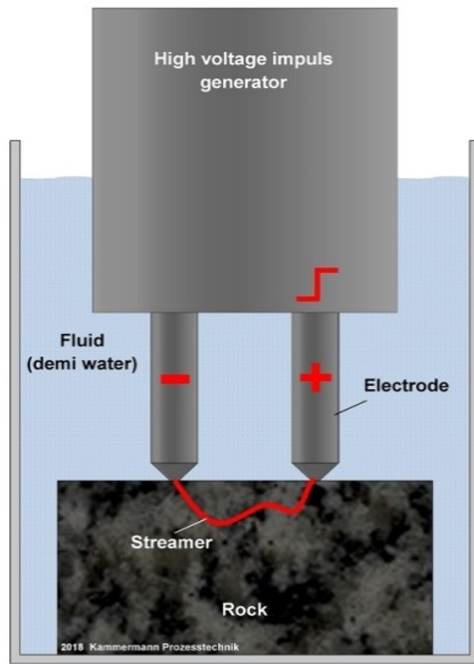
2.5.2 Plasma-Pulse Geo-Drilling (PPGD)

Plasma-Pulse Geo-Drilling (PPGD) is a contact-less drilling technology that uses high-voltage electric pulses to break the rock. These nano-second-long electric pulses generate a plasma channel (streamer) inside the rock which breaks the rock apart from within, i.e. against its low tensile strength without any mechanical abrasion of the drilling tools (see Figure 11, Ushakov et al., 2019; Vogler et al., 2020b; Walsh and Vogler, 2020; Ezzat et al., 2021). Since the tensile strength of the rock material is much lower than its compressive strength, the PPGD technology features better rock-breaking efficiency prospects than conventional rotary drilling methods. It could also be well-suited for drilling large borehole diameters (Schiegg et al., 2015), a peculiarity of geothermal wells and one of the factors affecting the high costs of drilling and completion procedures.

Laboratory and field demonstration of the technology have shown enhanced penetration rates in hard granite rocks. Additionally, the contact-less nature of this drilling technology implies a practically wear-free drilling process, thereby reducing or completely avoiding any replacement of worn drilling tools, thus positively impacting the overall drilling costs. Extensive research is being carried out to provide better understanding of the fundamental mechanisms underlying the PPGD concept (Vogler et al., 2020b; Walsh and Vogler, 2020; Ezzat et al., 2021). Further investigations comprise to study the effects of in-situ (high pressures and temperatures) conditions on the PPGD technology. This will provide insights on the potential use of the technology for deep drilling projects, and more specifically, in the frame of (deep) geothermal energy utilization.

2.6 Wellbore Trajectory Optimisation Workflow

An important performance factor for drilling is to ensure the stability of the borehole. When a borehole is unstable, more material needs to be carried back to the surface by the drilling fluids and rock fragments that are released to the borehole environment can cause operation difficulties like stuck pipes. Such difficulties generate costly delays. In addition, wellbore failure results in out of gauge boreholes with irregular borehole wall geometries. Such situation generates further difficulties for cementation and borehole completion.

Figure 11: *Plasma-Pulse Geo-Drilling (PPGD) principle (Rossi et al., 2020a).*

Borehole stability problems are well-known in the oil & gas industry and solutions exist for this case where many boreholes are drilled mostly in sedimentary rocks. Optimal drilling parameters for a field are estimated by trial and error on many wells. For the deep geothermal industry the conditions are very different: boreholes are drilled in crystalline rocks with a failure mode that often differs to the sedimentary conditions encountered in oil & gas.

In addition, only few boreholes are drilled and they must be stable to enable the high rate production completions required for geothermal projects. The knowledge development by trial and error over many boreholes is not an option.

In a collaborative project between industry and academia (DG-WOW, 2019), a wellbore stability estimation workflow adequate for deep geothermal boreholes was developed. At the heart of the workflow, a systematic parameter estimation approach allows to calibrate both the stresses and the strength simultaneously. The approach is not delivering a unique solution but the range of possible parameters based on the observations. It calibrates both the (first order) overall trends of strength and stresses and the (second order) variability about theses trends. The output of these models give us a unique insight in the stress conditions and variability in the earth crust. They allow also to make stochastic predictions for subsequent wellbore sections and to optimise wellbore trajectory and drilling parameters to keep wellbore failure under an acceptable limit.

The workflow has been implement in a software tool that guides the user through the different steps. The main steps included in this workflow are presented in Figure 12.
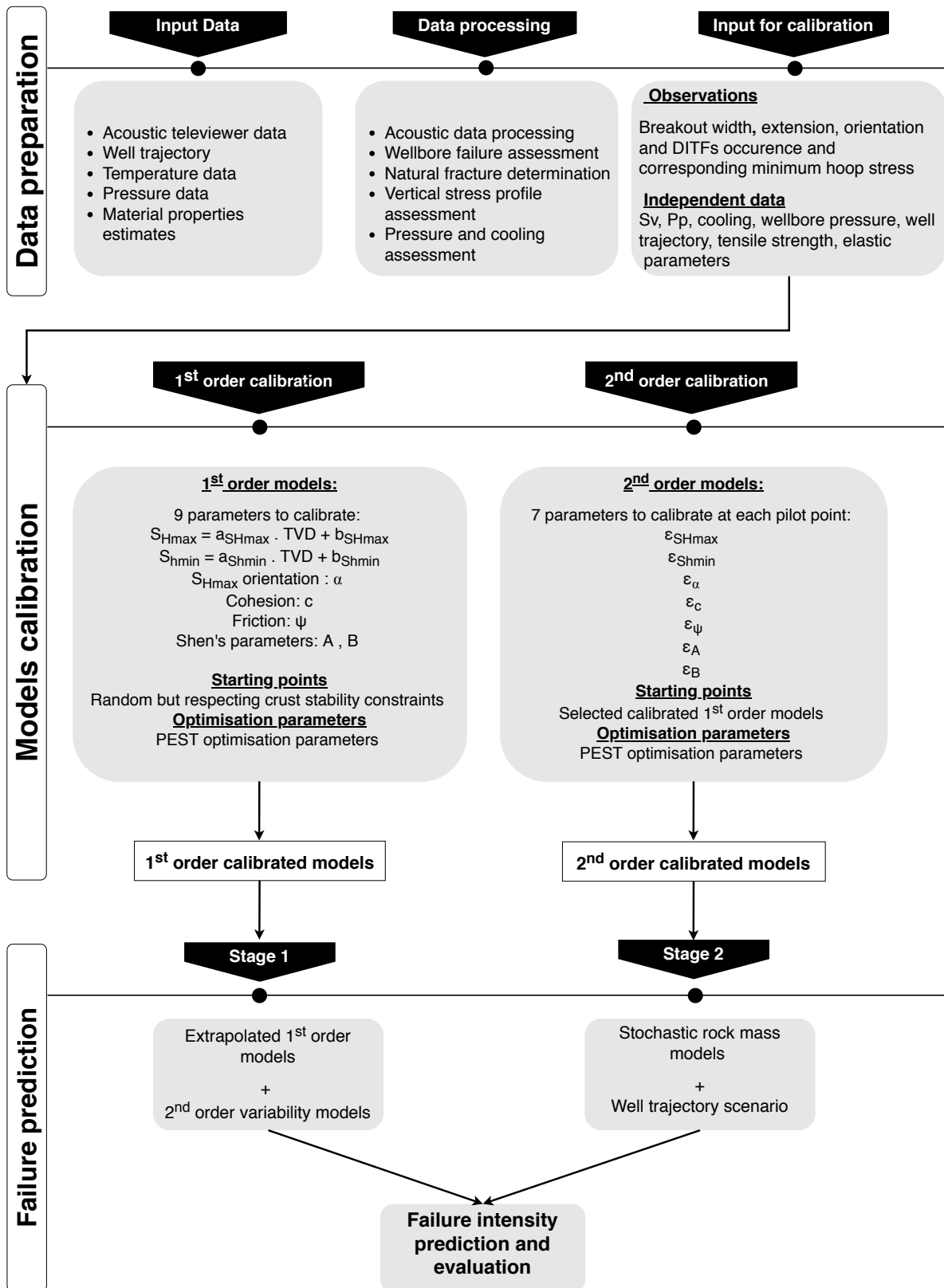
Figure 12: *Steps of the Deep Geothermal Well Optimisation Workflow (DGWOW) application (Dahrabou, 2021).*

3 Deep Geothermal Reservoirs

A geothermal reservoir is a rock mass at depth that can be accessed from the surface, usually via a number of boreholes. In order to extract heat it is important that a fluid can circulate. Various aspects of geothermal reservoirs have been studied in SCCER-SoE; characterization aims at understanding the network of fractures at various scales that allow for fluid circulation; simulation shall allow to predict the fluid flow and heat extraction in the reservoir; finally, reservoir stimulation targets at the generation of permeability while at the same time controlling the negative effects of induced seismicity.

3.1 Reservoir Characterisation

3.1.1 Joint characterisation of fracture network, stresses and microseismicity

An interplay exists between the fracture network, the in-situ stresses and the seismicity. These elements share the commonality of following scale-invariant laws. It is believed that these laws stem from the processes at play in self-organised critical systems, although the details of these processes and relationships remain unknown.

Better understanding these relationships is however critical for understanding system response to perturbations like fluid pressure change during stimulation. This problem is approached by studying scaling relationships of fractures and stresses as they can be observed at the borehole well.

Moein et al. (2019) investigated the scaling characteristics of fracture patterns in deep geothermal boreholes. It was shown that fracture patterns present fractal characteristics over more than two orders of magnitude in scale and in all cases the fractal dimensions lay in the range 0.86–0.88. These characteristics can be used for better constraining fracture network models. Valley and Evans (2014) studied also the scaling relationships that are present in stress related data. Different methods to estimate fractal dimension from stress-induced wellbore failure data were compared.

By using a similar approach to characterise microseismic data, Moein et al. (2018b) developed a methodology to forecast maximum magnitude during hydraulic stimulation. This methodology was applied to the Basel stimulation dataset.

Another by-product of these analyses is a methodology for fracture network characterisation using stress based tomography (Moein et al., 2018a). The approach uses a Bayesian inversion technique to produce fracture models that honor both the fracture intersection observation with a borehole and the stress perturbation induced by such fractures. An example of such reconstruction is presented in Figure 13.

3.1.2 New Stress Measurement Techniques based on Injection-induced Dislocation Measurements

While stresses are recognized as the most important parameter controlling reservoir response during hydraulic stimulation, their measurement in deep reservoirs remains challenging. There is no technique that can provide all stress component from a single measurements. However, new tools have been developed, partly based on fiber optic sensors. One example is the SIMFIP probe that allows to measure the resulting dislocations during the injection in fault zones (Guglielmi et al., 2015). The data generated by this new tool is used to propose a stress inversion technique that provides the complete stress tensor from a single set of measurements.

The general principle of the methodology is based on the well-known stress inversion approach used in structural geology for estimating paleo-stresses from fault orientation and slip direction. This approach was enriched by including the pressure and flow rate data measurement captured during the test to propose full-stress tensor solution
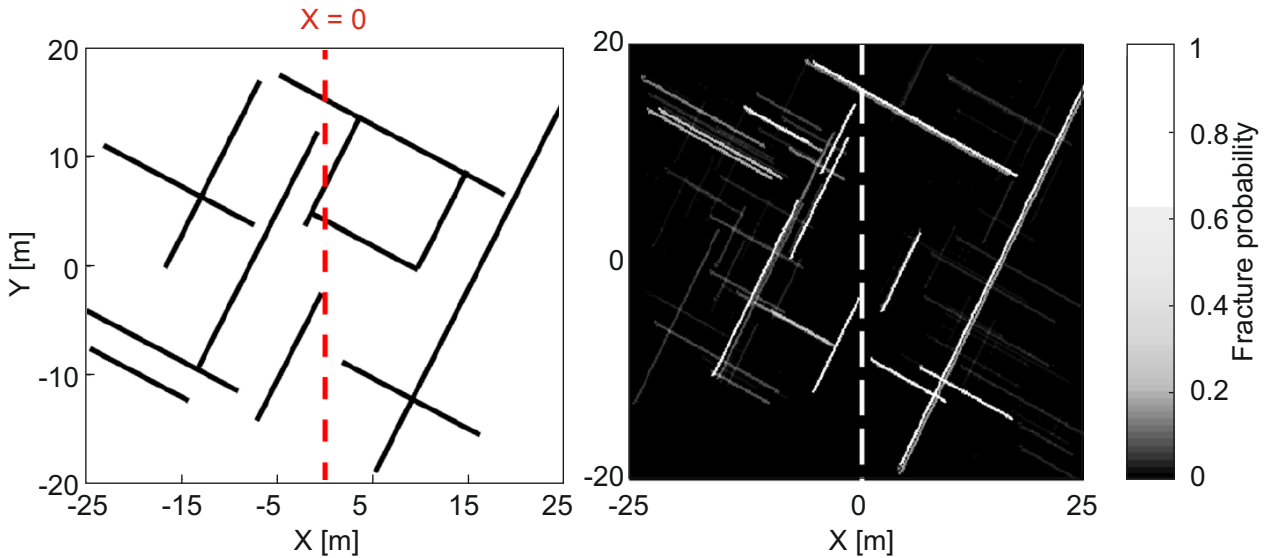
Figure 13: *Results of fracture tomography analyses: (left) synthetic fracture network used as a training case. The red dashed line represent a borehole across this fracture network along which data are collected. (right) Bayesian reconstruction of the fracture network based on observation of fracture and stresses at the borehole only (dashed lined). Modified after Moein et al. (2018a).*

that honor all the available observation. Theoretical developments were required to verify the validity under non-uniform pore pressure conditions of the Wallace-Bott hypothesis that underpin the stress inversion approach (Kakurina et al., 2019). Also the necessary data processing and reduction steps were developed, that are required to extract the information from a SIMFIP test needed for stress inversion (Kakurina et al., 2020).

3.2 Reservoir Simulation

3.2.1 Coupled Processes in Fractures

To accurately predict and describe the performance of enhanced geothermal systems (EGS), a number of coupled physical processes have to be understood. Notably, during initial injection, high-fluid pressures can cause seismic activity due to fault slip. Additionally, EGS relies on sufficiently high permeabilities of the rock mass under investigation. If the initial permeability is insufficient, permeability can be further increased by inducing slip in critically stressed faults or fractures. Given the highly complex fracture topologies, investigation of the hydro-mechanical stresses in the fractures is notoriously difficult.

Recent research addressed these problems by focusing on fluid flow processes in the subsurface through complex geometries. All work is based on the use of transfer operators such as L²-projections, which enable information transfer between independent meshes in 3D.

Planta et al. (2020b) investigated the hydro-mechanical coupling in rough fractures, starting with the purely mechanical interaction of two fracture sides that are in contact, where the contact area and stress distribution changes as more normal load is applied to the system (Figure 14). This is representative of the processes occurring at depth, when changes in fluid pressure can cause fracture opening and thereby a change in contact area. Changing contact areas then also lead to a re-distribution of the flow field, which results in a change of permeability (Planta et al., 2018; Planta et al., 2019) (Figure 15).

To achieve a more realistic fracture configuration, as may be encountered in a reservoir setting as well, the numerical method was further extended to multiple fracture geometries such as fracture intersections (Planta et al., 2020a). Finally, first efforts were performed to further account for thermo-hydro-mechanical effects in fractures as well (Hassanjanikhoshkroud et al., 2020).

Besides hydro-mechanically coupled processes, further focus was put on flow phenomena in the subsurface in general. Here, fluid flow can occur either through fractures or the rock matrix. These processes can compete, with flow generally occurring through both media. Especially when larger reservoirs are considered, computing flow phenomena and the corresponding mesh generation through
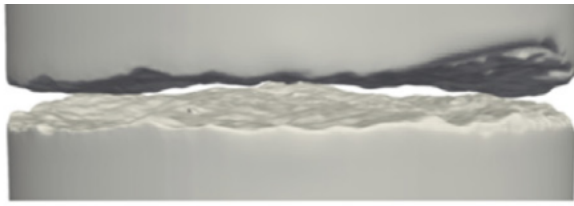
Figure 14: *Mechanical contact between two rough fracture surfaces, which results to a change in contact area when the applied load changes (Planta et al., 2020b).*
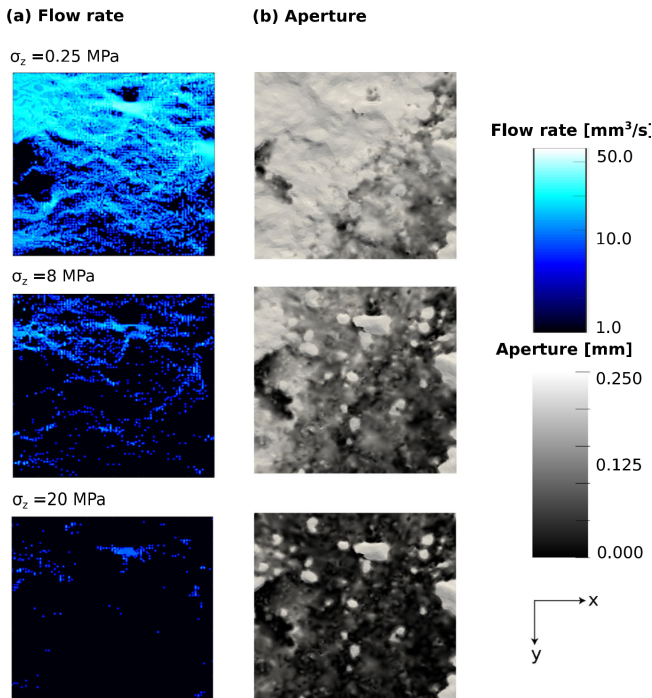
Figure 15: *Changing aperture and fluid flow field distribution with changes in normal load (Planta et al., 2018; Planta et al., 2019; Planta et al., 2020a).*

a fracture network, can become very computationally demanding. Coupling flow processes in fractures and porous media was also achieved with Lagrange multipliers, thus significantly easing fluid flow computations in fractured reservoirs (Schädle et al., 2019; Zulian et al., 2020).

3.2.2 Natural Convection in and Heat Production from Fracture Networks in Deep Reservoir Rocks

Surprisingly little is known about the natural convection of hot fluids in fractures in the earth's crust, namely about the amounts and styles of heat transport that directly influence the geothermal potential

of a certain site. Patterson et al. (2018b) and Patterson et al. (2018a) systematically explored convection in a single, kilometer-scale fracture zone and in arrays of several such fracture zones.

One key result of the studies was that convection leads to patterns in and near the fracture of temperatures higher and lower than the regional geothermal gradient. Depending on the fracture's transmissivity, these excess temperatures can reach up to 15 °C (Figure 16). Drilling into parts with higher-than-average temperature may significantly enhance the economic feasibility of a geothermal project by providing higher efficiency at the target depth or the targeted temperature at shallower depth. Drilling into a cooler part may have a significant negative impact. Future research will have to explore such pattern formation in site-specific fracture geometries.

An interesting result for future up-scaling of EGS-type geothermal projects is that the patterns of excess temperature can "sync" between parallel, hydraulically unconnected fracture zones if these have a close enough spacing of a few hundred meters or less. Then, the thermal anomalies that convection induces in the host rock will start to interact and eventually co-align convection cells in all fractures (Figure 17). Constraining these patterns in a given project could lead to optimal well siting strategies when up-scaling targets neighboring fracture zones.

All these findings are related to fracture zones that convect naturally. The two studies also found that fracture networks in deep crystalline basement can cause shallow heat flow anomalies if they are buried under sedimentary cover. This has important implications for prospecting and exploration: naturally convecting fracture zones may need softer stimulation approaches (or none as exemplified by the German Insheim example), thereby possibly providing an attractive exploration target. It could be shown that the amplitude of the significant shallow heat flow enhancement is directly tied to the convective heat transport in the underlying, buried fracture network and may therefore allow to estimate its thermo-hydraulic properties.

Additional research addressed the question how thermo-elastic coupling affect production from the typically (sub-)vertically aligned fractures in the upper crust. Injecting cold water will lead to contraction of the rock, thereby potentially opening fracture aperture while the flow of warmer water will tend to close aperture and, therefore, reduce permeability. However, such a picture turned out to be
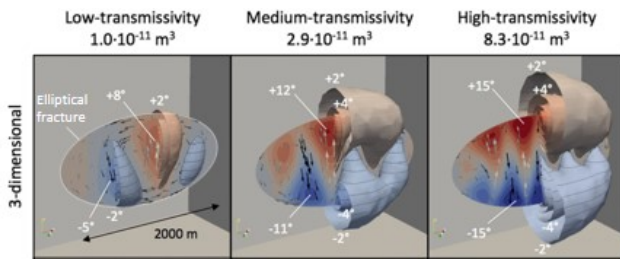
Figure 16: *Thermal anomalies (relative to the local geothermal gradient) develop in a naturally convecting fracture (elliptical shape) and its surrounding host rock (Patterson et al., 2018b).*
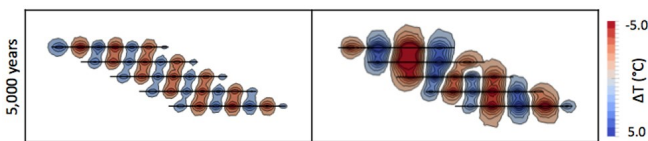
Figure 17: *Alignment of thermal anomalies across an array of five parallel fractures (black lines) that are hydraulically not connected and spaced 250 m apart, view from top, 5000 years after onset of convection. Left: homogeneous fracture permeability; right: fractures with significant in-plane variation of fracture permeability (Patterson et al., 2018b).*

too simplistic as opening or contraction induces stresses and strains that need to be balanced in the surrounding, leading to a "stress ring" around the injection point that may affect aperture further away. Also, if production occurs from a large vertical fracture that sits in a geothermal temperature gradient, then these effects may have significant impact on whether production from the upper or the lower part of the fracture is better suited for sustainable operation (Patterson and Driesner, 2020).

3.3 Reservoir Engineering and Permeability Creation

Developing and engineering geothermal reservoirs at depth has proven to be notoriously difficult in the past with failed deep geothermal projects outnumbering the successful ones. One problem lies in the challenge to establish fluid pathways between injection and production boreholes with optimal heat exchanger characteristics, while keeping induced seismicity below a harmful level. The outcomes of hydraulic stimulation operations – the key method to enhance the hydraulic conductivity and connectivity of the reservoir rock – has often been unpredictable.

Thus, exploitation of deep geothermal energy relies on a more fundamental understanding of the stimulation processes and the improved ability to control them.

Our current understanding of the seismic, thermo-hydromechanical and chemical processes during stimulations rely mostly on either decimeter-scale laboratory experiments or full-scale reservoir development projects. At the reservoir scale, indirect and sparse observations are usually recorded kilometers from where processes take place, and control of the stimulation processes is limited. Limited controlability and accessibility are eliminated at the laboratory scale, but scalability to the full-scale becomes an issue (Figure 18).

Recently, worldwide initiatives attempt to overcome these research obstacles by bridging these scales with underground in situ experiments, where process understanding and technological developments are advanced at the 10 to 100 m scales (Figure 18, Gischig et al., 2020). As part of the SCCER-SoE, such experiments were conducted at the Grimsel Test Site (GTS) between 2015 and 2017 and more recently in the newly established underground laboratory in the Bedretto tunnel.

3.3.1 Experiments at Grimsel Test Site (GTS)

The Grimsel experiment series performed at 450 m depth in crystalline rock included an extensive characterization of the target rock volume, twelve hydraulic stimulation experiments, as well as a post-characterization program (Amann et al., 2018). Characterization aimed at establishing a detailed 3D model of geological structures and rock properties, the stress field, and the hydraulic properties. Such a model provides indispensable information for both planning the stimulation experiment and analyzing the stimulation observations. Combining several methods for each characterization aspect was key to alleviate ambiguities and to improve validity of the results.

The geological model was based on tunnel mapping, systematic borehole logging as well as ground penetrating radar and 3D anisotropic seismic tomography (Krietsch et al., 2019; Doetsch et al., 2020). Stress characterization included both stress relief methods, hydraulic methods, microseismic monitoring and numerical modeling (Krietsch et al., 2020a; Gischig et al., 2018). Hydraulic characterization involved single- and cross-hole tests (Brixel et al., 2020a; Brixel et al., 2020b), and a range of
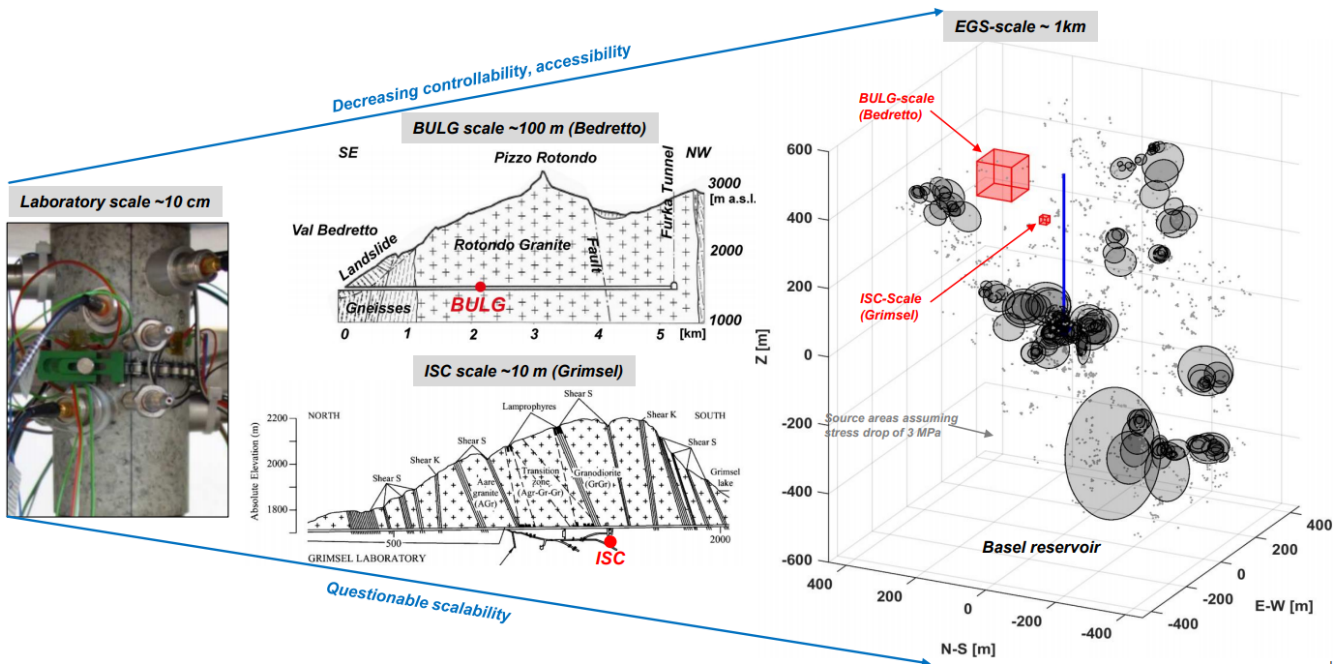
Figure 18: *Research on stimulation processes acts on different scales and at different depths.*

tracer tests (Kittilä et al., 2019; Kittilä et al., 2020a; Klepikova et al., 2020). At the same time, the characterization phase was a unique chance to explore innovative methods that go well beyond state-of-the-art: e.g. the utilization of DNA tracers (Kittilä et al., 2019); 3D anisotropic seismic tomography (Doetsch et al., 2020); time-lapse radar measurements during salt tracer tests (Giertzuch et al., 2020); using numerical models of anisotropic elasticity for the analysis of the overcoring tests for stress characterization (Krietsch et al., 2019); etc. The hydraulic stimulation experiment targeted six borehole intervals with pre-existing fracture to induce hydroshearing (HS), and six intact (i.e. fracture-free) intervals to initiate hydrofractures (HF). For the six HS and the six HF experiments each, a standardized injection protocol was utilized, so that the variability in the observations must primarily originate from local conditions and not from the injection strategy. The stimulations were monitored with extensive high-resolution and multi-parametric sensor network that included both passive and active seismic monitoring, a deformation monitoring system, various pressure monitoring intervals as well as distributed temperature sensing systems.

3.3.2   Insight from Grimsel Experiments

A rich dataset could be acquired during the Grimsel tests that sheds light on various aspects

of hydraulic stimulations with an unprecedented level detail. From the analysis, a range of important insights have crystalized so far, while further analysis is still in progress. Some key results, interpretations and conclusions are summarized in the following (see also http://www.sccer-soe.ch/en/publications/grimsel-isc-project/):

Creation of new flow paths: Transmissivity enhancement of up to three orders of magnitude and creation of new connections between boreholes – in general the primary goals of hydraulic stimulations – were successfully achieved during the stimulation experiments, as hydraulic characterization before and after experiments revealed (Krietsch et al., 2020b). Tracer tests after stimulation showed that the tracers accessed flow paths with larger hydraulic conductivities and thus swept larger volumes (Kittilä et al., 2020b). Interestingly, the stimulations did not enhance transmissivity throughout the reservoir; instead the target fractures showed a transmissivity decrease some distance from the injection. In an experiment involving circulation of hot water (i.e. 45 °C warm water in 13 °C rock) longer tracer recovery times indicate that flow might be impeded through thermoelastic effects leading to flow being diverted to the far-field (Kittilä et al., 2020b). A detailed analysis of one stimulation experiment (Krietsch et al., 2020a) showed how flow paths also changed

during stimulation: propagation of the seismicity cloud as well as complex pressure and deformation transients revealed that different flow channels had been activated during two subsequent stimulation cycles.

Limiting injectivity and transmissivity: Stimulations led to a very variable transmissivity and injectivity increase between experiments with enhancement factors ranging from < 10 only to more than 1000 (Figure 19, Brixel (2021)). It is noteworthy, that the injectivity after the HS stimulation reached similar values grouping around 1 l/min/MPa (range 0.4–1.7 l/min/MPa). Thus, the strong variability is owed to variable initial injectivities (0.0006–0.95 l/min/MPa) and not to a variable final injectivity. Initial transmissivities of the HS intervals range from 8.3×10^{-11} to 1.2×10^{-7} m^2/s (>3 orders of magnitude), while the final transmissivities lie between a narrow range of 5.5×10^{-8} to 2.3×10^{-7} m^2/s (0.6 orders of magnitude). Similar observations are made for the HF experiments.

The observation by Brixel (2021) raises the questions if the achievable injectivity/transmissivity is a characteristic of the reservoir rock mass, possibly mediated by the ambient stress field or geological properties. The existence of such a limiting transmissivity would have important implications for full-scale reservoir stimulations. While transmissivity (and thus productivity) of a single stimulated volume is limited, more productivity could be attained by stimulating multiple adjacent intervals, e.g. through zonal isolation stimulations.

Channelized heterogeneous flow: Only for few experiments (4 out of 6 HS experiments) and only at few monitoring locations, high-pressure signals away from the injection point (i.e. "pressure fronts") were observed, even though many non-linear pressure diffusion models of stimulations proposed in literature predict them (Krietsch et al., 2020a). We interpret the absence of such pressure signals as channelized flow within the fractures or fracture intersections.

Analysis of hydraulic tests prior to the stimulations (Brixel et al., 2020a; Brixel et al., 2020b) support a conceptual model of strongly heterogeneous and possibly channelized flow field that is characterized by a fractional flow model with a flow dimension of 1.3–1.5 (i.e. between linear flow and radial flow symmetry). Further, the flow field is dominated by either fractures of the damage zone around the core of shear zones, where permeability and fracture density scale with a simple power law, or by single fractures that link subparallel shear zones, for which simple permeability/fracture density-relationships break down.

Stress heterogeneity: Similar as observed in deep reservoirs (Valley and Evans, 2009), the stress field orientation was found to rotate and the stress magnitudes to decrease towards the main shear zones in the target rock volume (Krietsch et al., 2019). Both the HF and HS experiments imply that the shear zones may separate different stress compartments (Dutler et al., 2019; Krietsch et al., 2020b; Dutler et al., 2020) leading to a differences in the stimulation characteristics. Meter-scale stress heterogeneity possibly leads to dramatic changes of the source mechanism along adjacent fractures as was observed from seismicity distributions and moment tensors of one HS experiment (Villiger et al., 2020b).

Transient stress redistribution during stimulation, evident from the complex deformation patterns, is superimposed on the heterogeneous static stress field and gives rise to diverse fracture interactions and dislocation modes that include opening and shearing as well formation of new fracture off preexisting stimulated fractures. Often several adjacent fractures are observed to open simultaneously until one fracture opens faster and thus suppresses further opening or even closes neighboring fractures.

Mixed-mode stimulation: Various observations indicate that mode I (fracture opening) and mode II/III (slip) occur concurrently both during HS and HF stimulations as predicted by (McClure and Horne, 2014). Formation of a new fracture was observed during a HS dominated experiment from seismicity that propagated away from the main seismicity cloud and from a strain sensor that opened by almost 400 µm (Villiger et al., 2020b). Similarly, various HF experiments show that hydrofractures start out as clear mode I fractures, but quickly connect to the preexisting fracture network, where mode II/III dislocations become evident (Dutler et al., 2019; Dutler et al., 2020). During HF, often not a single but several fracture strands propagate simultaneously. Similarly, during HS several fractures are pressurized and open together, but start competing with each other through stress interaction.
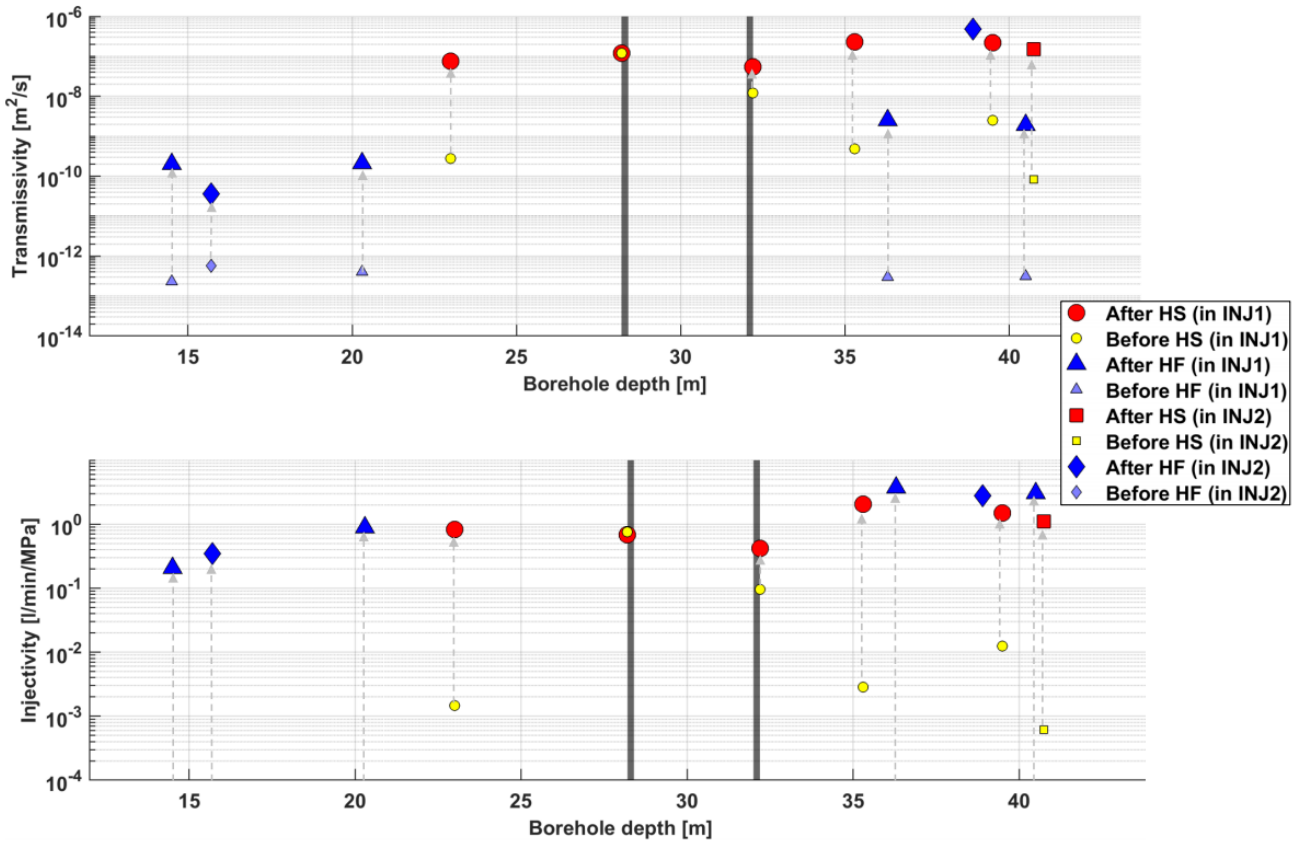
Figure 19: *Changes in transmissivity and injectivity during HS and HF experiments (Brixel, 2021).*

Noble gas release accompany fracturing: During the HF experiments an innovative insitu gas equilibrium membrane inlet mass spectrometer was able to monitor transient anomalies in the helium and argon concentrations (Roques et al., 2020). The anomalies are interpreted as originating from Helium and Argon-enriched fluids that were trapped in the pores of the rock mass and released by through fracturing processes. These intriguing and unique results demonstrate that geochemical monitoring complementing thermo- and hydromechanical observations may be of great value to understand stimulation processes.

Primary and secondary deformation field: Deformation and pressure observations from various distances around the stimulated rock volume suggest two deformation fields (Krietsch et al., 2020b; Dutler et al., 2020). In the near-field of the stimulation (i.e. < 15 m from injection), a so-called "primary field" exhibits the full complexity of the stimulation processes with transient and spatially variable extensional and compressive strain produced by fracture normal opening and

slip dislocation and the stress redistribution related to these processes. These processes are primarily governed pressure diffusion. In the far-field (> 15 m), a "secondary field" is observed, which shows both more systematic compressive and extensional deformations that exceed deformation magnitudes that are expected from pressure diffusion. Here, far-field poro-elastic volumetric deformations govern.

Size of the stimulated volume: The aforementioned observation of a diffusion-controlled near-field and a poro-elasticity-controlled far-field raise the question of how the stimulated volume is to be defined. The question becomes even more compelling, because it was observed that the seismicity cloud in our case was much smaller than the pressurized volume estimated from 4D seismic tomography (Schopper et al., 2020; Doetsch et al., 2020).

Based on clear correlations between seismic velocity and pressure found at the pressure monitoring locations, it was possible to delineate the volume that is likely affected by elevated pressure or – in the far-field – is compressed

through volumetric expansion in the near-field. The seismicity clouds have been much smaller that the implied pressurized volumes. Furthermore, observations of transmissivity decreases some distance away from the stimulated intervals additionally question if the pressurized volume or the seismically active volume encompass a rock mass volume with enhanced transmissivity.

Aseismic versus seismic deformation: A potentially larger stimulated volume as illuminated by the seismicity cloud may indicate that a large portion of the deformation – also the permanent one remaining after the stimulation – has occurred aseismically. In fact, a comparison of the total seismic moment per experiment with the total moment inferred from fracture dislocation magnitudes observed at the boreholes wall from acoustic televiewer images support the interpretation that seismic deformation accounts for only a small fraction of the total deformation (Villiger et al., 2020). Furthermore, fracture dislocation observed at various deformation sensors was found to be sometimes accompanied by seismicity and sometimes not (Krietsch et al., 2020b).

Variable stimulation outcomes in a small rock volume: Generally, stimulation outcomes were found to be surprisingly variable within the relatively small experimental volume and defined by very local rock mass conditions like fracture orientation and architecture, hydraulic conductivity and connectivity or stress conditions. Apart from the aforementioned variable transmissivity changes per experiment, the seismic productivity, spatial distribution and magnitude distribution (expressed as a- and b-values) has been very diverse (Figure 20): for instance, while for one experiment only about 100 seismic events were detected, more than >5000 events were located for another one (Villiger et al., 2020).

Predictability of induced seismicity: The variability of seismicity characteristics between experiments is so large that predicting seismicity (or seismic hazard) for one experiment based on the information from another seems futile. This raises the question to what degree a priori forecasts of seismicity are possible at a certain experimental scale but also across scales. The meter-scale complexity found for the most seismically active experiments further challenges the predictability towards larger
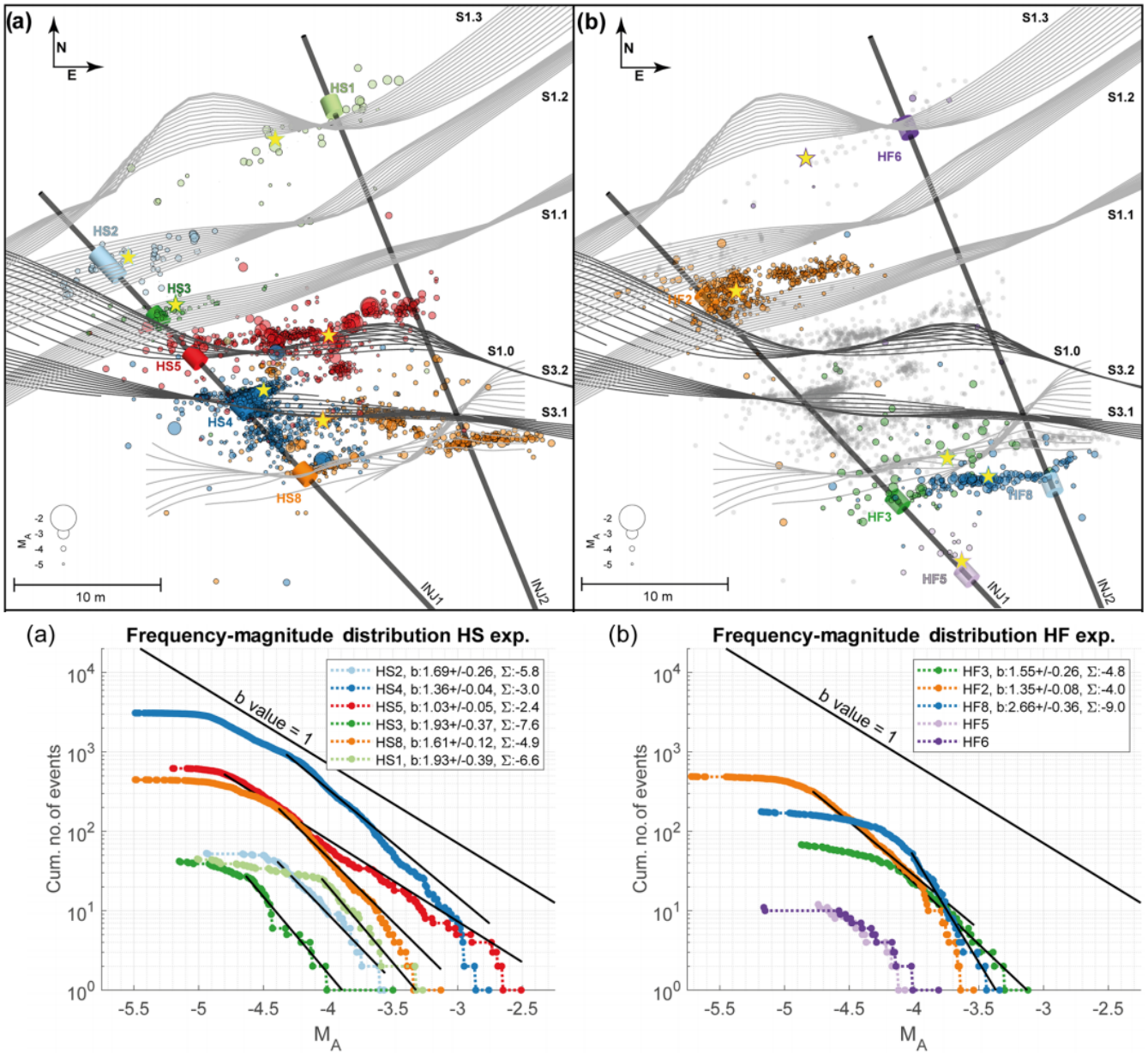
scales (Villiger et al., 2020b).

Moreover, this experiment exhibits an extraordinary tendency for repeating earthquakes that even lead to a partial breakdown of the anticipated Gutenberg-Richter distribution (Villiger et al., 2021; Experiment HS4 in Figure 20), which is the basis for seismic hazard forecasting. Here, further experimental work on different scales must tackle the question on scale-invariance of seismicity from the meter to the kilometer-scale.

A hypothetical open-hole stimulation: As most past reservoir development projects performed large open-hole stimulations, it is worth considering the following thought experiment (Villiger et al., 2020): What would have happened if instead of several 1–2 m long intervals, an extended borehole section including covering all intervals would have been stimulated at once? Most likely, the flow would have entered the most transmissive fractures. However, these correspond to the fractures of those intervals, for which the transmissivity and injectivity changed only marginally, and, at the same time, which were by far the most seismically active ones.

Thus, an open-hole stimulation may have produced little gain in transmissivity/injectivity but a lot of seismicity. Stimulation using zonal isolation (i.e. of several selected intervals as done in our experiment series) may be a more advantageous strategy in terms of transmissivity gain and seismic hazard, if already transmissive and seismically active structures can be avoided. However, our experiments also indicate that hydraulic communication between adjacent stimulation zones is conceivable making it difficult to fully avoid hydraulically and seismically active fracture systems.

3.3.3 Relation between Hydraulic and Mechanical Fracture Behavior

The geophysical characterization of the hydraulic stimulations performed at GTS did not only allow for monitoring the underlying processes but also for identifying new parameters and signatures providing further insight to its interpretation. A particularly valuable target parameter in this regard is the so-called fracture compliance Z_N, which characterizes the mechanical "softness" of a fracture with regard to compressive or tensile stresses acting perpendicular to its walls. Fracture compliance can be in-

Figure 20: *Seismicity clouds of all stimulation experiments in map view. A) HS experiments, b) HF experiments (Villiger et al., 2020). c) and d) Magnitude distributions of all experiments.*
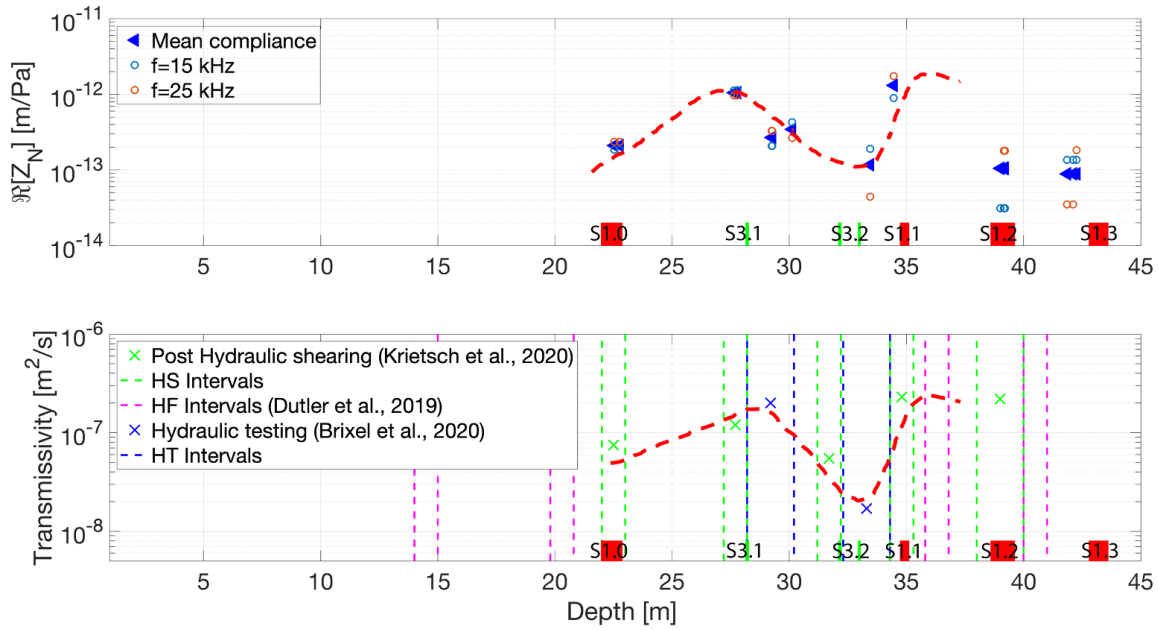
Figure 21: *a) Normal compliance of fractures intersecting borehole INJ1 (blue triangles) obtained from FWS log data. Red and green filled circles denote S1 and S3 shear zone depths, respectively (Figure 3). b) Green and blue crosses denote transmissivity values obtained by (Krietsch et al., 2020a; Brixel et al., 2020a), respectively. Blue, magenta, and green dashed lines denote borehole intervals for the experiments of Brixel et al., 2020a; Dutler et al., 2019; Krietsch et al., 2020a, respectively.*

ferred from the amplitude behavior of tube waves in vertical seismic profiling (VSP) experiments (Hunziker et al., 2020) and from the time delays and amplitude decays experienced by the critically refracted P-waves in full-waveform sonic (FWS) logs (Barbosa et al., 2019).

Figure 21 shows an example of new development of the latter technique (Barbosa et al., 2021), which allowed for the quasi-continuous estimations of fracture compliance along injection borehole INJ1 at GTS. Based on the results of various hydraulic characterization experiments performed on isolated fractures intersecting this borehole (Krietsch et al., 2020b; Dutler et al., 2019; Brixel et al., 2020a), the correlation between the mechanical and hydraulic behavior of fractures can be directly compared and analyzed (Figure 21). In spite of the fact that the transmissivities lie in a narrow range of less than one order-of-magnitude, the compliance profile was found to delineate the most permeable fractures along the borehole. Given the relative ease of measuring fracture compliance as compared to hydraulic transmissivity, this opens the perspective of enhancing the design and the effectiveness of subsequent hydraulic testing and stimulation experiments.

3.3.4 Scaling up - the Bedretto Experiment

The experiments at the Grimsel Test Site were a large step from lab scale to the kilometer scale that will be encountered in commercial EGS projects. A series of stimulations were conducted and monitored by a comprehensive sensor network in boreholes and the surrounding tunnels. This has resulted in a significantly improved understanding of stimulation induced processes.

Nevertheless, it was clear that an intermediate step at 100 meter scale would be needed. After the Bedretto tunnel had been identified as a suitable test-bed for a larger scale reservoir experiment, the necessary infrastructure was built, including high-power electric supply, ventilation, internet and safety installations. After several months of preparation/procurement and building, the lab was put in operation in Mai 2019 (Bedretto Lab, 2021).

The original plan was to execute a single SFOE-funded Pilot and Demonstration project (VLTRE, 2021), however, it soon became clear that there was a large interest in the Bedretto facility, therefore three projects were combined to the so-called Bedretto Reservoir Project, all with strong engagement of Geoenergy Suisse as industrial implementation partner (DESTRESS, 2021; ZoDrEx, 2021).

A vast multicomponent monitoring system had to be developed for the monitoring of the stimulation experiments (see Figure 23). The challenge being that most of the available sensors on the market were not capable to measure the required parameters in the local conditions and at the sensitivity required for the analysis of stimulation experiments. Thus, extensive development of sensors has taken place through over 20 different companies. Figure 22 shows the spatial arrangement of two stimulation and four monitoring boreholes that were drilled within the Bedretto reservoir project.

At the end of 2020, researchers of ETH together with the industrial partner Geo-Energy Suisse succeeded in establishing circulation by hydraulically stimulating 10 isolated borehole sections in consecutive stages (Geo-Energy Suisse, 2021).

A maximum of 100 m^3 of water were injected per interval, the permeability of the stimulated intervals could be increased on average by a factor of 10 to 100. The microseismicity induced by the stimulations, with magnitudes ranging between -3.3 and -1.8 Mw, was about 1 million times smaller than the earthquake that led to the abandonment of the Basel geothermal project in 2006.

The well characterized rock volume, the high-resolution monitoring system and the engineered reservoir is an outstanding test-bed for further geothermal and geoscientific research. This work will continue for the next years and address the fundamental issues related to the extraction of geothermal energy from crystalline rocks.
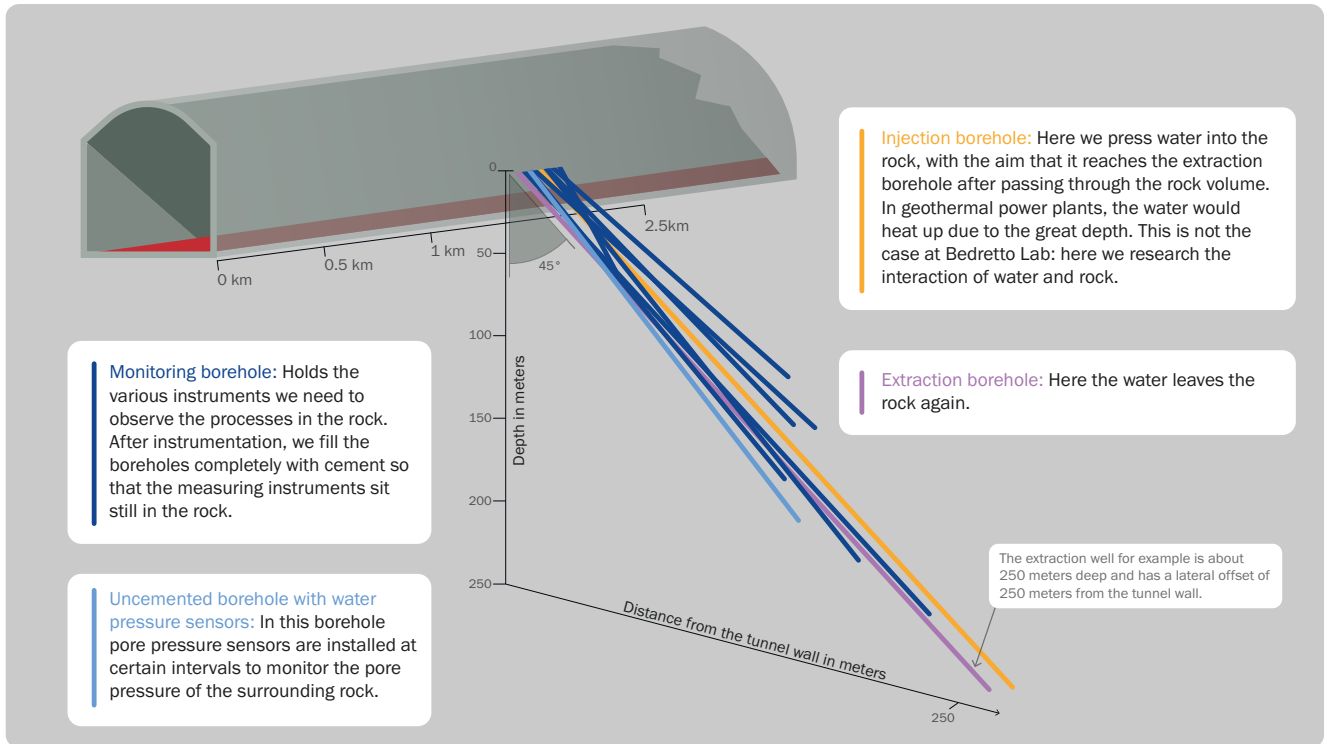
Figure 22: *Monitoring and stimulation boreholes for the Bedretto reservoir experiment (Swiss Seismological Service at ETH Zurich).*
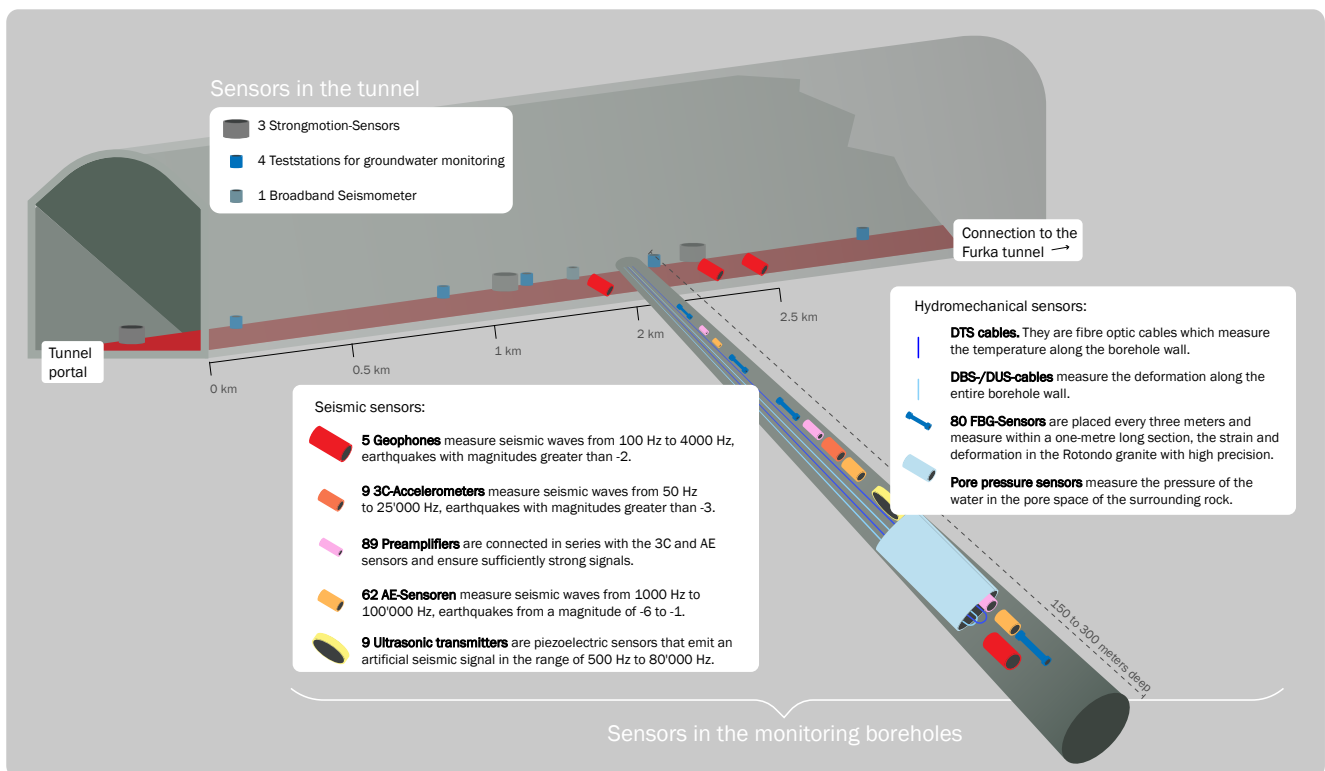

Figure 23: *Monitoring infrastructure in the boreholes (Swiss Seismological Service at ETH Zurich).*

4 Usage of the Subsurface for CO₂ Storage

The Swiss climate goal of net-zero greenhouse gas emissions by 2050 requires options to avoid emissions from large industrial installations such as cement or waste incineration plants and to generate negative emissions to compensate unavoidable emissions, e.g. from agriculture. While an array of biological and technical options exists to permanently lock away CO₂ from the biosphere, the geological storage of CO₂ seems to be the most promising route.

The Federal Council decided on 28 Aug 2019 to strive for net-zero greenhouse gas emissions in Switzerland by 2050. This objective forms the basis for the recently revised Swiss Energyperspectives 2050+ (Prognos, 2020). Cornerstones will be the decarbonization of the demand sectors buildings, industry and mobility with efficiency measures, electro-mobility, heat pumps, etc.

Recent scenarios published by SFOE (Prognos, 2020) and the Joint Activity Scenarios and Modelling (JASM, www.sccer-jasm.ch) agree that CO₂ Capture and Storage (CCS) is needed as an additional means to reach the net-zero emission target (Panos et al., 2021; Panos and Kober, 2020; Guidati et al., 2021; Marcucci et al., 2021). This concerns emissions from cement and municipal waste incineration plants (see Figure 24) but also technologies to generate negative emissions, for instance Bio Energy with CCS (BECCS) and Direct Air Capture with CCS (DACCS). The key requirement for all these approaches is the possibility of geological CO₂ storage at a sufficient scale of 10–20 Mt$_{CO_2}$/a. Some of the challenges to realize this in Switzerland were addressed within the SCCER-SoE.
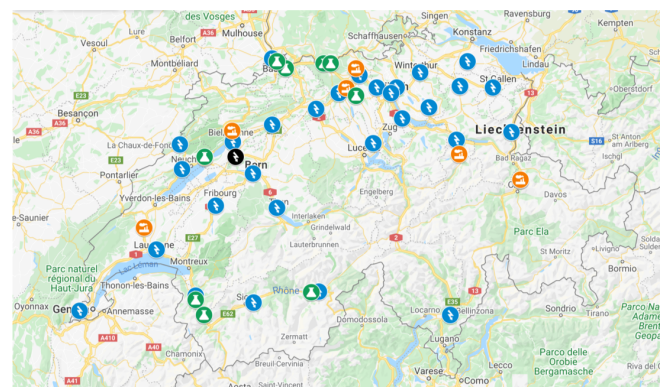
4.1 Swiss CO₂ Storage Potential

A first thorough and comprehensive study on the potential CO₂ storage capacity was carried out by Chevalier et al. (2010). It was a first-order appraisal based solely on geological data and criteria available at that time. The only possible realms for CO₂ storage in saline aquifers (no other options are viable) in Switzerland are the Swiss Molasse Basin (SMB) and the adjacent Folded Jura. The authors adopted the approach and criteria established in the literature (Bachu, 2003; Chadwick et al., 2008),

adapted for the Swiss case. By carrying out both a basin-wide and an aquifer-wide analysis, and by accounting for the many uncertainties, they estimated a large potential for CO₂ geological storage in the Swiss Molasse Basin, namely of the order of 2500 Mt$_{CO_2}$ (see Figure 25).

Five potential aquifer/seal pairs have been identified as potentially interesting in a depth range of 800–2500 m, the most promising of which is a carbonatic Triassic formation (Upper Muschelkalk) overlayered by a shaly/evaporitic formation (Gypskeuper). The storage potential in the Muschelkalk alone was estimated to be about 700 Mt$_{CO_2}$ (see Figure 25).

This first appraisal was revisited by the same authors, on the basis of new data acquired in the last decade (Diamond, 2019). The main factors determining whether an aquifer formation can serve as an industrial-scale reservoir for gas storage are rock-matrix porosity, rock-matrix permeability and the porosity and permeability of any fracture

Figure 24: *Map of main point-source Swiss emitters: WtE (blue), cement (orange), and chemical (green) plants.*
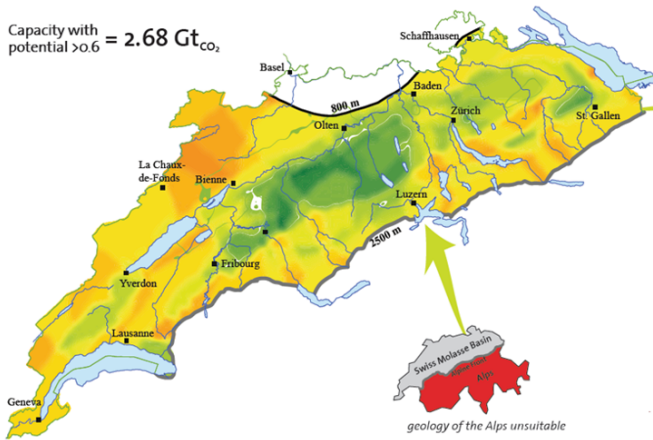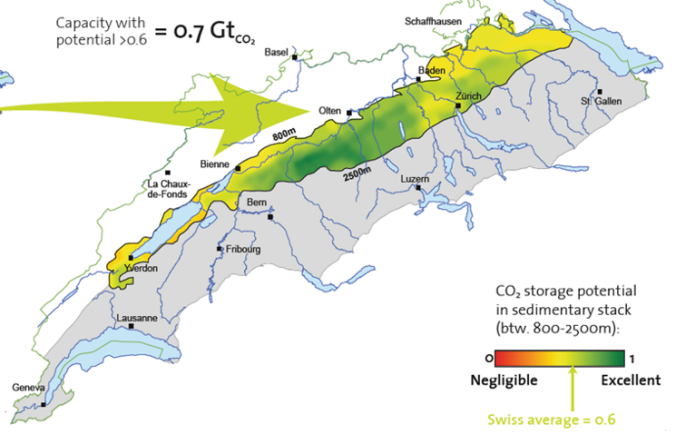
Figure 25: *Potential for CO₂ storage in Switzerland, modified after Chevalier et al., 2010.*
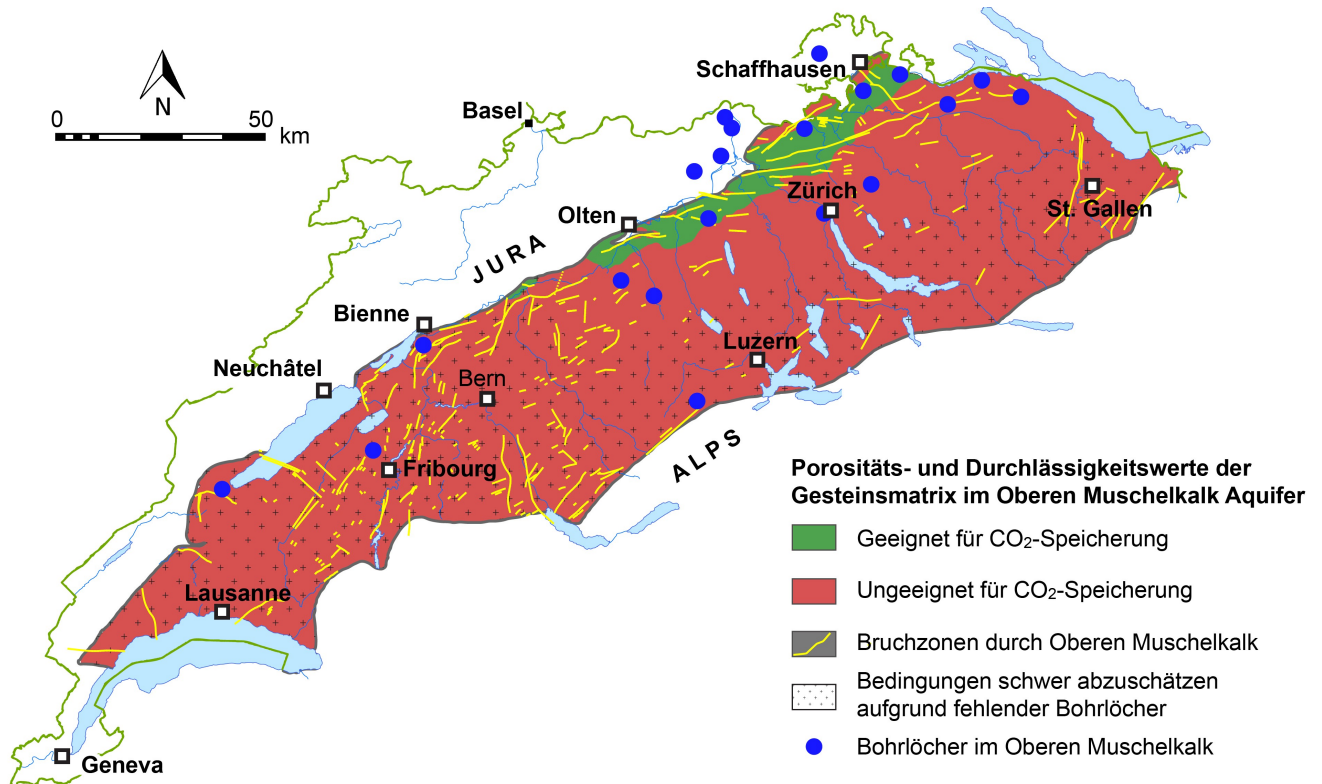
Figure 26: *New map of reservoir properties of the Trigonodus Dolomit (green + red areas) in the Upper Muschelkalk, Swiss Molasse Basin. Green area with-out faults has properties nominally suitable for industrial-scale gas sequestration. Red area is unsuitable (Diamond, 2019).*

networks. Current industrial techniques require rock-matrix porosities > 10 vol.% and permeabilities > 10 mD to efficiently inject gas. Considering these factors, the most promising part of the Upper Muschelkalk is the 20–30 m thick layer known as the Trigonodus Dolomit, which is hydraulically sealed above by the Gipskeuper layer. The Trigonodus Dolomit occurs throughout the Swiss Molasse Basin between <100 m depth in the north and > 5000 m in the south (combined green and red areas in Figure 26).

Regarding gas storage, it appears that the Trigonodus Dolomit exceeds the minimum useful matrix porosity and permeability values only at depths < 1130 m. Applying the technical limit of 800 m minimum depth for gas injection, a feasible depth window of 800–1130 m results. This combination of depth and matrix properties is attained only within the green area (640 km^2) in Figure 26, between Olten and Schaffhausen. This area is cross-cut by discrete faults (yellow lines in Figure 26), which may or may not be potential gas-leakage pathways through the overlying Gipskeuper seal. Some of the faults are flanked by networks of fractures that enhance porosity and permeability of the Trigonodus Dolomit and that do not breach the overlying Gipskeuper seal, but whose distribution is difficult to quantify. The theoretical CO_2 storage capacity of the unfaulted green regions (~300 km^2 at 5.5% injection efficiency) is ~52 Mt$_{CO_2}$, considerably less than the previous estimate of 700 Mt$_{CO_2}$. The red area in Figure 26 is unsuitable for CO_2 storage.

## 4.2 Combining CO_2 Storage with Geothermal Energy Extraction

Deep saline aquifers and depleted natural gas and oil reservoirs that are targets for geologic CO_2 storage are naturally porous and permeable and thus do not require hydraulic stimulation as for crystalline baserock (see Section 3.3). Since Randolph and Saar (2011a) first considered extracting geothermal energy with subsurface CO_2 from such naturally permeable geologic reservoirs in what they termed CO_2-Plume Geothermal (CPG) energy systems, many more theoretical studies followed and are being conducted on CPG to date. Current efforts regarding CPG research and development focus on deploying a first pilot, and then demonstration, CPG system with candidate sites being evaluated also in Switzerland (see also Section 4.3). These efforts are being led by Prof. Saar and his Geother-

mal Energy and Geofluids (GEG.ethz.ch) group at ETH Zurich but involve several academic, industry, and agency research and development groups worldwide.

CPG power plants produce a portion of the geologically stored and geothermally heated and pressurized CO_2 intentionally back to the land surface to expand it in a turbine with a generator to generate electricity. Thereafter, the CO_2 is cooled, any water is removed, before or after the turbine as discussed by Garapati et al. (2015) and Fleming et al. (2020), and the dry CO_2 is re-injected along with the CO_2 coming from the CO_2 capture facility into the geologic CO_2 storage reservoir. Supercritical CO_2 has advantageous thermophysical properties (Adams et al., 2014; Walsh et al., 2017; Hefny et al., 2020) compared to water (the conventional subsurface heat extraction fluid), which allows CPG power plants to extract heat at a higher rate (Randolph and Saar, 2011a; Adams et al., 2015; Adams et al., 2020), given the same reservoir conditions, e.g. thickness and transmissivity (see lower-left half of Figure 27). Furthermore, as all produced CO_2 is re-injected into the reservoir during CPG operations, 100% of the CO_2 is still eventually permanently stored underground so that CPG power plants can be viewed as add-ons to CCS. Thus, future CPG power plants would reduce, and have under favorable geologic conditions the potential to eliminate, the cost of CCS by providing heat, electricity and/or revenue (from power sales) for CCS operations (Randolph and Saar, 2011b).

While (future) CO_2-Plume Geothermal (CPG) power plants are expected to generate more power when implemented in deep saline aquifers, due to potentially significant heating during exothermic exsolution of any water that was dissolved in the CO_2 (Fleming et al., 2020), expected deployment of CPG in depleted gas or oil fields (see also Section 4.3 and Figure 31) also yields certain advantages for both CCS and CPG, such as large CO_2 storage capacity, proven seal, reservoir characterization knowledge and existing (sub)surface infrastructure (Kovscek, 2002; Bachu, 2003; Raza et al., 2018; Hoteit et al., 2019; Ezekiel et al., 2020; Hefny et al., 2020).

Furthermore, and of particular potential importance to Switzerland, with its largely low geothermal temperature gradients (e.g. Section 2.4) and reservoir transmissivities, Garapati et al. (2020) have shown that under certain conditions, CPG can serve as a geothermal pre-heater before further working
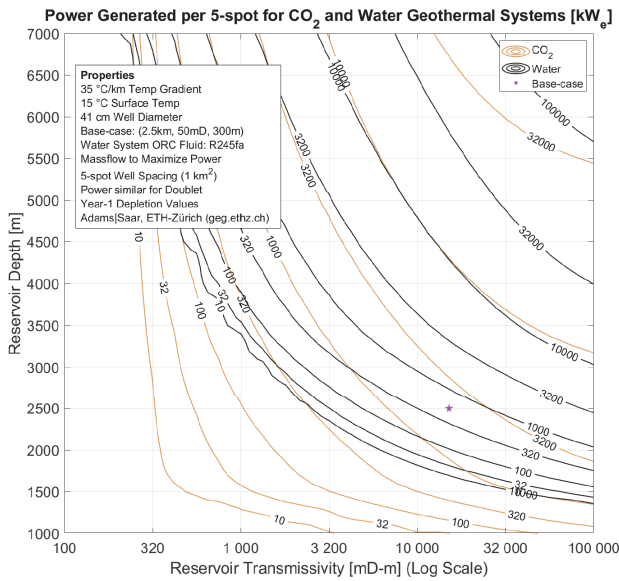
Figure 27: *Power Generated per 5-spot for CO₂ and water geothermal systems as a function of reservoir depth and transmissivity. The star indicates the power generated at the CPG base case: 2.5 km depth; 300 m thickness; and 50 mD permeability (Adams et al., 2020).*

fluid heating and electricity generation, resulting in larger power generation efficiencies than when separate geothermal and higher-temperature power plants are employed.

All implementations of CPG require careful system design, in terms of injection-to-production well spacing, production well diameter, required minimum CO_2 saturation (compared to water) around the production well inlet and several other factors to optimize production well fluid flow conditions, heat energy extraction rates and longevity of the geothermal reservoir, i.e. minimize reservoir heat depletion rates (Garapati et al., 2015; Adams et al., 2021).

The CPG concept has also been expanded to include systems that can use geologically stored CO_2 and geothermal energy to provide energy storage services to the electricity system (Buscheck et al., 2016; Fleming et al., 2018; Adams et al., 2019). In these systems, excess electricity can be used (stored) to cool, condense, and inject CO_2 into the subsurface, for example during times when more electricity is being generated by wind or solar energy technologies than is demanded. Later, this stored CO_2 can be extracted and used to generate electricity when demanded, for example when the wind is not blowing or the sun is not shining. In this way, these emerging CO_2-based geothermal

energy systems can directly reduce CO_2 emissions by sequestering them in the subsurface while indirectly reducing CO_2 emissions by increasing the utilization of variable renewable energy technologies on the electricity grid (Ogland-Hand et al., 2019; Ogland-Hand et al., 2021).

4.3 Assessment of CO₂ Storage Sites

Within the ELEGANCY project (ELEGANCY, 2021), a renewed screening activity for site selection was carried out in other segments of the Swiss Molasse Basin. The work aimed at characterizing geological structures capable of trapping CO_2, taking advantages of new seismic data acquisition and/or reinterpretation, accompanied by new porosity and permeability data.

4.3.1 Available Deep Subsurface Data

Switzerland can be classified into three geological domains: (1) Jura, (2) Swiss Molasse Basin (SMB) and (3) Alps (Trumpy, 1980, see Figure 28). Earlier studies suggested that a CO_2 storage potential exists in the SMB and parts of the Jura, but not in the Alps because of its metamorphic nature and structural complexity (Chevalier et al., 2010).

The SMB spans over 300 km in the SW-NE direction from the Savoy region (France) to Lake Constance (at the border between Switzerland and Germany), and has a variable width ranging between 30 km near Geneva to 80 km towards Lake Constance. The nature of the SMB subsurface is heterogeneous and exhibits different structural and lithological configurations, some of which may favour the implementation of CO_2 storage.

The critical question regarding any implementation of CO_2 storage is whether the subsurface data available is suitable and complete enough, so as to be able to estimate with an acceptable level of confidence the fate of any injected CO_2 and the potential impact of such injection on the environment (Ireland et al., 2020). Over the years, the main source of deep subsurface geological information, namely wells > 500 m below ground level (bgl) and 2D/3D seismic reflection data, have been from hydrocarbon exploration (see Figure 29). Although a depth of > 800 m bgl is required for supercritical CO_2 storage in aquifers and depleted hydrocarbon reservoirs (Bachu, 2003), critical information on the overburden units is still necessary, particularly their sealing properties and the risk of contamination
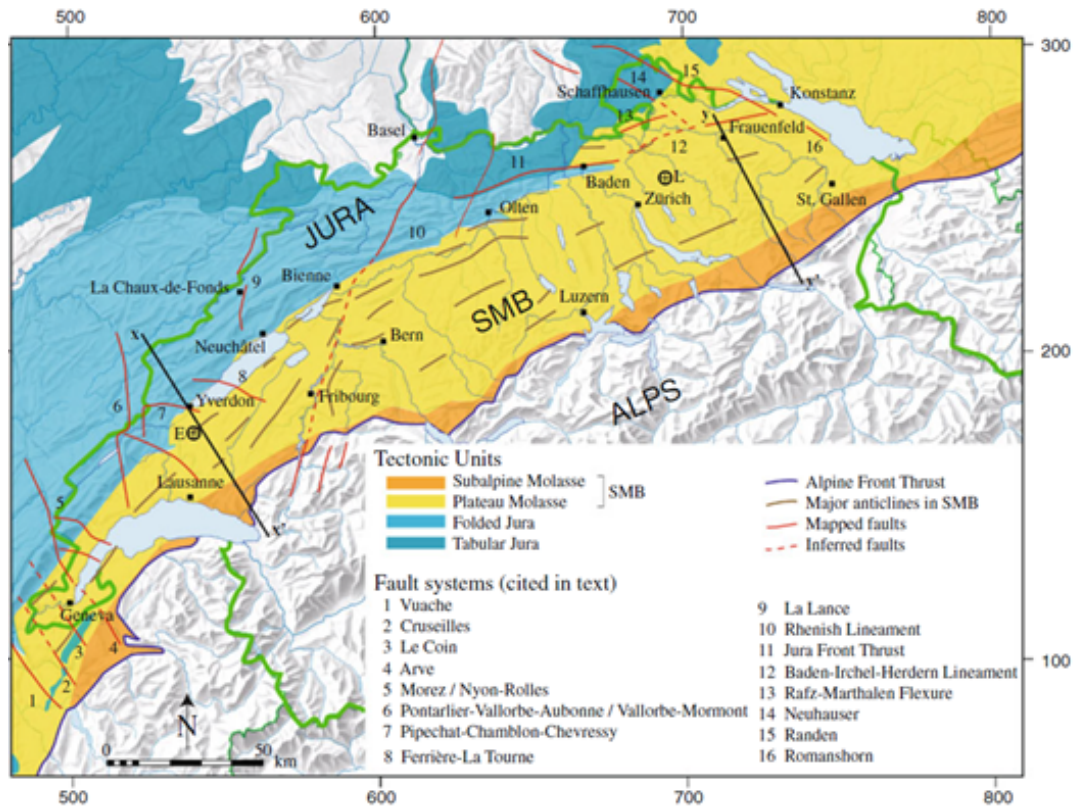
Figure 28: *Geological Configuration of the Swiss Molasse Basin (SMB) showing the major fault systems (Modified from Chevalier et al., 2010).*

of shallower resources, e.g. fresh water aquifers. Based on the aforementioned subsurface dataset available to this study, the SMB can be classified into four main regions (see Figure 30):

- High data density region: In this area, 3D seismic reflection datasets and borehole controls are available. This includes the St. Gallen area in northeastern Switzerland and other locations in northwestern Switzerland where the National Cooperative for the Disposal of Radioactive Waste (NAGRA) has acquired high-resolution 3D seismic surveys. 3D seismic data allow a detailed structural delineation of traps that may enable geological storage of CO_2. In these areas, the images of the subsurface have typically a higher signal to noise ratio.
- Moderate-high density region: This region includes parts of Canton of Vaud. This category encompasses regions lacking 3D seismic dataset but characterized by high-density 2D seismic lines (spacing < 5 km) and abundant well controls associated with past hydrocarbon exploration.

- Moderate-low density region: This includes areas lacking 3D seismic dataset and characterized by moderate density 2D seismic lines (spacing < 10 km) and limited borehole controls. A significant portion of the Swiss Molasse Basin falls in this category.
- Low data density region: This region is representative of other areas across the Swiss Molasse Basin having poor subsurface data coverage characterized by sparse grid of 2D seismic lines with little or no well control.

4.3.2 Workflow for Site Screening

Switzerland is characterized by a complex subsurface geological framework in terms of (i) underground usage (i.e. existing and future geoenergy exploitation, nuclear waste repository and large scientific infrastructure projects), (ii) subsurface manifestation of geofluids (water and hydrocarbons) and (iii) regulatory framework (cantonal and federal laws). These geological and technical factors must be considered during the screening of suitable
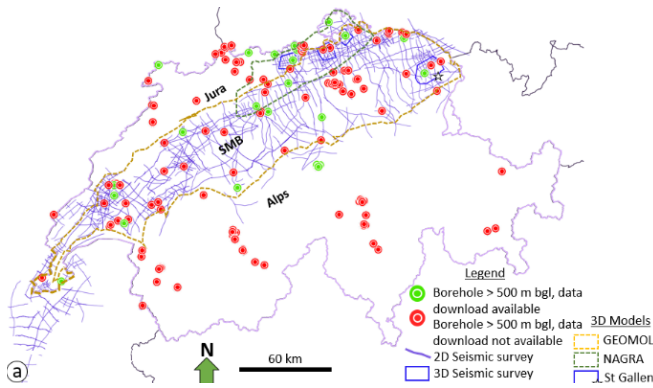
Figure 29: *Subsurface dataset available in the SMB and part of the Jura.*

Figure 30: *Data density (seismic and well data) classification of the SMB; location of test sites for screening.*
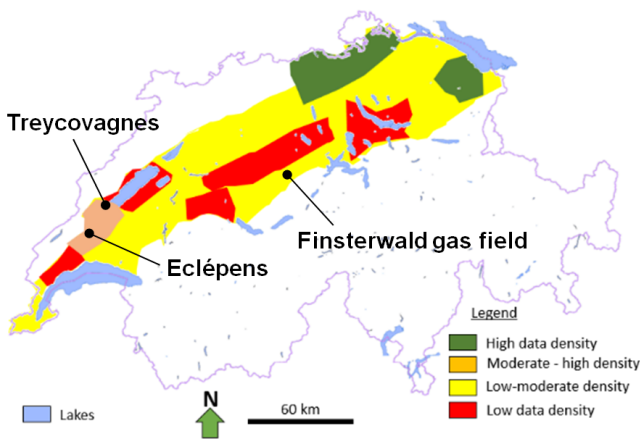
sites for CO_2 storage in Switzerland.

Overall, the site screening process involves quantifying the key geological properties necessary for CO_2 injection by identifying and quantifying the key parameters (i.e. reservoir storativity, sealing integrity etc.) and assessing their uncertainties in order to predict and mitigate the risk associated with them. The workflow can be applied to any site across the SMB and other onshore sedimentary basins elsewhere where a detailed assessment of CO_2 storage potentials needs to be carried out (Mazzotti et al., 2021).

4.3.3 Assessment for Selected Sites

The proposed workflow was tested for three sites in sub-regions of the SMB with moderate-high data density and subsurface knowledge (well penetrations with good quality logs and/or seismic and a pre-existing knowledge of the geological structure with storage and sealing potential, Figure 30).

Finsterwald Natural Gas Field, Entlebuch. Depleted hydrocarbon reservoirs are recognized as the most suitable candidate for CO_2 sequestration based on their storage capacity, proven seal, reservoir characterization knowledge and existing (sub)surface infrastructure (Kovscek, 2002; Bachu, 2003; Raza et al., 2018; Hoteit et al., 2019). Furthermore, where these reservoirs have adequate temperature as well as permeability and thickness (i.e. transmissivity), the injected CO_2 can be employed as a subsurface working fluid for CO_2-Plume Geothermal (CPG) power plants, increasing the subsurface energy extraction rate, compared to groundwater, all else being equal, while still eventually sequestering 100 % of the initially injected CO_2, as discussed in Section 4.2.

In Switzerland, only the Finsterwald gas field in Entlebuch (Canton of Lucerne) had a marginal production of natural gas for a decade until depletion (Lahusen and Wyss, 1995). It may therefore be considered as a CO_2 storage site assuming that the volume occupied previously by the produced hydrocarbons will be filled entirely by the injected CO_2 (Hoteit et al., 2019).

The Entlebuch-1 well targeted an anticlinal structure in the Finsterwald gas field and produced 74 mio Nm^3 of gas from a 20 m-thick karstified Malm limestone reservoir (Malm Karst, Upper Jurassic) at > 4 km depth (Figure 31). This reservoir is sealed
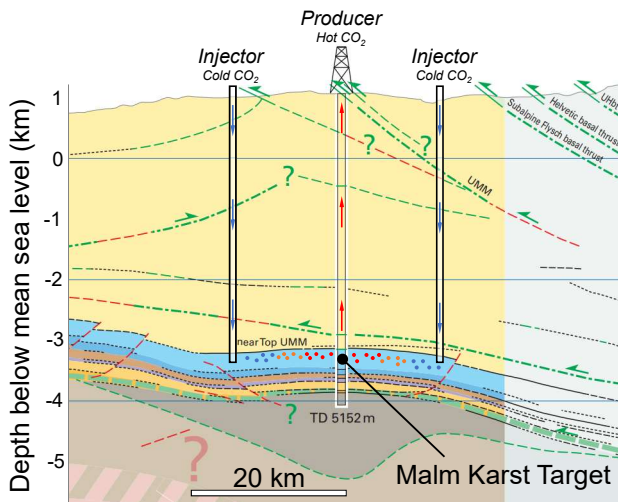
Figure 31: *Structure of the CO₂ storage complex at Entlebuch (modified from Sommaruga et al., 2012) with possible arrangement of CO₂ injector and producer wells for CPG (Section 4.2).*

Figure 32: *3D top reservoir structure of the target interval for storing CO₂ at the Eclépens area.*
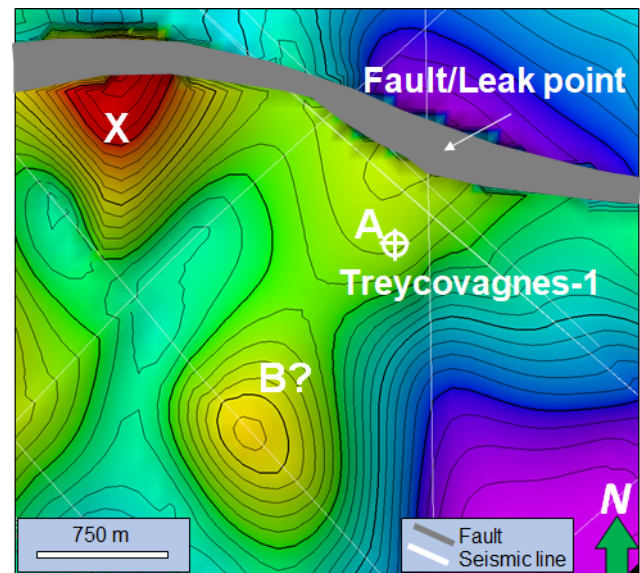
Figure 33: *Top reservoir structure of the target interval for storing CO₂ in Treycovagnes site.*

by a 4 km thick Molasse overburden containing impermeable shale-rich layers. Based on the volume of hydrocarbons produced, a static CO_2 storage capacity for the Finsterwald gas field in the order of $0.2\,\mathrm{Mt}_{CO_2}$ can be estimated.

The depth of this Upper Jurassic reservoir suggests a reservoir temperature of 100–120 °C using a reasonable geothermal gradient of 30 °C/km. This may allow for power generation using CPG (Section 4.2). CO_2 could be introduced through injector wells an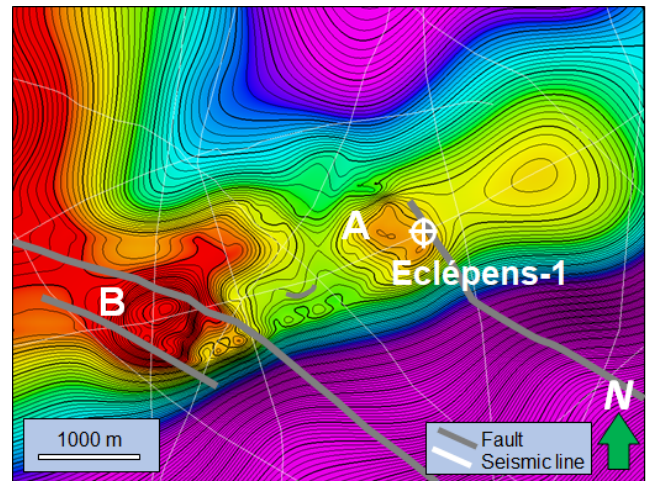d retrieved through the original Entlebuch-1 well (Figure 31; for illustrative purposes only, injector and produces wells will usually be only 1 km apart).

Eclépens. The site is located in the Canton of Vaud between the towns of Lausanne and Yverdon (Figure 30). It is close to a large-scale cement factory owned by the Holcim Group with a nearby quarry exploiting the topographic expression of a deeply rooted structure known as the Mormont anticline. The Eclepens-1 borehole, a former hydrocarbon exploration well drilled in the 80s is currently plugged and abandoned.

A potential reservoir interval suitable for storing CO_2 was identified within the Upper Triassic and Lower Jurassic strata at a depth of 2042.5–2105 m, with a thickness of 62.5 m. A reasonably dense set of 2D seismic lines allows to build a model of the subsurface. Figure 32 shows the height profile of the upper boundary of the possible reservoir. Of

interest are two anticlinal structures with 4-way dip closure. The area of the reservoir above spill point is approx. 2.8 mio m² for anticline A and 1 mio m² for anticline B. The porosity of this interval ranges between 1–7.5 %. The combined P50 estimated static CO_2 storage capacity for both structures considering a spill and fill scenario is $0.12\,\mathrm{Mt}_{CO_2}$.

Treycovagnes. The Treycovagnes site is also located in the Canton of Vaud between the towns of Lausanne and Yverdon (Figure 30), approx. 20 km from the same Holcim cement factory. The structural framework of this site consists of a half anticline bounded by faults (Figure 33). This site was selected based on the large thickness (62 m) of the

Triassic Buntsandstein aquifer/reservoir found in the Treycovagnes-1 well.

There is an anticline A spanning ca 0.4 mio m^2 above spill point/ leak point. A second anticlinal structure – albeit poorly constrained by the 2D seismic line – may exist, spanning ca 0.6 mio m^2 above spill point. The porosity distribution for the Buntsandstein found here ranges between 2–6 %. We estimated a P50 static CO$_2$ storage capacity for both structures in the order of 0.03 Mt$_{CO_2}$. Generally, the density of seismic lines is lower than for the Eclépens site, leading to a larger uncertainty of the exact structure of the reservoir.

4.3.4 Next Steps on Site Selection

The outcome of the screening activities for CO$_2$ storage on selected sites across the SMB has substantially increased the understanding of the properties of these sites (especially the reservoir tightness in terms of porosity and permeability), indicated a very small capacity for CO$_2$ storage, and revealed the unsatisfactory level of knowledge regarding the nature of the Swiss subsurface.

The primary data needed for assessing the potential of CO$_2$ storage is presented in Table 2, of which seismic data (3D or high density 2D) and well data are of paramount importance. Sparse seismic data coverage limits detailed mapping and modelling of potential subsurface structures and traps capable of sequestering CO$_2$ in the SMB.

Absence of sufficient data has also consequences in understanding surface fault behaviors, which may have implications on storage integrity at specific sites. In addition, this may result in inaccurate CO$_2$ storage volume estimation at selected sites. Limited deep well data in the SMB will limit deployment of geostatistical reservoir/aquifer modelling techniques especially facies constrained petrophysical modelling of the target reservoirs/aquifers. Therefore, the only possible choice of assuming homogeneous reservoir/aquifer facies or petrophysical properties over a considerably large vertical and lateral extent in inter-well regions does not give a good approximation of the subsurface properties of the SMB.

Importantly, this study highlights some challenges related to the subsurface aquifer/reservoir quality of the sites. Since most of the reservoirs in the SMB are tight systems, the possibility that a porosity and permeability contribution from fracture systems might play an important role in controlling storativity and fluid flow behaviour, needs to be considered.

Fracture evaluation is vital in tight reservoirs since fractures are well known to influence the reservoir porosity (Nelson, 2001; Land et al., 2013), hence the capacity of storing considerable volumes of fluids, as well as the rock permeability and transmissivity. Indeed, incorporation of one or multiple open fracture systems in the conceptual geological model (Moscariello, 2016) can result in a higher estimates of CO$_2$ storage capacity.

However, estimating fracture porosity and permeability requires detailed assessment of the reservoir/aquifer parameters. This can be achieved by characterizing subsurface image logs such as formation micro-imager (FMI) and electrical micro-imager (EMI), and core samples. Unfortunately, such data were acquired only in recently drilled wells in the SMB such as the St Gallen GT-1, Geneva GEo-01 and NAGRA's boreholes in North-eastern Switzerland.

In addition, cores may have only been recovered from borehole sections of interest to the actual project, and this may be different to promising subsurface intervals for CO$_2$ storage. Ways to ameliorate this is analyzing any data from well-tests (i.e. Drill Stem Tests, Modular Formation Dynamics), production surveys (i.e. Production Logging Tool) and mud-loss records. These data may indeed provide information about possible fractured intervals having high aperture that may develop into a fracture network (Aghli et al., 2020). However, such data are also limited in the SMB subsurface (Table 2) and outcrop analogues can be used to characterize the fracture system representative of the Swiss subsurface.

During a possible follow-up project, a robust probabilistic assessment of the geological storage capacity could be developed for the sites described above. This should be based on realistic geological conceptual models that are corroborated by relevant analogue data sets. This will allow to build detailed 3D static models which consider realistic complex-porosity and permeability systems, that are representative of aquifer/reservoir intervals, including matrix, fracture and karstic networks. Such procedure will allow to better estimate a range of different CO$_2$ storage capacity scenarios across Switzerland.

Ultimately, the 3D static model will then be used as input for dynamic simulations aimed at understanding the fate of the CO$_2$ plume and will serve

as basis for geomechanical modelling (i.e. slip tendency, discrete network modeling, etc.), to predict fault behaviour and related risks of induced seismicity associated with injectivity tests.

In summary, this preliminary study has identified only a small storage capacity in the three sites analyzed in the SMB (in total $< 1\,Mt_{CO_2}$). This is mainly because of the tight nature (i.e. low matrix porosity and permeability) of the potential reservoirs and aquifers under consideration. Further work should be carried out to complete the assessment of CO_2 storage potential as not all geological uncertainties (i.e. existence of fractured and/or karst porosity and permeability) have been fully assessed in this work.

4.4   Experiments on a Faulted Cap-rock

A potential risk of any subsurface CO_2 storage is leakage through a faulted caprock that should seal the reservoir from above. This situation was studied within the ELEGANCY project by performing an injection experiment in a fault hosted in clay at the Mont Terri underground rock laboratory in northwestern Switzerland (ELEGANCY, 2021; Wenning et al., 2019; Wenning et al., 2020a; Wenning et al., 2020b; Zappone et al., 2020).

The experiment aimed at improving our understanding on the main physical and chemical mechanisms controlling the migration of CO_2 through a fault damage zone, and the impact of the injection on the transmissivity in the fault. To this end, we injected a CO_2-saturated saline water in the top of a 3 m thick fault in the Opalinus Clay, a clay formation that is a good analogue of common caprock for CO_2 storage at depth. The mobility of the CO_2 within the fault was studied at decameter scale, by using an integrated monitoring system composed of a seismic network, pressure temperature and electrical conductivity sensors, fiber optics, extensometers, and an in situ mass spectrometer for dissolved gas monitoring.

Figure 34 shows the full time series for the flow rate and recorded pressure for one year of injection. The flow rate drops in the first few days of injection from an average value of 0.2 ml/min to about 0.05 ml/min, then slowly decreases up to a steady-state value of about 0.035 ml/min (Figure 34a). In one year, only about 20 litres of CO_2-saturated water were injected into the fault zone.

The injection pressure is overall constant at 4.5 MPa (Figure 34b – blue line), while the pressure monitored at the interval M1 is first increasing to a maximum change of 0.08 MPa, then starting a slow decrease with a negative trend at time of writing (Figure 34 – red line). Worth to note that the two major pressure drops in the monitoring interval in June and December 2019 were due to incorrect manoeuvres of the operators, while the "jumps" observed in the period January–March 2020 where poroelastic effects caused by a nearby excavation. Overall, the pressure at the monitoring interval reaches a maximum around October/November 2019, and decreases afterward: this could be indicative of a compressive front with pressure increasing before the fluid from the injection breakthrough in the monitoring interval and decreasing afterwards. The pressure at injection is set constant, but at regular interval (every 30 days), we perform a little shut-in/restart cycle to check for possible reactivation of the micro-fractures in the fault (Figure 34b – blue line). Figure 34c shows an example of these tests, at the start of the injection activities. The time of pressure decay of 0.3 MPa (from 4.8 to 4.5 MPa) is of 1 min on June 12th, 2019, and 30 min on June 13th, 2019. All following tests show a progressive increase in the decay time, as expected for a pressure front propagating further away from injection point.

Modelling of pressure observations indicate some potential porosity decrease in the near injection region. This would represent a sort of healing mechanism, that in the long term would prevent the leakage to happen. Upscaling of the results and assuming far-worse conditions than in the Mon Terri experiment (i.e. much more permeable fault) shows relatively large leakage only if the permeability is above 10^{-17} m^2. In the worst simulated case (permeability 10^{-15} m^2, distance injection well-fault of only 50 m), about 0.1 %/year of injected CO_2 migrated at shallow depth. Worth to mention that here we do not simulate a seismic reactivation of the fault, and therefore assume the permeability changes are negligible.

Table 2: *Assessment of key subsurface data needed for characterizing the potential for CO$_2$ storage.*

Dataset	Implication	Availability
Seismic reflection data (2D and 3D)	Definition of structures and traps, definition of faults systems	Moderate
Borehole Data (Well logs, cores, temperature log and well reports)	Lithological description, petrophysical properties such as porosity and permeability. Temperature log is necessary to constrain the reservoir temperature for CPG consideration.	Moderate
Geochemistry - Seep information (Hydrocarbon, water)	Manifestation of seep e.g. gas or oil questions the seal integrity and the fate of the injected CO$_2$.	Moderate
Reservoir engineering and production data (well test or pumping test)	Understanding of reservoir injectivity, permeability and temperature. Information on porewater geochemistry and salinity are important for modelling.	Low
Geological Models (GEOMOL, sector models)	3D depth structure of the Swiss Molasse Basin necessary for development of static and dynamic reservoir model. Local refinement may be necessary in region with anomalous configuration. Limited areas covered by well penetration, high density 2D-seismic and/or 3D seismic are suitable for high-res models.	Moderate
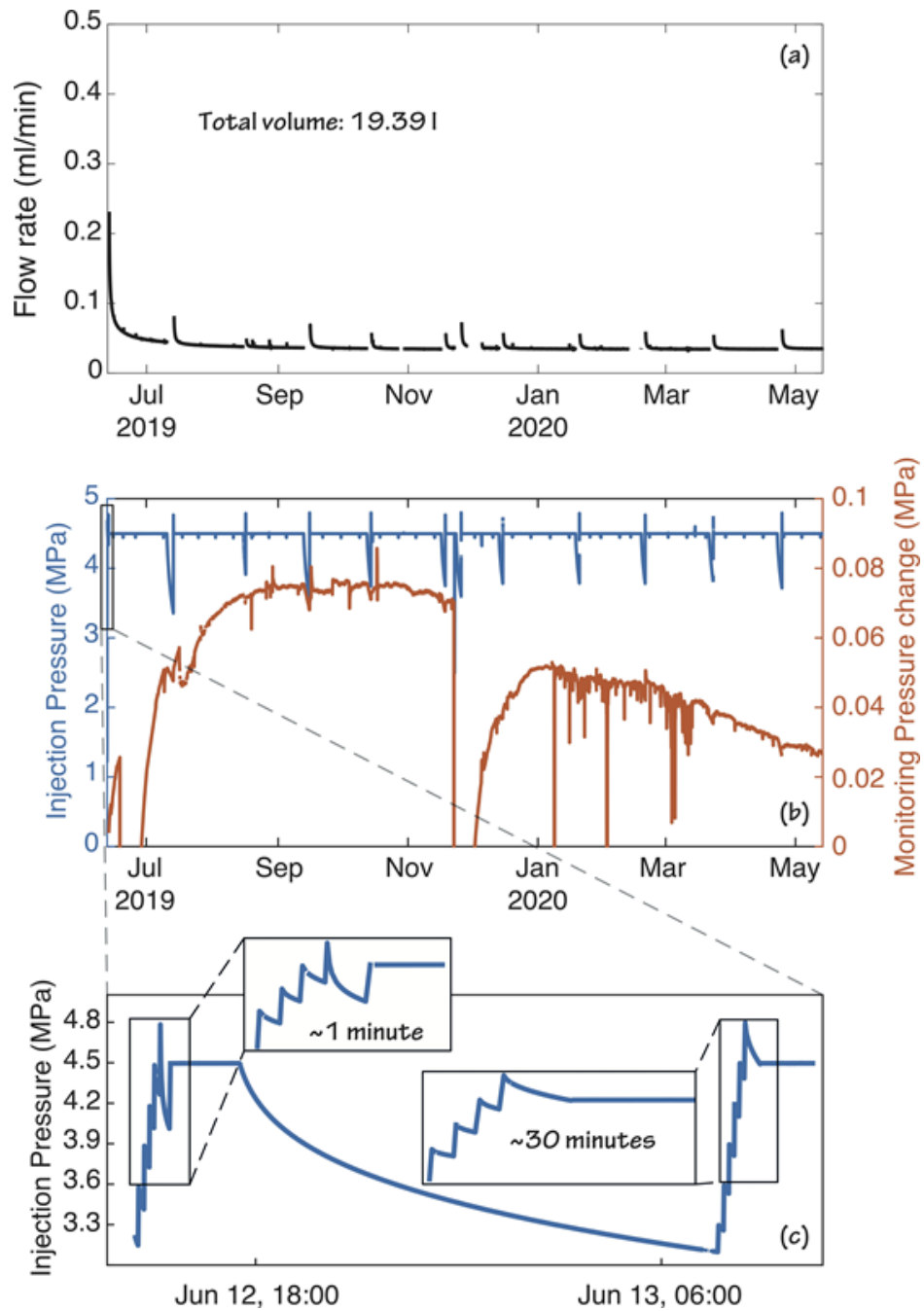
Figure 34: *(a) Flow rate recorded during the one year-long injection of CO₂ saturated fluid. (b) Pressure at injection interval (blue line) and pressure changes recorded at the monitoring interval (red line). (c) Zoom on injection pressure in the first days of injection.*

5 Risk Management and Sustainability

When a new technology like geothermal heat or power generation is deployed, a number of factors need to be considered that go beyond the mere technical aspects. One factor is risk, both during reservoir creation (induced seismicity) and during operation. In addition, a number of sustainability indices were considered from various domains such as environment, economy and social perception.

5.1 Advanced Traffic Light System (ATLS)

One main goal of the SCCER-SoE activities was promoting and testing of data-based self-learning systems to manage and mitigate fluid-induced seismicity. A critical lesson learned from failed EGS projects such as the one in Pohang (South Korea, 2017; causing a M5.4 earthquake) is that "static" quantitative risk assessments are necessary yet not sufficient to mitigate fluid-induced seismicity. In fact, a preliminary risk analysis should be used as prior information and updated in near-real-time as new data arrives during and stimulation.

We tested and demonstrated the capabilities of such an Adaptive Traffic Light Systems (ATLS) in Geldinganes (Iceland) in October 2019. Geldinganes is a peninsula within the city limits of Reykjavik. The exceptional geothermal gradient in this area allows economic heat production for the district heating system of the city if the wells deliver sufficient flow rates. One existing production well was drilled in 2001 through basalts and dolerite intrusions into a gabbro body with limited success.

Within the framework of the European DE-STRESS project (DESTRESS, 2021), cyclic injection schemes were applied at multiple stages to increase the productivity of the well. In parallel, the seismic activity was monitored and used for updating the seismic risk using the ATLS system developed at the SED. In brief, the ATLS used as prior information a priori risk assessment (Broccardo et al., 2017) and fed it into a Bayesian learning system (Broccardo et al., 2017; Mignan et al., 2017) to obtain online risk updating. Each update was used for decision making and to modify the injection profile.

The performance of the ATLS system was satisfying. The preliminary risk assessment was character-ized by large uncertainties present at all levels of the analysis, which was substantially reduced based on the near-real-time recorded micro-seismicity. In addition, the seismic risk expressed in terms of individual risk (IR) decreased as new data were encoded into the system. Figure 35 shows the IR at the beginning (left) and at the end (right) of the project. The IR is reported as a probabilistic measure such that it can be expressed by its median and confidence intervals. In the same Figure, the iso-risk curves are reported. The threshold of IR = 10^{-6} for the median of the IR represented the discriminant for continuing or stopping the project (i.e. if the median was crossing the IR = 10^{-6} contour the project would have been stopped). As next steps, ATLS approaches will be tested in the Bedretto underground lab, in the Hengill area in Iceland and also at next EGS demonstration project in the US, the Utah FORGE (utahforge.com).

5.2 Accident Risk

In addition to induced seismicity and aspects related to public acceptance and risk aversion, a comprehensive risk assessment of deep geothermal systems should consider various types of risk related to accidental events with potential consequences to human health and the environment (Spada and Burgherr, 2015; Spada et al., 2014; Spada et al., 2021). In fact, along the full life cycle (i.e. drilling, stimulation and operation phases) of a deep geothermal project it has been found that blowouts and the release of hazardous chemicals in different life cycle stages present potential areas of concerns. Blowouts can happen during the drilling and the stimulation phases, while the release of hazardous substances can occur in all
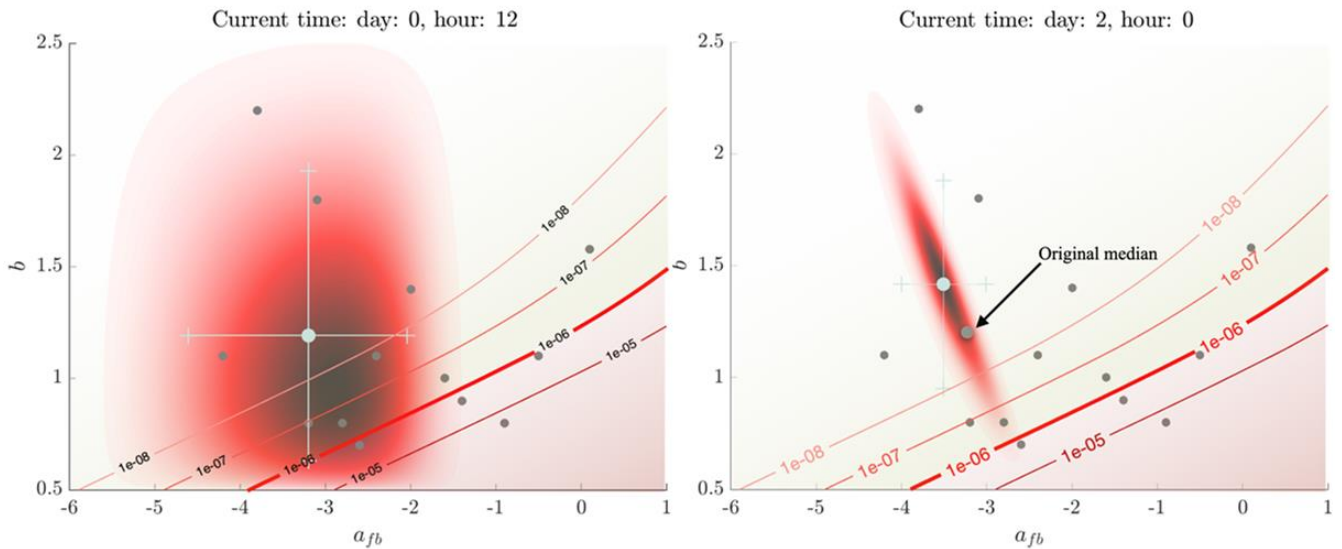
Figure 35: *IR as a function of the b-value and the underground feedback parameter a_{fb}, (better known as seismogenic index). Light green domain represents the "safe domain", the light red domain represents the "failure" domain. The limit state function is represented by the iso-risk curve IR = 10⁻⁶. The left panel shows the IR and the associated uncertainties at the beginning of the project. The right panel represents the IR and the associated uncertainties towards the end of the project.*

phases. Hazardous substances are transported, stored and used for different purposes:

- Caustic soda commonly provides a short time additive in the drilling mud.
- Hydrochloric and hydrofluoric acids, ammonium persulfate and boric acid are typical chemical utilized for cleaning purposes during the hydraulic stimulation.
- Working fluids (e.g. benzene) are used in the operation of the geothermal plant.
- The brine can contain so-called NORMs (naturally occurring radioactive materials), or others hazardous substance, as for example arsenic, depending on the geology of the subsurface.

Accident risk for blowouts in both drilling and stimulation phases and the use of hydrochloric and hydrofluoric acids in the stimulation phase pose a significantly higher (at least one order of magnitude) expected risk than other hazardous substances used in the different phases. In contrast, the risk of extreme events is higher in the operational phase due to the use of highly explosive and inflammable substances, e.g. benzene. Finally, accident risk for deep geothermal energy systems compares favorably to all the fossil energy chains (coal, oil, natural gas), hydropower, hydrogen and most new renewable technologies (e.g. wind offshore). These results suggest that improvements

of safety procedures and standards should rather focus on the level of "every day" or operational risk aspects associated with deep geothermal systems, but also that potential catastrophic events should not be discarded a priori.

5.3 Suitability of Deep Geothermal Energy Systems

Possible geothermal power plant locations are constrained by geological conditions as well as economic, environmental and social aspects. In order to consider the plethora of criteria in the potential site selection and decision-making process, a spatial Multi-Criteria Decision Analysis (sMCDA) has been applied (Ferretti and Montibeller, 2016). It combines MCDA with a Geographical Information System (GIS) at the level of a total of 1684 municipalities for the Swiss Molasse basin. MCDA allows to consider a wide variety of aspects, e.g. environmental, economic, etc., in a transparent manner (Volkart et al., 2017), while GIS accounts for the spatial variability of the problem (Yalcin and Gul, 2017). The Swiss Molasse basin has been selected, since more pilot projects are expected due to the less heterogeneous geological conditions compared to the Alpine region.

Currently, no DGE plants are operational in Switzerland. Therefore, six hypothetical geothermal plants with two (duplet) or three (triplet) wells
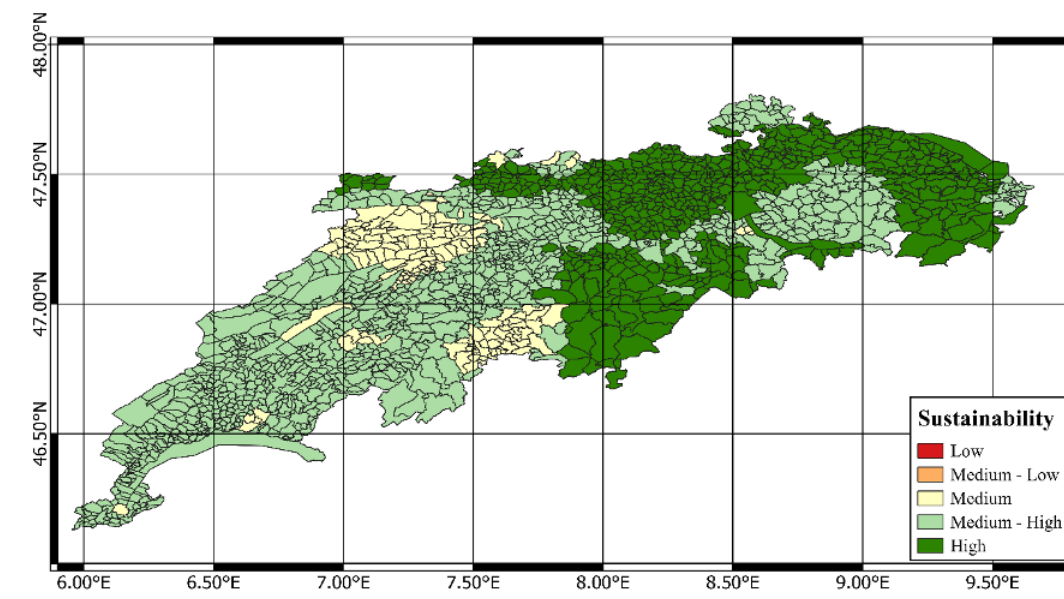
Figure 36: *Average Sustainability map for Deep Geothermal Energy in Switzerland based on a set of sample preference profiles.*

and three plant capacities for each have been analyzed (Bauer et al., 2017). In total, 12 indicators are considered and assigned to the three pillars of sustainability. Five environmental indicators (Climate Change, Human Toxicity, Particulate Matter Formation, Water Depletion, Metal Depletion), two economic (Average Generation Cost, Company Taxation), and five social (Non-Seismic Accident Risk, Natural Seismic Risk, Induced Seismicity, Population, Presence of National/Regional Parks).

The environmental and the Average Generation Cost indicators are sensitive to the temperature gradient (Hirschberg et al., 2015). Therefore, they have been estimated for each municipality based on the ratio between the heat flux and the average thermal conductivity of rocks for Switzerland (Bodmer, 1982). In contrast, no spatial effects are present for non-seismic Accident Risk, since it depends only on the number of drilled wells (Spada et al., 2014). The Company Taxation, which vary at the cantonal level, refers to the taxation in percentage to the industries. The Natural Seismic Risk is expressed on an ordinal scale as low, medium or high based on Federal office for the Environment (FOEN) (2020). It is considered a proxy for social acceptance, i.e. high values correspond to lower social acceptance. The Population size in a municipality indicates the risk of potentially affected inhabitants due to, for example, induced seismicity. The presence or absence of National/Regional Parks indicates whether a municipality is more suited for a potential DGE

system, since parks can be subjected to specific regulations that can affect the start or even the acceptance of a DGE project. The Induced Seismicity Indicator is estimated based on the expected total volume of fluid injected for the stimulation. The higher the volume, the higher the risk of induced seismicity (Evans et al., 2012).

The indicator values have been calculated for the six hypothetical geothermal plants in each municipality and were then used as input for the sM-CDA. Since no stakeholder elicitation has been performed, a number of representative, artificial preference profiles have been defined. First, a Monte Carlo approach was used to generate an average sustainability map. Second, four distinct profiles were defined: equal weights for all indicators, which corresponds to the spirit of sustainability, and three weighting profiles that strongly favor one sustainability pillar (weight 80 %), whereas the two other pillars are both weighted 10 %.

Figure 36 shows that the sustainability performance of DGE in Switzerland is high in the Northeast of Switzerland. However, the different artificial profiles clearly indicate that different weighting profiles can influence the sustainability performance of a municipality. This illustrates the sensitivity of the ranking to subjective preferences by various stakeholders. Therefore, trade-offs have to be considered for an informed decision-making process, and to guide the public debate and participatory processes.

6   Conclusions

For the past seven years, researchers at federal universities, cantonal universities and universities of applied science collaborated to advance the science and application of geothermal energy exploitation. Important steps towards the industrialization have been made, mostly by collaborating with industrial partners from the private and public sector.

Currently, Switzerland imports more than 70 % of its primary energy input, mostly in form of fossil oil and gas that is used in the heating and mobility sector. In order to realize the ambitious goal of net-zero greenhouse gas emissions, the use of fossil energy will have to be stopped. Simply switching to imports of biogenic liquids and gases is a risky strategy since it is unknown whether such resources can be produced in sufficient quantity at an attractive price.

The majority of the heat demand in Switzerland occurs at temperatures that can in principle be covered by geothermal sources. This includes the complete sector of space heat and domestic hot water and parts of the industrial process heat demand, for instance in food production. The challenges to unlock this potential are manifold, the most important being the insufficient knowledge of the subsurface, and the immaturity of technologies to efficiently extract the heat from several kilometers depth.

Over the past seven years, researchers in the SCCER-Supply of Electricity addressed these challenges in a comprehensive way. Their results are condensed in the present report, and the most important conclusions and recommendations are the following.

Advancing Knowledge of the Subsurface

As for any subsurface activity, sufficient knowledge is a key prerequisite to increase the probability of success of a project. An important step was the development of the geological model of the Swiss Molasse Basin (GeoMol) by Swisstopo. Based also on Geomol, various workflows have been developed and tested with concrete case studies (see Section 2).

Creation of Geothermal Reservoirs

Once a suitable target has been identified, the heat that is stored in the underground needs to be brought to the surface. For sedimentary targets that exhibit a sufficient permeability, this may be achieved by a suitable combination of injection and production wells that aim at the aquifer. SCCER-SoE researchers participated in successful campaigns in the Geneva area (see Section 1).

In presence of crystalline base rock, permeability has to be artificially generated. Fundamental knowledge on the processes of hydrofracking and hydroshearing have been generated during experiments at the Grimsel test site. Permeability could be increased by orders of magnitude, while controlling the inevitable rock movements that may be perceived as induced seismicity at the surface. Recent experiments at a considerably larger scale in the Bedretto Laboratory confirmed the viability of such soft hydraulic stimulation techniques (see Section 3). Part of this endeavour was the development and validation of workflows to reduce risks of wellbore failure and excessive seismicity during drilling.

Testing at various scales is only one tool available to the researchers. Complementary approaches in simulating the coupled processes of fluid dynamics, heat transfer and rock mechanics have been further developed. These allow to gain insights into the processes during stimulation but also during the operation of the reservoir.

Storage of CO₂

The latest updates of the Energyperspectives 2050+ highlights the importance of CO_2 storage from large scale emitters in Switzerland, e.g. waste incineration and cement plants (see Section 4). The prerequisites for geological storage are reservoirs with

sufficient porosity and permeability that are sealed by an impermeable cap rock.

A first rough assessment of the domestic storage potential yielded a considerable value of 2500 Mt, roughly 50 times the annual emissions in Switzerland. Unfortunately, this estimate had be revised with more data being available: for the most promising geological formation, the Upper Muschelkalk, this led to a more than 10-fold reduction of storage potential from 700 Mt down to 50 Mt.

Recent studies established and tested a workflow for assessing a storage site. This workflow was applied to three cases which gave again only a small amount of CO$_2$ storage potential. Further assessment of existing subsurafce data will be needed to better appraise the potential for domestic CO$_2$ storage. In parallel, it is recommended to develop an alternative solution, namely to collect CO$_2$ within Switzerland and to transport it via a joint European infrastructure to storage sites in the North Sea.

7 Recommendations

Geothermal energy can play a decisive role in the decarbonization of the heating sector, replacing fossil oil and gas. To unlock the potential of geothermal heat it is recommended to demonstrate the technology at increasing depth. Starting point are medium deep sedimentary layers where the natural permeability of aquifers can be used, feeding into district heating networks and low temperature industrial processes. Deeper crystalline rocks can then be exploited using the techniques developed in SCCER-SoE. This allows to feed medium temperature industrial processes and to eventually also produce electricity.

Geothermal electricity generation played a prominent role in the original Energy strategy of 2012. 4.4 TWh/a were planned to be generated in 2050. This gave a tremendous push to geothermal research in Switzerland, coordinated within the SCCER-Supply of Electricity.

The latest update of the Energy Perspectives 2050+ took a broader view on all aspects of a future net-zero greenhouse gas emission energy system (Prognos, 2020). It highlighted also the challenge of de-carbonizing the heating sector which – together with mobility – is the main emitter of CO$_2$ in Switzerland. In the scenarios generated within the JASM project but also by the Prognos consortium (Marcucci et al., 2021; Prognos, 2020), the tremendous value of using geothermal energy as it is, namely as heat, became clear.

This is not surprising since in a total system optimization any resource is used in a way that maximizes its value in reducing CO$_2$ emissions at minimum cost. This makes the generation of electricity less attractive, since 85–90 % of the geothermal heat is degraded to useless ambient heat (anergy) in the power generation process, whereas the direct use of geothermal heat for district heating or industrial processes has a utilization rate of close to 100 %.

The challenges in exploiting geothermal energy increase with depth. Today's extraction of heat from the underground is limited to less then 400 m depth where the rock temperature is not much higher than the mean ambient temperature and therefore heat pumps need to be employed. Going deeper will increase the source temperature and eventually make the use of heat pumps unnecessary. The first

target should therefore be aquifers at a depth of 1–2 km that deliver heat to district heating networks or to agricultural and industrial processes that require heat at low temperatures.

With increasing experience, larger depths can be targeted, eventually entering the crystalline baserock where the soft hydraulic stimulation techniques can be employed that are being demonstrated and further developed in the Bedretto Laboratory. With source temperatures exceeding 100 °C at depth of more than 3 km, medium temperature industrial processes can be served.

SCCER-SoE largely focused on the subsurface challenges of geothermal energy. Going forward it is necessary to consider the configuration of the energy systems where geothermal energy will be integrated. Therefore, identifying which geothermal for what application is a key process to define the site-specific contribution of geothermal heat

This can be achieved by developing a harmonised workflow based on a step-wise approach which will focus on the definition of the thermal demand characteristics (annual quantities, temperature levels, and different geographical extension) and in a second step on the identification of the more efficient and sustainable usage of the geothermal resource.

The approach is to create an integrated solution that can help decision makers to understand what portion of the heating demand at a specific location can be supplied by geothermal energy. This mission is carried on by a new project termed De-carbonization of Cooling and Heating in Switzerland (DeCarbCH) under the umbrella of the new SWEET program (SFOE, 2021).

References

Adams, B. M., Fleming, M. R., Bielicki, J. M., Hansper, J., Glos, S., Langer, M., Wechsung, M., and Saar, M. O. (2019). "Grid Scale Energy Storage Using CO$_2$ in Sedimentary Basins: The Cost of Power Flexibility". In: *Proceedings European Geothermal Congress 2019*. Den Haag, The Netherlands, 11-14 June 2019.

Adams, B. M., Saar, M. O., Bielicki, J. M., Ogland-Hand, J. D., and Fleming, M. R. (2020). "Using Geologically Sequestered CO$_2$ to Generate and Store Geothermal Electricity: CO$_2$ Plume Geothermal (CPG)". In: *Proceedings MIT A+B Applied Energy Symposium 2020*. Cambridge, USA.

Adams, B. M., Kuehn, T. H., Bielicki, J. M., Randolph, J. B., and Saar, M. O. (2014). "On the Importance of the Thermosiphon Effect in CPG (CO$_2$ Plume Geothermal) Power Systems". In: *Energy* 69, pp. 409–418. DOI: 10.1016/j.energy.2014.03.032. URL: http://dx.doi.org/10.1016/j.energy.2014.03.032.

– (2015). "A Comparison of Electric Power Output of CO$_2$ Plume Geothermal (CPG) and Brine Geothermal Systems for Varying Reservoir Conditions". In: *Applied Energy* 140, pp. 365–377. DOI: 10.1016/j.apenergy.2014.11.043. URL: http://dx.doi.org/10.1016/j.apenergy.2014.11.043.

Adams, B. M., Vogler, D., Kuehn, T. H., Bielicki, J. M., Garapati, N., and Saar, M. O. (2021). "Heat depletion in sedimentary basins and its effect on the design and electric power output of CO2 Plume Geothermal (CPG) systems". In: *Renewable Energy* 172, pp. 1393–1403. ISSN: 18790682. DOI: 10.1016/j.renene.2020.11.145. URL: https://doi.org/10.1016/j.renene.2020.11.145.

Aghli, G., Moussavi-Harami, R., and Mohammadian, R. (2020). "Reservoir heterogeneity and fracture parameter determination using electrical image logs and petrophysical data (a case study, carbonate Asmari Formation, Zagros Basin, SW Iran)". In: *Petroleum Science* 17.1, pp. 51–69.

Amann, F., Gischig, V., Evans, K., Doetsch, J., Jalali, R., Valley, B., Krietsch, H., Dutler, N., Villiger, L., Brixel, B., Klepikova, M., Kittilä, A., Madonna, C., Wiemer, S., Saar, M. O., Loew, S., Driesner, T., Maurer, H., and Giardini, D. (2018). "The seismo-hydromechanical behavior during deep geothermal reservoir stimulations: open question tackled in a decameter-scale in situ stimulation experiment". In: *Solid Earth* 9.1, pp. 115–137.

Bachu, S. (2003). "Screening and ranking of sedimentary basins for sequestration of CO2 in geological media in response to climate change". In: *Environmental Geology* 44, pp. 277–289.

Barbosa, N. D., Caspari, E., Rubino, J. G., Greenwood, A., Baron, L., and Holliger, K. (2019). "Estimation of fracture compliance from attenuation and velocity analysis of full-waveform sonic log data". In: *Journal of Geophysical Research: Solid Earth* 124(3), 2738–2761.

Barbosa, N. D., Greenwood, A., Caspari, E., Dutler, N., and Holliger, K. (2021). "Estimates of Individual Fracture Compliances Along Boreholes From Full-Waveform Sonic Log Data". In: *Journal of Geophysical Research: Solid Earth* 126(5). DOI: https://doi.org/10.1029/2021JB022015.

Bauer, C., Hirschberg, S., Bauerle, Y., Biollaz, S., Calbry-Muzyka, A., Cox, B., Heck, T., Lehnert, M., Meier, A., Prasser, H.-M., Schenler, W., Treyer, K., Vogel, F., Wieckert, H. C., Zhang, X., Zimmermann, M., Burg, V., Bowman, G., Erni, M., Saar, M., and Tran, M. Q. (2017). *Potentials, costs and environmental assessment of electricity generation technologies*. Villigen PSI, Switzerland: Paul Scherrer Institute.

Bedretto Lab (2021). *Bedretto Underground Laboratory for Geoenergy and Geoscience*. URL: http://www.bedrettolab.ethz.ch/home/.

Bodmer, P. H. (1982). "Beiträge zur Geothermie der Schweiz". PhD thesis. Zurich, Switzerland: ETH Zurich.

Brixel, B. (2021). "Fluid flow in sparse fracture systems, prior to and after fault slip". PhD thesis. Zurich, Switzerland: ETH Zurich.

Brixel, B., Klepikova, M., Jalali, M. R., Lei, Q., Roques, C., Kriestch, H., and Loew, S. (2020a). "Tracking fluid flow in shallow crustal fault zones: 1. Insights from single-hole permeability estimates." In: *Journal of Geophysical Research: Solid Earth* 125(4). DOI: e2019JB018200.

Brixel, B., Klepikova, M., Lei, Q., Roques, C., Jalali, M. R., Krietsch, H., and Loew, S. (2020b). "Tracking fluid flow in shallow crustal fault zones: 2. Insights from cross-hole forced flow experiments in damage zones." In: *Journal of Geophysical Research: Solid Earth* 125(4). DOI: e2019JB019108.

Broccardo, M., Mignan, A., Wiemer, S., Stojadinovic, B., and Giardini, D. (2017). "Hierarchical Bayesian modeling of fluid-induced seismicity". In: *Geophysical Research Letters* 44(22), pp. 11–357.

Buscheck, T. A., Bielicki, J. M., Edmunds, T. A., Hao, Y., Sun, Y., Randolph, J. B., and Saar, M. O. (2016). "Multi-Fluid Geo-Energy Systems: Using Geologic CO2 Storage for Geothermal Energy Production and Grid-Scale Energy Storage in Sedimentary Basins". In: *Geosphere* 12.3. ISSN: 1553-040X. DOI: 10.1130/GES01207.1.

Chadwick, A., Arts, R., Bernstone, C., May, F., Thibeau, S., and Zweigel, P. (2008). "Best practice for the storage of CO2 in saline aquifers-observations and guidelines from the SACS and CO2STORE projects (Vol. 14)". In: *British Geological Survey*.

Chevalier, G., Diamond, L. W., and Leu, W. (2010). "Potential for deep geological sequestration of CO 2 in Switzerland: a first appraisal". In: *Swiss Journal of Geosciences* 103.3, pp. 427–455.

Clerc (in prep.). "PhD Thesis University of Geneva". PhD thesis. Swisstopo.

Dahrabou (2021). "Calibration methodology of near-field wellbore stress and strength to predict failure severity in deep geothermal boreholes: From theory to industrial applications". PhD thesis. Emille-Argand 11, CH-2000 Neuchâtel: Université de Neuchâtel.

DESTRESS (2021). *Demonstration of soft stimulation treatments of geothermal reservoirs.* URL: http://www.destress-h2020.eu/en/home/.

DG-WOW (2019). *Deep Geothermal Well Optimization Workflow (DG-WOW).* URL: https://www.aramis.admin.ch/Grunddaten/?ProjectID=37661.

Diamond, L. (2019). *Deep underground heat reservoirs, Joint NRP70 project "Hydropower and geo-energy".* Tech. rep. URL: https://nfp-energie.ch/en/projects/960/.

Diaz, M. B., Kim, K. Y., Kang, T. H., and Shin, H. S. (2018). "Drilling data from an enhanced geothermal project and its pre-processing for ROP forecasting improvement". In: *Geothermics* 72.December 2017, pp. 348–357. ISSN: 03756505. DOI: 10.1016/j.geothermics.2017.12.007. URL: https://doi.org/10.1016/j.geothermics.2017.12.007.

Doetsch, J., Krietsch, H., Schmelzbach, C., Gischig, M. J. V., Villiger, L., Amann, F., and Maurer, H. (2020). "Characterizing a decametre-scale granitic reservoir using ground-penetrating radar and seismic methods." In: *Solid Earth* 11(4), pp. 1441–1455.

Dutler, N., Valley, B., Gischig, V., Jalali, M., Brixel, B., Krietsch, H., Roques, C., and Amann, F. (2020). "Hydromechanical insight of fracture closure during in-situ hydraulic fracturing in crystalline rock." In: *International Journal of Rock Mechanics and Mining Sciences* 135. DOI: 104450.

Dutler, N., Valley, B., Gischig, V., Villiger, L., Krietsch, H., Doetsch, J., and Amann, F. (2019). "Hydraulic fracture propagation in a heterogeneous stress field in a crystalline rock mass." In: *Solid Earth* 10(6), pp. 1877–1904.

ELEGANCY (2021). *Efficient generation of renewable H2 from biomass, while harvesting geothermal heat and enabling negative CO₂ emissions.* URL: https://www.aramis.admin.ch/Texte/?ProjectID=40148.

Evans, K. F., Zappone, A., Kraft, T., Deichmann, N., and Moia, F. (2012). "A survey of the induced seismic responses to fluid injection in geothermal and CO₂ reservoirs in Europe". In: *Geothermics* 41, pp. 30–54. DOI: https://doi.org/10.1016/j.geothermics.2011.08.002.

Ezekiel, J., Ebigbo, A., Adams, B. M., and Saar, M. O. (2020). "Combining natural gas recovery and CO2-based geothermal energy extraction for electric power generation". In: *Applied Energy* 269.April,

p. 115012. ISSN: 03062619. DOI: 10.1016/j.apenergy.2020.115012. URL: https://doi.org/10.1016/j.apenergy.2020.115012.

Ezzat, M., Vogler, D., Saar, M. O., and Adams, B. M. (2021). "Simulating Plasma Formation in Pores under Short Electric Pulses for Plasma Pulse Geo Drilling (PPGD)". In: *Energies* 14.16, p. 4717. ISSN: 1996-1073. URL: https://www.mdpi.com/1996-1073/14/16/4717.

Fay, H. (1993). "Practical Evaluation of Rock-Bit Wear During Drilling". In: *Proceedings SPE Drilling & Completion*, pp. 99–104. DOI: 10.2118/21930-PA.

Federal office for the Environment (FOEN) (2020). *Seismic zones according to the SIA 261 standard.* Ittigen, Switzerland: FOEN.

Ferretti, V. and Montibeller, G. (2016). "Key challenges and meta-choices in designing and applying multi-criteria spatial decision support systems". In: *Decision Support Systems* 84, pp. 41–52. DOI: https://doi.org/10.1016/j.dss.2016.01.005.

Fitzgerland, T. (2013). "Frackonomics: Some economics of hydraulic fracturing". In: *Case W. Res. L. Rev.* 63.4, pp. 1337–1362. DOI: 10.3868/s050-004-015-0003-8.

Fleming, M. R., Adams, B. M., Randolph, J. B., Ogland-Hand, J. D., Kuehn, T. H., Buscheck, T. A., Bielicki, J. M., and Saar, M. O. (2018). "High Efficiency and Large-scale Subsurface Energy Storage with CO$_2$". In: *Proceedings 43rd Workshop on Geothermal Reservoir Engineering*. Stanford University USA.

Fleming, M. R., Adams, B. M., Kuehn, T. H., Bielicki, J. M., and Saar, M. O. (2020). "Increased Power Generation due to Exothermic Water Exsolution in CO2 Plume Geothermal (CPG) Power Plants". In: *Geothermics* 88.April, p. 101865. ISSN: 03756505. DOI: 10.1016/j.geothermics.2020.101865. URL: https://doi.org/10.1016/j.geothermics.2020.101865.

Garapati, N., Adams, B. M., Fleming, M. R., Kuehn, T. H., and Saar, M. O. (2020). "Combining brine or CO2 geothermal preheating with low-temperature waste heat: A higher-efficiency hybrid geothermal power system". In: *Journal of CO2 Utilization* 42.October, p. 101323. ISSN: 22129820. DOI: 10.1016/j.jcou.2020.101323. URL: https://doi.org/10.1016/j.jcou.2020.101323.

Garapati, N., Randolph, J. B., and Saar, M. O. (2015). "Brine displacement by CO2, energy extraction rates, and lifespan of a CO2-limited CO2-Plume Geothermal (CPG) system with a horizontal production well". In: *Geothermics* 55, pp. 182–194. ISSN: 03756505. DOI: 10.1016/j.geothermics.2015.02.005. URL: http://dx.doi.org/10.1016/j.geothermics.2015.02.005.

Geo-Energy Suisse (2021). *Breakthrough for deep geothermal energy - Small steps with great success.* URL: http://www.destress-h2020.eu/export/sites/destress/stay-informed/.galleries/pdf/Mediarelease_GES_Bedretto_21012021.pdf_2063069299.pdf.

Giertzuch, P. L., Doetsch, J., Jalali, M., Shakas, A., Schmelzbach, C., and Maurer, H. (2020). "Time-lapse ground penetrating radar difference reflection imaging of saline tracer flow in fractured rock." In: *Geophysics* 85(3), H25–H37.

Gischig, S., Doetsch, J., Maurer, H., Krietsch, H., Amann, F., Evans, K. F., Nejati, M., Jalali, M., Obermann, A., Valley, B., Wiemer, S., and Giardini, D. (2018). "On the link between stress field and small-scale hydraulic fracture growth in anisotropic rock derived from micro-seismicity". In: *Solid Earth* 9(1), pp. 39–61.

Gischig, V. S., Giardini, D., Amann, F., Hertrich, M., Krietsch, H., Loew, S., Maurer, H., Villiger, L., Wiemer, S., Bethmann, F., Brixel, B., Doetsch, J., Doonechaly, N. G., Driesner, T., Dutler, N., Evans, K. F., Jalali, M., Jordan, D., Kittilä, A., Ma, X., Meier, P., Nejati, M., Obermann, A., Plenkers, K., Saar, M. O., Shakas, A., and Valley, B. (2020). "Hydraulic stimulation and fluid circulation experiments in underground laboratories: Stepping up the scale towards engineered geothermal systems". In: *Geomechanics for Energy and the Environment* 24, p. 100175. ISSN: 23523808. DOI: 10.1016/j.gete.2019.100175. URL: https://doi.org/10.1016/j.gete.2019.100175.

Griesser, J.-C. and Rybach, L. (1989). "Numerical Thermohydraulic Modeling of Deep Groundwater Circulation in Crystalline Basement: An Example of Calibration". In: *Hydrogeological Regimes and Their Subsurface Thermal Effects*. American Geophysical Union (AGU), pp. 65–74. ISBN: 978-1-118-66650-0. DOI: 10.1029/GM047p0065. URL: https://agupubs.onlinelibrary.wiley.com/doi/abs/10.1029/GM047p0065 (visited on 02/18/2020).

Gruber, M. (2017). "Structural Investigations of the Western Swiss Molasse Basin – From 2D Seismic Interpretation to a 3D Geological Model." PhD thesis. University of Fribourg.

Guglielmi, Y., Cappa, F., Lançon, H., Janowczyk, J. B., Rutqvist, J., Tsang, C. F., and Wang, J. S. Y. (2015). "ISRM Suggested Method for Step-Rate Injection Method for Fracture In-Situ Properties (SIMFIP): Using a 3-Components Borehole Deformation Sensor". en. In: *The ISRM Suggested Methods for Rock Characterization, Testing and Monitoring: 2007-2014*. Ed. by R. Ulusay. Cham: Springer International Publishing, pp. 179–186. ISBN: 978-3-319-07713-0. DOI: 10.1007/978-3-319-07713-0_14. URL: https://doi.org/10.1007/978-3-319-07713-0_14 (visited on 10/01/2019).

Guidati, G., Marcucci, A., and Giardini, D. (2021). *Probabilistic Assessment of the Swiss Energy Stragegy - Scenario analysis with the SES-ETH model*. Tech. rep. ETH Zurich - JASM. URL: https://sccer-jasm.ch/JASMpapers/JASM_results_ses_eth.pdf.

Hassanjanikhoshkroud, N., Nestola, M. G. C., Zulian, P., Planta, C. von, Vogler, D., Köstler, H., and Krause, R. (2020). "Thermo-Fluid-Structure Interaction Based on the Fictitious Domain Method: Application to Dry Rock Simulations". In: pp. 1–12.

Hefny, M., Qin, C. Z., Saar, M. O., and Ebigbo, A. (2020). "Synchrotron-based pore-network modeling of two-phase flow in Nubian Sandstone and implications for capillary trapping of carbon dioxide". In: *International Journal of Greenhouse Gas Control* 103.April. ISSN: 17505836. DOI: 10.1016/j.ijggc.2020.103164. arXiv: 2004.06792.

Hirschberg, S., Wiemer, S., and Burgherr, P. (2015). *Energy from the earth: Deep geothermal as a resource for the future?* Bern, Switzerland: vdf Hochschulverlag AG an der ETH Zürich.

Höser, D., Meier, T., Patru, A., Kant, M., and Rudolf von Rohr, P. (2018). "An experimental study of the influence of uniaxial load on flame jet drilling". In: *International Journal of Rock Mechanics and Mining Sciences* 106.April, pp. 311–318. DOI: 10.1016/j.ijrmms.2018.04.007.

Hoteit, H., Fahs, M., and Soltanian, M. R. (2019). "Assessment of CO2 Injectivity during Sequestration in Depleted Gas Reservoirs". In: *Geosciences* 9.5, p. 199.

Hunziker, J., Greenwood, A., Minato, S., Barbosa, N. D., Caspari, E., and Holliger, K. (2020). "Bayesian full-waveform inversion of tube waves to estimate fracture aperture and compliance". In: *Solid Earth* 11(2).

Ireland, M., Rachel, B., Miles, W., Paul, S., and Richard, D. (2020). "Paucity of Legacy Oil and Gas Subsurface Data Onshore United Kingdom: Implications for the Expansion of Low Carbon Subsurface Activities and Technologies". In: *EarthArXiv* 4. DOI: 10.31223/osf.io/rdv2s.

Jamali, S., Wittig, V., and Bracke, R. (2017). "Mechanically assisted thermal type laserjet process for deep hard rock drilling". In: *Oil Gas European Magazine* 43.4, pp. 192–196.

Kakurina, M., Guglielmi, Y., Nussbaum, C., and Valley, B. (Apr. 2019). "Slip perturbation during fault reactivation by a fluid injection". In: *Tectonophysics* 757, pp. 140–152. ISSN: 0040-1951. DOI: 10.1016/j.tecto.2019.01.017. URL: http://www.sciencedirect.com/science/article/pii/S0040195119300083 (visited on 03/27/2019).

– (Oct. 2020). "In Situ Direct Displacement Information on Fault Reactivation During Fluid Injection". en. In: *Rock Mechanics and Rock Engineering* 53.10, pp. 4313–4328. ISSN: 1434-453X. DOI: 10.1007/s00603-020-02160-w. URL: https://doi.org/10.1007/s00603-020-02160-w (visited on 10/21/2020).

Kant, M. A., Rossi, E., Duss, J., Amann, F., Saar, M. O., and Rudolf von Rohr, P. (2018). "Demonstration of thermal borehole enlargement to facilitate controlled reservoir engineering for deep geothermal, oil

or gas systems". In: *Applied Energy* 212, pp. 1501–1509. DOI: https://doi.org/10.1016/j.apenergy.2018.01.009.

Kant, M. A., Rossi, E., Höser, D., and Rudolf von Rohr, P. (2017). "Thermal Spallation Drilling, an Alternative Drilling Technology for Deep Heat Mining - Performance Analysis, Cost Assessment and Design Aspects". In: *Proceedings 42nd Workshop on Geothermal Reservoir Engineering, Stanford University, Stanford, California, February 13-15, 2017 - SGP-TR-212*, pp. 1–10.

Kittilä, A., Jalali, M., Saar, M. O., and Kong, X. Z. (2020b). "Solute tracer test quantification of the effects of hot water injection into hydraulically stimulated crystalline rock." In: *Geothermal Energy* 8(1), pp. 1–21.

Kittilä, A., Jalali, M. R., Evans, K. F., Willmann, M., Saar, M. O., and Kong, X. Z. (2019). "Field comparison of DNA-labeled nanoparticle and solute tracer transport in a fractured crystalline rock." In: *Water Resources Research* 55(8), pp. 6577–6595.

Kittilä, A., Jalali, M. R., Somogyvári, M., Evans, K. F., Saar, M. O., and Kong, X. Z. (2020a). "Characterization of the effects of hydraulic stimulation with tracer-based temporal moment analysis and tomographic inversion". In: *Geothermics* 86. DOI: 101820.

Klepikova, M., Brixel, B., and Jalali, M. (2020). "Transient hydraulic tomography approach to characterize main flowpaths and their connectivity in fractured media". In: *Advances in Water Resources* 136.

Kovscek, A. R. (2002). "Screening criteria for CO2 storage in oil reservoirs". In: *Petroleum Science and Technology* 20.7-8, pp. 841–866.

Krietsch, H., Gischig, V., Evans, K., Doetsch, J., Dutler, N. O., Valley, B., and Amann, F. (2019). "Stress measurements for an in situ stimulation experiment in crystalline rock: integration of induced seismicity, stress relief and hydraulic methods." In: *Rock Mechanics and Rock Engineering* 52(2), pp. 517–542.

Krietsch, H., Gischig, V. S., Doetsch, J., Evans, K. F., Villiger, L., Jalali, M., Valley, B., Loew, S., and Amann, F. (2020b). "Hydro-mechanical processes and their influence on the stimulation effected volume: Observations from a decameter-scale hydraulic stimulation project." In: *Solid Earth* 11, pp. 1699–1729. DOI: https://doi.org/10.5194/se-11-1699-2020.

Krietsch, H., Villiger, L., Doetsch, J., Gischig, V. S., Evans, K. F., Brixel, B., Jalali, M., Loew, S., Giardini, D., and Amann, F. (2020a). "Changing flow paths caused by simultaneous shearing and fracturing observed during hydraulic stimulation". In: *Geophysical Research Letters*. DOI: doi.org/10.1029/2019GL086135.

Lahusen, P. H. and Wyss, R. (1995). "Erdöl-und Erdgasexploration in der Schweiz: Ein Rückblick". In: *Bullettin Association Suisse des Geologues et Ingenieurs du Petrole* 62, pp. 43–72.

Laloui, L. and Loria, A. R. (2019). *Analysis and Design of Energy Geostructures, Theoretical Essentials and Practical Application*. Elsevier. ISBN: 9780128206232.

Land, C. V. der, Wood, R., Wu, K., Dijke, M. van, Jiang, Z., Pwm, C., et al. (2013). "Modelling the permeability evolution of carbonate rocks". In: *Marine and Petroleum Geology* 48, pp. 1–7.

Landesgeologie (2017). "GeoMol: Geologisches 3D-Modell des Schweizer Molassebeckens". PhD thesis.

Link, K. (2021). *Statistik der geothermischen Nutzung in der Schweiz - Ausgabe 2019*. energieschweiz. URL: https://geothermie-schweiz.ch/wp_live/wp-content/uploads/2020/08/10154-Geothermiestatistik_Schweiz_Ausgabe_2019_final.pdf.

Lukawski, M. Z., Anderson, B. J., Augustine, C., Capuano, L. E., Beckers, K. F., Livesay, B., and Tester, J. W. (2014). "Cost analysis of oil, gas, and geothermal well drilling". In: *Journal of Petroleum Science and Engineering* 118, pp. 1–14. DOI: 10.1016/j.petrol.2014.03.012.

Marcucci, A., Guidati, G., Giardini, D., Bauer, C., Berger, M., Bollinger, A., Burg, V., Carbonell Sanchez, D., Damartzis, T., Evangelos, P., Gupta, R., Hirschberg, S., Kober, T., Li, X., Lordan-Perret, R., Marechal, F., Murray, P., Paolone, M., Patel, M., Ramachandran, K., Schildhauer, T., Schlecht, I., Streicher, K., Weigt, H., Yilmaz, S., and Zuberi, J. (2021). *Transformation of the Swiss energy system towards net-zero greenhouse gas emissions - Results from the Joint Activity Scenarios & Modelling*. ETH Zurich. URL: https://www.sccer-jasm.ch.

Mazzotti, M., Becattini, V., and Guidati, G. (2021). *CO₂ Capture and Storage (CCS) - An Essential Element of the Swiss Climate Strategy. Results from the Elegancy project*. URL: https://www.aramis.admin.ch/Dokument.aspx?DocumentID=67419.

McClure, M. W. and Horne, R. N. (2014). "An investigation of stimulation mechanisms in Enhanced Geothermal Systems." In: *International Journal of Rock Mechanics and Mining Sciences* 72, pp. 242–260.

Mignan, A., Broccardo, M., Wiemer, S., and Giardini, D. (2017). "Induced seismicity closed-form traffic light system for actuarial decision-making during deep fluid injections". In: *Scientific Reports* 7(1), pp. 1–10.

Mock, S. (2017). "The Neogene tectonic and geodynamic evolution of the central Swiss Molasse Basin: An integrative 3-D modeling, tectonic and thermochronological study." PhD thesis. University of Berne.

Moein, M. J. A., Somogyvári, M., Valley, B., Jalali, M., Loew, S., and Bayer, P. (Nov. 2018a). "Fracture Network Characterization Using Stress-Based Tomography". en. In: *Journal of Geophysical Research: Solid Earth* 123.11, pp. 9324–9340. ISSN: 21699313. DOI: 10.1029/2018JB016438. URL: http://doi.wiley.com/10.1029/2018JB016438 (visited on 03/30/2019).

Moein, M. J. A., Tormann, T., Valley, B., and Wiemer, S. (2018b). "Maximum Magnitude Forecast in Hydraulic Stimulation Based on Clustering and Size Distribution of Early Microseismicity". en. In: *Geophysical Research Letters* 45.0, pp. 6907–6917. ISSN: 1944-8007. DOI: 10.1029/2018GL077609. URL: https://agupubs.onlinelibrary.wiley.com/doi/abs/10.1029/2018GL077609 (visited on 08/20/2018).

Moein, M. J. A., Valley, B., and Evans, K. F. (Jan. 2019). "Scaling of Fracture Patterns in Three Deep Boreholes and Implications for Constraining Fractal Discrete Fracture Network Models". en. In: *Rock Mechanics and Rock Engineering*. ISSN: 1434-453X. DOI: 10.1007/s00603-019-1739-7. URL: https://doi.org/10.1007/s00603-019-1739-7 (visited on 03/30/2019).

Moscariello, A. (2016). "Reservoir geo-modeling and uncertainty management in the context of geo-energy projects". In: *Swiss Bulletin für angewandte Geologie* 21.1, pp. 29–43.

Moscariello, A., Guglielmetti, L., Omodeo-Salé, S., De Haller, A., Eruteya, O., Lo, H., Clerc, N., Makloufhi, Y., Do Couto, D., Ferreira De Oliveira, G., Perozzi, L., DeOliveira, F., Hollmuller, P., Quiquerez, L., Nawratil De Bono, C., F, F. M., and Meyer, M. (2020). "Heat production and storage in Western Switzerland: advances and challenges of intense multidisciplinary geothermal exploration activities, an 8 years progress report". In: *Proceedings World Geothermal Congress 2020, Reykjavik, Iceland, April 26 – May 2*.

Nelson, R. (2001). *Geologic analysis of naturally fractured reservoirs*. New York: Gulf Professional Publishing.

Niederau, J., Ebigbo, A., and Saar, M. O. (Apr. 2020). "Characterization of Subsurface Heat-Transport Processes in the Canton of Aargau Using an Integrative Workflow". In: *Proceedings World Geothermal Congress 2020*. Reykjavik Iceland. URL: https://pangea.stanford.edu/ERE/db/WGC/papers/WGC/2020/11116.pdf.

Ogland-Hand, J. D., Bielicki, J. M., Adams, B. M., Nelson, E. S., Buscheck, T. A., Saar, M. O., and Sioshansi, R. (2021). "The value of CO2-Bulk energy storage with wind in transmission-constrained electric power systems". In: *Energy Conversion and Management* 228.October 2020, p. 113548. ISSN: 01968904. DOI: 10.1016/j.enconman.2020.113548. URL: https://doi.org/10.1016/j.enconman.2020.113548.

Ogland-Hand, J. D., Bielicki, J. M., Wang, Y., Adams, B. M., Buscheck, T. A., and Saar, M. O. (2019). "The Value of Bulk Energy Storage for Reducing CO₂ Emissions and Water Requirements from Regional Electricity Systems". In: *Energy Conversion and Management* 181.April, pp. 674–685. DOI: 10.1016/j.enconman.2018.12.019.

Panos, E. and Kober, T. (2020). *Report on energy model analysis of the role of H2-CCS systems in Swiss energy supply and mobility with quantification of economic and environmental trade-offs, including market assessment and business case. Deliverable 5.3.6 of the ACT ELEGANCY EU Project 274498 (upcoming)*.

Panos, E., Kober, T., Kannan, R., and Hirschberg, S. (2021). *Long-term energy transformation pathways - Integrated scenario analysis with the Swiss TIMES energy systems model*. Tech. rep. PSI - JASM. URL: https://sccer-jasm.ch/JASMpapers/JASM_results_stem.pdf.

Patterson, J. and Driesner, T. (2020). "The effect of thermo-elastic stress re-distribution on geothermal production from a vertical fracture zone". In: *Geothermics* 85.

Patterson, J., Driesner, T., and Matthai, S. K. (2018a). "Self-organizing fluid convection patterns in an echelon fault array". In: *Geophysical Research Letters* 45, 4799–4808. DOI: https://doi.org/10.1029/2018GL078271.

Patterson, J., Driesner, T., Matthai, S. K., and Tomlinson, R. (2018b). "Heat and fluid transport induced by convective fluid circulation within a fracture or fault". In: *Journal of Geophysical Research: Solid Earth* 123, 2658–2673. DOI: https://doi.org/10.1002/2017JB015363.

Planta, C. von, Vogler, D., Chen, X., Nestola, M. G. C., Saar, M. O., and Krause, R. (2018). "Variational Parallel Information Transfer between Unstructured Grids in Geophysics - Applications and Solution Methods". In: pp. 1–4.

– (2019). "Simulation of hydro-mechanically coupled processes in rough rock fractures using an immersed boundary method and variational transfer operators". In: *Computational Geosciences* 23.5, pp. 1125–1140. DOI: 10.1007/s10596-019-09873-0.

– (2020a). "Modelling of hydro-mechanical processes in heterogeneous fracture intersections using a fictitious domain method with variational transfer operators". In: *Computational Geosciences*. DOI: 10.1007/s10596-020-09936-7.

Planta, C. von, Vogler, D., Zulian, P., Saar, M. O., and Krause, R. (2020b). "Solution of contact problems between rough body surfaces with non matching meshes using a parallel mortar method". In: *International Journal of Rock Mechanics and Mining Sciences* 133, p. 104414. DOI: 10.1016/j.ijrmms.2020.104414.

Prognos (2012). *Die Energieperspektiven für die Schweiz bis 2050*. Prognos AG. URL: https://www.prognos.com/publikationen/alle-publikationen/292/show/7f9a4382d75cc40032147306d423aaca/.

– (2020). *Energieperspektive 2050+*. Swiss Federal Office of Energy. URL: https://www.bfe.admin.ch/bfe/de/home/politik/energieperspektiven-2050-plus.html.

Randolph, J. B. and Saar, M. O. (2011a). "Combining geothermal energy capture with geologic carbon dioxide sequestration". In: *Geophysical Research Letters* 38.10, pp. 1–7. ISSN: 0094-8276. DOI: 10.1029/2011GL047265.

– (2011b). "Coupling carbon dioxide sequestration with geothermal energy capture in naturally permeable, porous geologic formations: Implications for CO2 sequestration". In: *Energy Procedia* 4.2010, pp. 2206–2213. ISSN: 18766102. DOI: 10.1016/j.egypro.2011.02.108.

Raza, A., Gholami, R., Rezaee, R., Bing, C. H., Nagarajan, R., and Hamid, M. A. (2018). "CO2 storage in depleted gas reservoirs: A study on the effect of residual gas saturation". In: *Petroleum* 4.1, pp. 95–107.

Reinsch, T., Paap, B., Hahn, S., Wittig, V., and Berg, S. van den (2018). "Insights into the radial water jet drilling technology – Application in a quarry". In: *Journal of Rock Mechanics and Geotechnical Engineering* 10.2, pp. 236–248. DOI: 10.1016/j.jrmge.2018.02.001.

Roques, C., Weber, U. W., Brixel, B., Krietsch, H., Dutler, N., Brennwald, M. S., Villiger, L., Doetsch, J., Jalali, M., Gischig, V., Amann, F., Valley, B., Klepikova, M., and Kipfer, R. (2020). "In situ observation of helium and argon release during fluid-pressure-triggered rock deformation". In: *Scientific Reports* 10(1), pp. 1–9.

Rossi, E., Adams, B. M., Vogler, D., Rudolf von Rohr, P., Kammermann, B., and Saar, M. O. (2020a). "Advanced drilling technologies to improve the economics of deep geo-resource utilization". In: *Proceedings MIT A+B Applied Energy Symposium 2020*. MIT, Cambridge, USA, pp. 1–6.

Rossi, E., Jamali, S., Saar, M. O., and Rudolf von Rohr, P. (2020b). "Field test of a Combined Thermo-Mechanical Drilling technology. Mode I: Thermal spallation drilling". In: *Journal of Petroleum Science and Engineering* 190.107005, pp. 1–14. DOI: 10.1016/j.petrol.2020.107005.

Rossi, E., Jamali, S., Schwarz, D., Saar, M. O., and Rudolf von Rohr, P. (2020c). "Field test of a Combined Thermo-Mechanical Drilling technology. Mode II: Flame-assisted rotary drilling". In: *Journal of Petroleum Science and Engineering* 190.106880, pp. 1–12. DOI: 10.1016/j.petrol.2019.106880.

Rossi, E., Jamali, S., Wittig, V., Saar, M. O., and Rudolf von Rohr, P. (2020d). "A combined thermo-mechanical drilling technology for deep geothermal and hard rock reservoirs". In: *Geothermics* 85C, pp. 1–11. DOI: 10.1016/j.geothermics.2019.101771.

Rossi, E., Kant, M. A., Borkeloh, O., Saar, M. O., and Rudolf von Rohr, P. (2018a). "Experiments on Rock-Bit Interaction during a Combined Thermo-Mechanical Drilling Method". In: *Proceedings 43rd Workshop on Geothermal Reservoir Engineering, Stanford University, Stanford, California, February 12-14, 2018 - SGP-TR-213*. Stanford University, Stanford, CA, pp. 1–9.

Rossi, E., Kant, M. A., Madonna, C., Saar, M. O., and Rudolf von Rohr, P. (2018b). "The Effects of High Heating Rate and High Temperature on the Rock Strength: Feasibility Study of a Thermally Assisted Drilling Method". In: *Rock Mechanics and Rock Engineering* 51.9, pp. 2957–2964. DOI: 10.1007/s00603-018-1507-0.

Rossi, E., Saar, M. O., and Rudolf von Rohr, P. (2020e). "The influence of thermal treatment on rock-bit interaction: a study of a combined thermo-mechanical drilling (CTMD) concept". In: *Geothermal Energy* 8.16, pp. 1–22. DOI: 10.1186/s40517-020-00171-y.

Rudolf von Rohr, P., Rothenfluh, T., and Schuler, M. (2015). *Rock drilling in great depths by thermal fragmentation using highly exothermic reactions evolving in the environment of a water-based drilling fluid.* Patent US8967293 B2.

Rybach, L., Eugster, W., and Griesser, J.-C. (1987). "Die geothermischen Verhältnisse in der Nordschweiz". In: *Eclogae geologicae helvetiae* 80.2, pp. 521–534.

Schädle, P., Zulian, P., Vogler, D., Bhopalam, S. R., Nestola, M. G. C., Ebigbo, A., Krause, R., and Saar, M. O. (2019). "3D non-conforming mesh model for flow in fractured porous media using Lagrange multipliers". In: *Computers & Geosciences* 132, pp. 42–55. DOI: https://doi.org/10.1016/j.cageo.2019.06.014.

Schiegg, H. O., Rødland, A., Zhu, G., Yuen, D. A., and AG, S. (2015). "Electro-Pulse-Boring (EPB): Novel Super-Deep Drilling Technology for Low Cost Electricity". In: *Journal of Earth Science* 26.1, pp. 37–46. DOI: 10.1007/s12583-015-0519-x.

Schopper, F., Doetsch, J., Villiger, L., Krietsch, H., Gischig, V. S., Jalali, M., Dutler, N., and Maurer, H. (2020). "On the Variability of Pressure Propagation during Hydraulic Stimulation based on Seismic Velocity Observations." In: *Journal of Geophysical Research: Solid Earth* 125(2). DOI: e2019JB018801.

SFOE (2021). *SWEET guiding theme: Integration of renewables.* URL: https://www.bfe.admin.ch/bfe/en/home/research-and-cleantech/funding-program-sweet/calls-for-proposals-overview/sweet-integration-of-renewables.html.

Shah, N., Samrock, F., and Saar, M. O. (2020a). "3-D magnetotelluric survey at northern Swiss heat flow anomaly". In: *Under review at Geothermics*.

– (2020b). "Resistics: an open source Python 3 package for processing of magnetotelluric data". In: *Under review at Computers and Geosciences*.

Sommaruga, A., Eichenberger, U., and Marillier, F. (2012). *Seismic Atlas of the Swiss Molasse Basin. Edited by the Swiss Geophysical Commission.* Tech. rep.

Spada, M. and Burgherr, P. (2015). "Accident Risk". In: *Energy from the Earth. Deep Geothermal as a Resource for the Future?* Ed. by S. Hirschberg, S. Wiemer, and P. Burgherr. Zurich, Switzerland: vdf Hochschulverlag AG. Chap. 6, pp. 229–262.

Spada, M., Sutra, E., and Burgherr, P. (2021). "Comparative accident risk assessment with focus on deep geothermal energy systems in the Organization for Economic Co-operation and Development (OECD) countries". In: *Geothermics* 95. DOI: https://doi.org/10.1016/j.geothermics.2021.102142..

Spada, M., Sutra, E., Wolf, S., and Burgherr, P. (2014). "Accident risk assessment for deep geothermal energy systems". In: *Safety and Reliability: Methodology and Applications?* Ed. by T. Nowakowski, M. Mlynczak, A. Jodejko-Pietruczuk, and S. Werbinska-Wojciechowska. London, UK: CRC Press, pp. 1523–1530.

Stefánsson, V. (1992). "Success in geothermal development". In: *Geothermics* 21.5-6, pp. 823–834. DOI: 10.1016/0375-6505(92)90033-6.

Team GeoMol (2015). "GeoMol—assessing subsurface potentials of the Alpine Foreland Basins for sustainable planning and use of natural resources—project report". In: *Augsburg: Bavarian Environment Agency*.

Teodoriu, C. (2011). "Use of Downhole Mud-Driven Hammer for Geothermal Applications". In: *Proceedings 37th Workshop on Geothermal Reservoir Engineering Stanford University, Stanford, California, January 30 - February 1, 2011 - SGP-TR-194*.

Tester, J. W., Anderson, B., Batchelor, A., Blackwell, D., DiPippo, R., Drake, E., Garnish, J., Livesay, B., Moore, M. C., and Nichols, K. (2006). *The Future of Geothermal Energy*. Tech. rep. November. Idaho National Laboratory.

Thiele, S. T., Jessell, M. W., Lindsay, M., Ogarko, V., Wellmann, J. F., and Pakyuz-Charrier, E. (2016). "The topology of geology 1: Topological analysis". In: *Journal of Structural Geology* 91, pp. 27–38.

Trumpy, R. (1980). *Geology of Switzerland: a guide-book. Part A: An outline of the geology of Switzerland.*

Ushakov, V. Y., Vajov, V. F., and Zinoviev, N. T. (2019). *Electro-discharge Technology for Drilling Wells and Concrete Destruction*. Springer, Cham. DOI: 10.1007/978-3-030-04591-3.

Valley, B. and Evans, K. F. (2009). "Stress orientation to 5 km depth in the basement below Basel (Switzerland) from borehole failure analysis." In: *Swiss Journal of Geosciences* 102(3), p. 467.

– (2014). "Preliminary assessment of the scaling relationships of in-situ stress orientation variations indicated by wellbore failure data". In: *EUROCK 2014: Rock Engineering and Rock Mechanics: Structures in and on Rock Masses*. Ed. by L. R. Alejano, Perucho, C. Olalla, and R. Jimémez. CRC Press.

Valley, B. and Miller, S. A. (2020). "Play-fairway analysis for deep geothermal resources in Switzerland". In: *Proceedings World Geothermal Congress 2020*. Reykjavik Iceland.

Varga, M. d. l., Schaaf, A., and Wellmann, F. (2019). "GemPy 1.0: open-source stochastic geological modeling and inversion". In: *Geoscientific Model Development* 12.1, pp. 1–32.

Villiger, L., Gischig, V. S., Doetsch, J., Krietsch, H., Dutler, N. O., Jalali, M., Valley, B., Selvadurai, P. A., Mignan, A., Plenkers, K., Giardini, D., Amann, F., and Wiemer, S. (2020). "Influence of reservoir geology on seismic response during decameter scale hydraulic stimulations in crystalline rock, Solid Earth Discuss." In: *Solid Earth* 11(2), pp. 627–655. DOI: doi.org/10.5194/se-2019-159.

Villiger, L., Gischig, V. S., Kwiatek, G., Krietsch, H., Doetsch, J., Jalali, M., Amann, F., Giardini, D., and Wiemer, S. (2020b). "Meter-scale stress heterogeneities and stress redistribution drive complex fracture slip and fracture growth during a hydraulic stimulation experiment." In: *In review for Geophysical Journal International*.

Villiger, L., Kraft, T., Gischig, V. S., Krietsch, H., Doetsch, J., Jalali, M., Amann, F., Giardini, D., and Wiemer, S. (2021). "Breaking in scale invariance due to repeated earthquakes induced during decameter-scale hydraulic stimulation." In: *In preparation*.

VLTRE (2021). *Validierung von Technologien zur Reservoir Entwicklung*. URL: https://www.aramis.admin.ch/Grunddaten/?ProjectID=38726.

Vogler, D., Walsh, S. D. C., Rudolf von Rohr, P., and Saar, M. O. (2020a). "Simulation of rock failure modes in thermal spallation drilling". In: *Acta Geotechnica* 15.8, pp. 2327–2340. DOI: 10.1007/s11440-020-00927-7.

Vogler, D., Walsh, S. D. C., and Saar, M. O. (2020b). "A numerical investigation into key factors controlling hard rock excavation via electropulse stimulation". In: *Journal of Rock Mechanics and Geotechnical Engineering* 12.4, pp. 793–801. DOI: 10.1016/j.jrmge.2020.02.002.

Volkart, K., Weidmann, N., Bauer, C., and Hirschberg, S. (2017). "Multi-criteria decision analysis of energy system transformation pathways: A case study for Switzerland". In: *Energy Policy* 106, pp. 155–168. DOI: https://doi.org/10.1016/j.enpol.2017.03.026.

Walsh, S. D. C. and Vogler, D. (Apr. 2020). "Simulating electropulse fracture of granitic rock". In: *International Journal of Rock Mechanics and Mining Sciences* 128, p. 104238. DOI: 10.1016/j.ijrmms.2020.104238.

Walsh, S. D., Garapati, N., Leal, A. M., and Saar, M. O. (2017). "Calculating thermophysical fluid properties during geothermal energy production with NESS and Reaktoro". In: *Geothermics* 70.December 2016, pp. 146–154. ISSN: 03756505. DOI: 10.1016/j.geothermics.2017.06.008. URL: http://www.sciencedirect.com/science/article/pii/S0375650516302048.

Wellmann, J. F. and Regenauer-Lieb, K. (2012). "Uncertainties have a meaning: Information entropy as a quality measure for 3-D geological models". In: *Tectonophysics* 526, pp. 207–216.

Wellmann, J. F., Varga, M. D. L., Murdie, R. E., Gessner, K., and MarkJessell (2018). "Uncertainty estimation for a geological model of the Sandstone greenstone belt, Western Australia–insights from integrated geological and geophysical inversion in a Bayesian inference framework". In: *Geological Society, London, Special Publications* 453.1, pp. 41–56.

Wenning, Q., Madonna, C., Kurotori, T., and Pini, R. (2019). "Spatial mapping of fracture aper-ture changes with shear displacement using X-ray computerized tomography". In: *J. Geophysical Research – Solid Earth*.

Wenning, Q., Madonna, C., Kurotori, T., Petrini, C., Hwang, J., Zappone, A., Giardini, D., Wiemer, S., and Pini, R. (2020a). "Chemo-mechanical coupling in fractured shale with water and hydrocarbon flow". In: *Geo. Res. Let. submitted*.

Wenning, Q., Madonna, C., Zappone, A., Grab, M., Rinaldi, A., Plötze, M., Nussbaum, C., Giardini, D., and Wiemer, S. (2020b). "Shale fault zone structure and stress dependent anisotropic permeability and seismic velocity properties (Opalinus Clay, Switzerland)". In: *Journal of Structural Geology submitted*.

Yalcin, M. and Gul, F. K. (2017). "A GIS-based multi criteria decision analysis approach for exploring geothermal resources: Akarcay basin (Afyonkarahisar)". In: *Geothermics* 67, pp. 18–28. DOI: https://doi.org/10.1016/j.geothermics.2017.01.002.

Zappone, A., Rinaldi, A., Grab, M., Wenning, Q., Roques, C., Madonna, C., Obermann, A., Bernasconi, S., Soom, F., Cook, P., Guglielmi, Y., Nussbaum, C., Giardini, D., and Wiemer, S. (2020). "Fault sealing and caprock integrity for CO$_2$ storage: an in-situ injection experiment". In: *Solid Earth submitted*.

ZoDrEx (2021). *Zonal Isolation, Drilling and Exploitation of EGS projects*. URL: http://www.geothermica.eu/projects/zodrex/.

Zulian, P., Schädle, P., Karagyaur, L., and Nestola, M. (2020). "Comparison and Application of non-Conforming Mesh Models for Flow in Fractured Porous Media using dual L agrange multipliers". In: *arXiv preprint arXiv:2008.06360*.